



UNIL | Université de Lausanne

Unicentre

CH-1015 Lausanne

<http://serval.unil.ch>

---

2013

## The congenital sodium diarrhea and Spint2: from the molecules to the disease

Nicolas Faller

Nicolas Faller, 2013, The congenital sodium diarrhea and Spint2: from the molecules to the disease

Originally published at : Thesis, University of Lausanne

Posted at the University of Lausanne Open Archive.  
<http://serval.unil.ch>

### **Droits d'auteur**

L'Université de Lausanne attire expressément l'attention des utilisateurs sur le fait que tous les documents publiés dans l'Archive SERVAL sont protégés par le droit d'auteur, conformément à la loi fédérale sur le droit d'auteur et les droits voisins (LDA). A ce titre, il est indispensable d'obtenir le consentement préalable de l'auteur et/ou de l'éditeur avant toute utilisation d'une oeuvre ou d'une partie d'une oeuvre ne relevant pas d'une utilisation à des fins personnelles au sens de la LDA (art. 19, al. 1 lettre a). A défaut, tout contrevenant s'expose aux sanctions prévues par cette loi. Nous déclinons toute responsabilité en la matière.

### **Copyright**

The University of Lausanne expressly draws the attention of users to the fact that all documents published in the SERVAL Archive are protected by copyright in accordance with federal law on copyright and similar rights (LDA). Accordingly it is indispensable to obtain prior consent from the author and/or publisher before any use of a work or part of a work for purposes other than personal use within the meaning of LDA (art. 19, para. 1 letter a). Failure to do so will expose offenders to the sanctions laid down by this law. We accept no liability in this respect.



**UNIL** | Université de Lausanne

Faculté de biologie  
et de médecine

**Département de Pharmacologie et Toxicologie**

**The congenital sodium diarrhea and Spint2:  
from the molecules to the disease**

**Thèse de doctorat en médecine et ès sciences (MD – PhD)**

présentée à la

Faculté de biologie et de médecine  
de l'Université de Lausanne

par

**Nicolas Faller**

Médecin diplômé de la Confédération Helvétique

**Jury**

Prof. Peter Vollenweider, président et répondant de la commission MD-PhD

Prof. Laurent Schild, directeur de thèse

Prof. François Verrey, expert

Dr. Eric Grouzmann, expert

Lausanne 2013

# Imprimatur

Vu le rapport présenté par le jury d'examen, composé de

Président	Monsieur Prof. Peter Vollenweider
Directeur de thèse	Monsieur Prof. Laurent Schild
Répondant Commission MD-PhD	Monsieur Prof. Peter Vollenweider
Experts	Monsieur Prof. François Verrey Monsieur Dr Eric Grouzmann

le Conseil de Faculté autorise l'impression de la thèse de


**Monsieur Nicolas Faller**

Médecin diplômé de la Confédération Helvétique

intitulée

**The congenital sodium diarrhea and Spint2:  
from the molecules to the disease**

Lausanne, le 30 mai 2013

pour Le Doyen  
de la Faculté de Biologie et de Médecine  
  
Prof. Peter Vollenweider

# TABLE OF CONTENTS

<b>SUMMARY (ENGLISH)</b> .....	5
<b>RESUME (FRANCAIS)</b> .....	6
<b>ABBREVIATIONS</b> .....	7
<b>INTRODUCTION</b> .....	8
<b>PROLOGUE ABOUT SALT AND WATER BALANCE</b> .....	8
<b>1. INTESTINAL ION TRANSPORT</b> .....	9
1.1. General considerations .....	9
1.2. Na <sup>+</sup> absorption .....	10
1.2.1. Nutrient-coupled Na <sup>+</sup> absorption .....	11
1.2.2. Electroneutral NaCl absorption .....	11
1.2.3. Electrogenic Na <sup>+</sup> absorption.....	12
1.3. Cl <sup>-</sup> absorption.....	13
1.4. Cl <sup>-</sup> secretion .....	14
1.5. Regulation of intestinal Na <sup>+</sup> and Cl <sup>-</sup> transport .....	15
1.5.1. The endocrine / paracrine system .....	16
1.5.2. The neuroenteric system .....	18
1.5.3. The immune system.....	18
<b>2. DIARRHEA</b> .....	18
<b>3. CONGENITAL DIARRHEAL DISORDERS AND FAMILIAL DIARRHEA SYNDROMES</b> .....	20
3.1. General considerations .....	20
3.2. Congenital chloride diarrhea .....	22
3.3. Glucose-galactose malabsorption .....	23
3.4. Familial diarrhea syndrome and mutation of GUCY2C .....	23
<b>4. THE CONGENITAL SODIUM DIARRHEA</b> .....	24
4.1. Description and pathophysiology .....	24
4.2. Mutations in the Spint2 gene .....	26
<b>5. SPINT2</b> .....	28
5.1. Definition .....	28
5.2. Tissue distribution and expression of Spint2 .....	29
5.3. Function of Spint2.....	30

5.4. Spint2 and cancers .....	31
5.5. Spint2 in mouse models .....	32
5.6. Putative roles of Spint2 in vivo .....	33
<b>6. SPINT1/HAI-1 .....</b>	<b>34</b>
6.1. Definition .....	34
6.2. Tissue distribution, expression and function of HAI-1 .....	34
6.3. Interaction HAI-1-CAP3 .....	35
6.4. HAI-1 knockout mouse models .....	35
<b>7. PROTEASES AND THEIR INHIBITORS.....</b>	<b>36</b>
7.1. General considerations about proteases .....	36
7.2. Mechanisms of proteolysis .....	38
7.3. General consideration about protease inhibitors .....	40
7.4. Classifications of serine protease inhibitors .....	41
7.5. Mechanisms of protease inhibition .....	42
7.5.1. <i>General considerations</i> .....	42
7.5.2. <i>Canonical inhibition</i> .....	43
7.5.3. <i>Structure of canonical inhibitors</i> .....	44
7.5.4. <i>Examples of canonical inhibition</i> .....	47
I) <u>Complex trypsin-CMTI1 inhibitor</u> .....	47
II) <u>Complex HGFA-Kunitz domain 1 of HAI-1</u> .....	48
III) <u>Complex CAP3-Aprotinin</u> .....	49
7.5.5. <i>Non-canonical inhibition</i> .....	49
7.5.6. <i>Mechanism of inhibition used by serpins</i> .....	50
<b>8. MEMBRANE-BOUND SERINE PROTEASES AS POTENTIAL PARTNERS OF SPINT2 .....</b>	<b>52</b>
8.1. General considerations .....	52
8.2. Physiological role of membrane-bound serine proteases .....	53
8.3. Membrane-bound serine proteases and Spint2 .....	54
<b>9. NHE3 AS A CANDIDATE GENE IN THE CONGENIAL SODIUM DIARRHEA ...</b>	<b>55</b>
9.1. General considerations .....	55
9.2. Physiological role of NHE3.....	55
9.3. Regulation of NHE3 .....	56
9.4. NHE3 and serine proteases .....	58
<b>AIMS OF THE PROJECT .....</b>	<b>59</b>

<b>MATERIAL AND METHODS</b> .....	63
<b>RESULTS</b> .....	68
<b>1. STRUCTURE-ACTIVITY STUDY OF SPINT2 WILD TYPE AND MUTANTS; A FUNCTIONAL ASSAY IN XENOPUS OOCYTES</b> .....	68
1.1. Functional assay in <i>Xenopus</i> oocytes .....	68
1.2. Complementary data to the functional assay in <i>Xenopus</i> oocytes.....	68
1.2.1. Assessment of the Spint2 R48L and R143L mutations.....	68
1.2.2. Dipeptidyl peptidase IV as putative target of Spint2.....	71
<b>2. GENERATION OF A SPINT2 KNOCKOUT MOUSE MODEL</b> .....	73
2.1. The gene-trap approach.....	73
2.2. Constitutive and conditional Spint2 knockout mice.....	76
<b>3. AN EPITHELIAL CELL MODEL FOR SPINT2</b> .....	81
3.1. Characterization of Caco-2 cells .....	81
3.2. Overexpression of Spint2 in Caco-2 cells.....	82
3.3. Knocking down Spint2 in Caco-2 cells.....	84
3.4. Stably transfection of Caco-2 cells.....	84
<b>4. THE NA-H-EXCHANGER NHE3 AND MEMBRANE-BOUND SERINE PROTEASES</b> .....	86
4.1. Cleavage of NHE3 by Tmprss3 .....	86
4.2. Functional consequence of the Tmprss3-dependent cleavage of NHE3 .....	91
<b>DISCUSSION</b> .....	96
<b>1. FUNCTIONAL ASSAY IN XENOPUS OOCYTES</b> .....	96
1.1. Dipeptidyl peptidase IV as putative partner of Spint2 .....	96
1.2. The R48L and R143L Spint2 mutations .....	98
<b>2. GENERATION OF A SPINT2 KNOCKOUT MOUSE MODEL</b> .....	98
<b>3. AN EPITHELIAL CELL MODEL FOR SPINT2</b> .....	103
<b>4. THE NA-H-EXCHANGER NHE3 AND MEMBRANE-BOUND SERINE PROTEASES</b> .....	105
<b>GENERAL CONCLUSIONS AND PERSPECTIVES</b> .....	109
<b>REFERENCES</b> .....	113
<b>RÉSUMÉ DESTINÉ À UN LARGE PUBLIC</b> .....	124
<b>ANNEXE: Article submitted to the Journal of Biological Chemistry</b> .....	125

# SUMMARY

The congenital sodium diarrhea is a very rare genetic disease. Children affected by this condition suffer from a severe diarrhea characterized by watery stools with a high fecal loss of sodium and bicarbonates, resulting in hyponatremic dehydration and metabolic acidosis. Genetic analyses have identified mutations in the Spint2 gene as a cause of this disease.

The spint2 gene encodes a transmembrane serine protease inhibitor expressed in various epithelial tissues including the gastro-intestinal tract and renal tubules. The physiological role of Spint2 is completely unknown. In addition, physiological partners of Spint2 are still to be identified and the mechanism of inhibition by Spint2 remains elusive. Therefore, the aim of this project was to get insights about the function and the role of Spint2 in the context of the congenital sodium diarrhea in order to better understand the pathophysiology of diarrheas and maybe identify new therapeutic targets.

A functional assay in *Xenopus* oocytes identified the membrane-bound serine proteases CAP1 and Tmprss13 as potential targets of Spint2 because both proteases were no longer inhibited by the mutant Spint2 Y163C that has been associated with the congenital diarrhea. Further functional and biochemical experiments suggested that the inhibition of Tmprss13 by Spint2 occurs through a complex interaction between both proteins.

The effects of membrane-bound serine proteases on the Na<sup>+</sup>-H<sup>+</sup> exchanger NHE3, which has been proposed to be involved in the pathogenesis of the congenital sodium diarrhea, were also tested. A specific cleavage of NHE3 by the membrane-bound serine protease Tmprss3 was observed in biochemical experiments.

Unfortunately, the physiological relevance of these results could not be assessed *in vivo* since the conditional Spint2 knockout mouse model that we generated showed a reduction in Spint2 expression of only 50% and displayed no phenotype.

Briefly, this work provides two new potential partners of Spint2 and emphasizes a putative regulation of NHE3 by membrane-bound serine proteases. Further work done in animal models and cell lines is required to assess the physiological relevance of these results and to obtain additional data about Spint2 and the congenital diarrhea.

# RÉSUMÉ

La diarrhée congénitale de sodium est une maladie génétique très rare. Les enfants touchés par cette maladie présentent une diarrhée aqueuse sévère accompagnée d'une perte fécale de sodium et bicarbonates causant une déshydratation hyponatrémique et une acidose métabolique. Des analyses génétiques ont identifié des mutations du gène *Spint2* comme cause de cette maladie.

Le gène *Spint2* code pour un inhibiteur de sérine protéase transmembranaire exprimé dans divers épithéliums tels que ceux du tube digestif ou des tubules rénaux. Le rôle physiologique de *Spint2* n'est pas connu. De plus, aucun partenaire physiologique de *Spint2* n'a été identifié et le mécanisme d'inhibition par *Spint2* nous est peu connu. Le but de ce projet est donc d'obtenir de plus amples informations concernant la fonction et le rôle de *Spint2* dans le contexte de la diarrhée congénitale de sodium, cela afin de mieux comprendre la physiopathologie des diarrhées et peut-être d'identifier de nouvelles cibles thérapeutiques.

Un test fonctionnel dans les ovocytes de *Xenopus* a identifié les sérine protéases transmembranaires CAP1 et Tmprss13 comme potentielles cibles de *Spint2* dans la mesure où ces deux protéases n'étaient plus bloquées par le mutant de *Spint2* Y163C qui est associé avec la diarrhée congénitale de sodium. Des expériences fonctionnelles et biochimiques plus poussées suggèrent que l'inhibition de Tmprss13 par *Spint2* est le résultat d'une interaction complexe entre ces deux protéines.

Les effets des sérine protéases transmembranaires sur l'échangeur  $\text{Na}^+\text{-H}^+$  NHE3, qui pourrait être impliqué dans la pathogenèse de la diarrhée congénitale de sodium ont aussi été testés. Un clivage spécifique de NHE3 par la sérine protéase transmembranaire Tmprss3 a été observé lors d'expériences biochimiques.

Malheureusement, la pertinence physiologique de ces résultats n'a pas pu être évaluée *in vivo*, étant donné que le modèle de souris knockout conditionnel de *Spint2* que nous avons créé ne montrait une réduction de l'expression de *Spint2* que de 50% et aucun phénotype.

En résumé, ce travail met en évidence deux nouveaux partenaires possibles de *Spint2*, ainsi qu'une potentielle régulation de NHE3 par des sérine protéases transmembranaires. Des expériences supplémentaires faites dans des modèles animaux et lignées cellulaires sont requises pour évaluer la pertinence physiologique de ces données et pour obtenir de plus amples informations au sujet de *Spint2* et de la diarrhée congénitale de sodium.



# ABBREVIATIONS

AE-1	Anion exchanger 1
AIDS	acquired immunodeficiency syndrome
BPTI	bovine pancreatic trypsin inhibitor (also known as aprotinin)
cAMP	cyclic adenosine monophosphate
CAP	channel activating protease
CFTR	cystic fibrosis transmembrane conductance regulator
cGMP	cyclic guanosine monophosphate
CMTI	cucurbita maxima trypsin inhibitor
DPPIV	dipeptidyl peptidase IV
DRA	down-regulated in colonic adenomas
DSS	dextran sodium sulfate
ENaC	epithelial sodium channel
ENS	enteric nervous system
ES cells	embryonic stem cells
GC-C	guanylate cyclase C receptor
GPI	glycophosphatidylinositol
GUCY2C	guanylate cyclase C receptor
HAI	hepatocyte growth factor activator inhibitor
HGF	hepatocyte growth factor
HGFA	hepatocyte growth factor activator
HIV	human immunodeficiency virus
INF $\gamma$	interferon $\gamma$
MDCK	Madin-Darby canine kidney (cells)
NBC-1	Na <sup>+</sup> -HCO <sub>3</sub> <sup>-</sup> cotransporter
NHE	Na <sup>+</sup> -H <sup>+</sup> -exchanger
NK2CL	Na <sup>+</sup> -K <sup>+</sup> -2Cl <sup>-</sup> cotransporter
OMSVP3	third domain of silver pheasant ovomucoid inhibitor (Kazal-type)
ORT	oral rehydration therapy
PAT-1	putative anion transporter 1
RCL	reactive center loop
SBTI	soybean trypsin inhibitor
SGLT1	Na <sup>+</sup> -couple glucose transporter, member 1
Slc	solute carrier
SSI	Subtilisin inhibitor
Tmprss	transmembrane protease, serine
TNF $\alpha$	tumor necrosis factor $\alpha$
VIP	vasoactive intestinal peptide

# INTRODUCTION

## PROLOGUE ABOUT SALT AND WATER BALANCE

Complex living organisms such as the human body are composed of a huge number of cells (about  $10^{14}$  for the human body). These cells not only live on their own but also interact with each other to form tissues, organs and finally systems, each having a specific role. From the level of the cells to the level of the systems, biological processes are tightly regulated to permit life. The control of all these parameters is called homeostasis and remarkably occurs even though the external environment surrounding complex living organisms varies a lot (e.g. changes in temperature, variable access to food and water, presence of other complex living organisms and microorganisms). This external world was called “milieu extérieur” by the French physiologist Claude Bernard, in opposite to the “milieu intérieur”, in which the cells of the human body live.

An adult with a body weight of 70 kg is made of 60% of water, namely 42 liters. Two-third (28 liters) of this volume is present within the cells: this is the intracellular fluid volume. One third (14 liters) is outside the cells: this is the extracellular fluid volume, which is subdivided in blood plasma (3 liters) and interstitial fluid (11 liters). Although, both the intracellular and extracellular fluid volumes have a similar osmolality (290 mOsm), their composition is different. In particular, cells have a high  $K^+$  concentration and low  $Na^+$  and  $Cl^-$  concentrations, whereas low  $K^+$  concentration and high  $Na^+$  and  $Cl^-$  concentrations are found in extracellular fluid. All these parameters are vital and are thus tightly regulated. The regulation of extracellular fluid volume is achieved by controlling the total body content of NaCl (the main electrolytes), whereas extracellular osmolality is regulated via the control of

total body water content. These phenomena constitute the salt and water balance or homeostasis.

Water / sodium homeostasis involves different organs, such as the gastro-intestinal tract, the central nervous system, endocrine glands, the lung, the skin and the kidney. By modulating the output of salt and water, the kidney plays a pivotal role in salt and water balance. Consequently, diseases of the kidney usually lead to disturbances of extracellular fluid that may be life-threatening.

The gastrointestinal tract is the organ where the food and water intake occurs and thus, also contributes importantly in the maintenance of salt and water balance. As for the kidney, diseases involving the gut can lead to severe disorders of water and electrolytes homeostasis. For instance, diarrhea is a major cause of death in the world, notably in children from developing countries, and a very common symptom in industrial countries. In spite of this, mechanisms of electrolytes and water transports in the gut and their regulation are still incompletely understood.

## **1. INTESTINAL ION TRANSPORT**

### **1.1. General considerations**

Unless otherwise specified, data of the following chapters come from the sources (1-5) and the textbook Medical Physiology, Boron and Boulpaep, 2<sup>nd</sup> updated edition, 2012, Saunders.

Fluid absorption takes place in the small intestine and in the colon. Although the average fluid intake is around 1.5 to 2 L/day, these organs absorb up to 10 L of fluid every day. As shown in figure 1, they also have to reabsorb fluid that has been secreted along the entire digestive tract, namely 1.5 L/day of saliva, 2.0 L/day of gastric secretion, 1.5 L/day of pancreatic secretion and 0.5 L/day of bile secretion. The small intestine itself, but also the

colon can secrete fluid that must be reabsorbed. Most of fluid is (re)absorbed by the small intestine (6.5 L/day), while remaining fluid is (re)absorbed by the colon. Finally, only 0.1 L/day is excreted with the feces. These numbers highlight the considerable capacity of intestinal tissues to transport water. Interestingly, water transport is entirely a passive process, whereas intestinal epithelial cells actively transport  $\text{Na}^+$  and  $\text{Cl}^-$ . This solute movement then drives fluid movement.

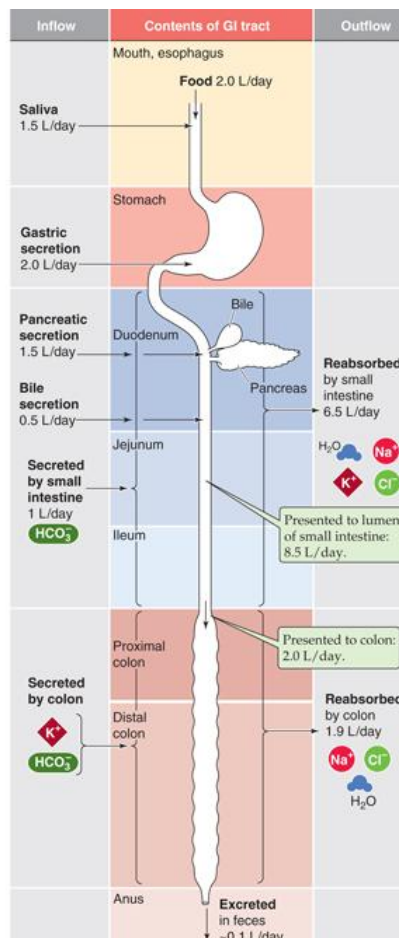


**Figure 1: Fluid balance in the gastro-intestinal tract** (from Boron and Boulpaep, Medical Physiology, 2<sup>nd</sup> updated edition, 2012)

## 1.2. $\text{Na}^+$ absorption

$\text{Na}^+$  absorption in the small intestine and colon occurs via three different mechanisms: (1) nutrient-coupled  $\text{Na}^+$  absorption, (2) electroneutral  $\text{NaCl}$  absorption and (3) electrogenic  $\text{Na}^+$  absorption. In each case, the  $\text{Na-K-pump}$  on the basolateral side of epithelial cells, which

actively pumps 3 Na<sup>+</sup> ions out of the cell and 2 K<sup>+</sup> ions into the cells, is the driving force for Na<sup>+</sup> entry in the apical side of epithelial cells.

### 1.2.1. Nutrient-coupled Na<sup>+</sup> absorption (figure 2)

First described in the 1960s (6), nutrient-coupled absorption is an important mechanism of Na<sup>+</sup> absorption directly after a meal. Its contribution between periods of food intake is of limited importance. Sugars, amino acids and other nutrients transport is coupled to Na<sup>+</sup> absorption. A classic example is glucose-coupled Na<sup>+</sup> absorption mediated by SGLT (Na/glucose cotransporter), which is followed osmotically by water absorption (7). Nutrient-coupled Na<sup>+</sup> absorption mainly occurs in jejunum. Because such transport remains intact during diarrheal disease, oral rehydration therapy (ORT) contains sugar, salt and water so that, in spite of active fluid secretion in the gut, sufficient salt and water absorption can occur by stimulating glucose-couple Na<sup>+</sup> transport. ORT constitutes a major progress in the management of diarrhea around the world (8).

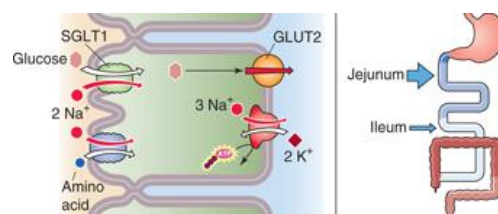


**Figure 2: Nutrient-coupled Na<sup>+</sup> absorption** (from Boron and Boulpaep, Medical Physiology, 2<sup>nd</sup> updated edition, 2012)

### 1.2.2. Electroneutral NaCl absorption

Na<sup>+</sup> absorption is also possible in the absence of nutrients as first shown in the 1970s (9,10). This uptake is mediated by the Na-H exchangers NHE2 and NHE3 (11), both localized in apical membrane of intestinal epithelial cells (see discussion of NHE3 later). This transport, which couples Na<sup>+</sup> entry into enterocytes to proton secretion into the intestinal

lumen, is stimulated in the duodenum and jejunum by  $\text{HCO}_3^-$  rich secretion from the pancreas (figure 3). In other parts of the small intestine and colon, Na-H exchange is coupled to Cl- $\text{HCO}_3$  exchange, resulting in electroneutral NaCl absorption (figure 4).

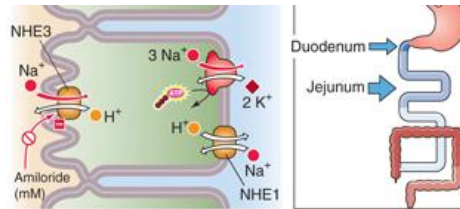


**Figure 3: Na-H exchange** (from Boron and Boulpaep, Medical Physiology, 2<sup>nd</sup> updated edition, 2012)

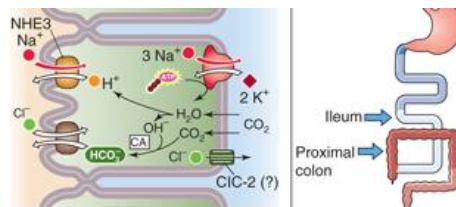


**Figure 4: Parallel Na-H and Cl- $\text{HCO}_3$  exchange** (from Boron and Boulpaep, Medical Physiology, 2<sup>nd</sup> updated edition, 2012)

### 1.2.3. Electrogenic $\text{Na}^+$ absorption

Electrogenic  $\text{Na}^+$  absorption is exclusively found in the distal part of the colon. In this process, epithelial sodium channels ENaC mediate the entry of  $\text{Na}^+$  from the apical side of colonic epithelial cells (figure 5). ENaC is a  $\text{Na}^+$ -selective ion channel responsible for transepithelial  $\text{Na}^+$  transport particularly in renal distal tubules, distal colon and lung (12,13). As in other tissues, electrogenic  $\text{Na}^+$  absorption is also regulated by the mineralocorticoid hormone aldosterone.

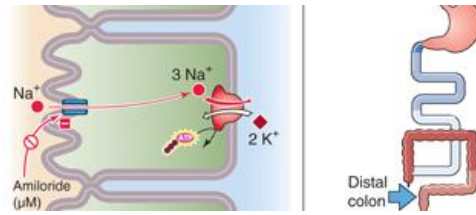


**Figure 5: electrogenic Na<sup>+</sup> absorption** (from Boron and Boulpaep, Medical Physiology, 2<sup>nd</sup> updated edition, 2012)

### 1.3. Cl<sup>-</sup> absorption

Cl<sup>-</sup> absorption either occurs in a passive manner driven by the negatively charged lumen generated by nutrient-coupled and electrogenic Na<sup>+</sup> absorption as seen in the jejunum and distal colon or via Cl<sup>-</sup>-HCO<sub>3</sub><sup>-</sup> exchangers working alone or in parallel with Na<sup>+</sup>-H exchangers (figure 6). Two Cl<sup>-</sup>-HCO<sub>3</sub><sup>-</sup> exchangers mediate most of Cl<sup>-</sup> absorption at the intestine brush border membrane: Slc26a3 and Slc26a6 (solute carrier family members 26a3 and 26a6 respectively). Slc26a3, first identified in the colon, is also known as DRA (down regulated in colonic adenomas) because of its low expression in such tumors (14). Slc26a6, also named PAT-1, was discovered via data mining (15). Both exchangers are widely expressed along the small intestine and colon (16-18), with a higher abundance in duodenum and colon for Slc26a3 and duodenum, jejunum and ileum for Slc26a6. They both play a significant role in Cl<sup>-</sup> absorption, mainly in duodenum and jejunum, as demonstrated by studies in knockout mice (16,19-21). In addition to its role in the proximal part of the small intestine, Slc26a3 also plays a role in the colon. The importance of this transporter is highlighted by the fact that recessive loss-of-function mutations in the SLC26A3 gene have been identified in children presenting a congenital chloride diarrhea (22). Although Slc26a3 and Slc26a6 have similar contributions in Cl<sup>-</sup> absorption (minor differences exist), Slc26a3 deficiency is more severe, probably because of its role in distal colon.

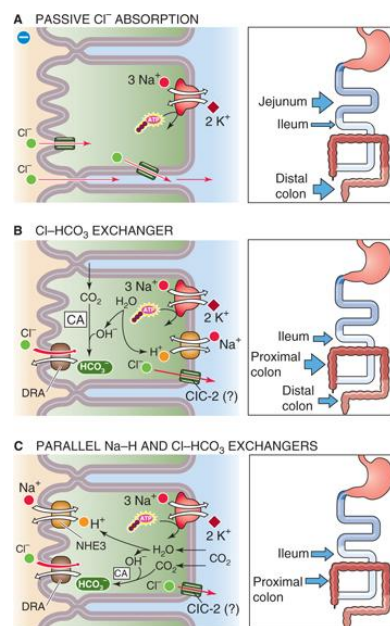


**Figure 6: Cl<sup>-</sup> absorption** (from Boron and Boulpaep, Medical Physiology, 2<sup>nd</sup> updated edition, 2012). Although not shown in this figure, Cl-HCO<sub>3</sub> exchange also occurs in duodenum and jejunum (1).

#### 1.4. Cl<sup>-</sup> secretion

For a long time, intestinal tissues have been considered to exclusively perform an absorptive task. Studies done during cholera outbreaks during the 1950-1960s have changed this concept (23-25), showing notably that supernatant of *Vibrio cholerae* culture instilled into rabbit ileum provokes a strong secretion of fluid. Experiments done in Ussing chambers clarified the pathophysiological mechanism of secretory diarrhea due to *Vibrio cholerae* and thus, with further molecular studies, provided a more comprehensive model of fluid secretion by intestinal epithelia (26-28). This model involves a chloride channel localized at the apical cell surface that allows secretion of Cl<sup>-</sup> ions into the intestinal lumen, basolateral membrane K<sup>+</sup> channels that repolarize the cell and a basolateral membrane NaK<sub>2</sub>Cl transporter that mediates Cl<sup>-</sup> entry into the enterocytes (figure 7). CFTR (for cystic fibrosis transmembrane conductance regulator) is the apical Cl<sup>-</sup> channel mentioned above. This channel first cloned in 1989 (29) is well known for its role in the genetic disease cystic fibrosis, which is characterized by meconium ileus and constipation, recurrent pulmonary infections with



progressive parenchymal destruction, pancreatic insufficiency and liver failure; disorders that are all consequences of abnormal  $\text{Cl}^-$  transport in the intestine, lung, pancreas and liver respectively (30). By increasing adenylate cyclase activity and thus intracellular cAMP levels, cholera toxin not only stimulates CFTR-mediated  $\text{Cl}^-$  secretion but also inhibits Na-H exchangers-mediated  $\text{Na}^+$  absorption (26,27,31,32). Regulation of  $\text{Na}^+$  and  $\text{Cl}^-$  transport is further discussed in the next chapter.

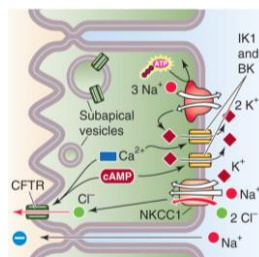


**Figure 7:  $\text{Cl}^-$  secretion** (from Boron and Boulpaep, Medical Physiology, 2<sup>nd</sup> updated edition, 2012).

### 1.5. Regulation of intestinal $\text{Na}^+$ and $\text{Cl}^-$ transport

This chapter sums up various aspects of the regulation of intestinal  $\text{Na}^+$  and  $\text{Cl}^-$  transport. In intestinal epithelial cells, intracellular levels of  $\text{Ca}^{2+}$ , cAMP and cGMP, and gluco- and mineralocorticoids all modulate ion transport either by changing the number of transporters at the cell surface and/or by modifying their intrinsic activity. In particular, increased  $\text{Ca}^{2+}$ , cAMP and cGMP intracellular levels leads to both a stimulation of  $\text{Cl}^-$  secretion and an inhibition of electroneutral  $\text{NaCl}$  absorption (26,31,33-35). The main targets of these modulating pathways are CFTR and NHE3 respectively (3,36). How  $\text{Cl}^-$ - $\text{HCO}_3^-$  exchangers are regulated is poorly known.

Based on immunohistochemical analyses, absorption is thought to mainly occur in the villous enterocytes, whereas secretion takes place in cryptic cells of the small intestine (37). This distinction is less clear in the colon, raising the possibility that some overlap does exist

and that a same cell might display(re-)absorptive and secretive capacity via molecular complexes involving NHE3, CFTR Slc26a3 and Slc26a6 (1).

The common cellular modulators of ion intestinal transport at the level of intestinal epithelial cells described above are all controlled by higher systems via an increasing list of active molecules (table 1): (1) the endocrine / paracrine system, (2) the neuroenteric system and (3) the immune system.

**Table 1**  
Local control of intestinal ion transport

Agonist	Source	Target cell(s)	Intracellular mediator(s)	Secondary mediator(s) of transporting epithelial cell effects
<b>Secretory/Antiabsorptive stimuli</b>				
VIP (S91)	Neural	Epith	cAMP	
ACh (S92, S93)	Neural	Epith, neural, mes	Ca <sup>2+</sup> , PKC	Eicos, ? VIP
SP (S94-S96)	Neural	Neural, mast, epith	Ca <sup>2+</sup> , PKC	Histamine, eicos
ATP/ADP (S97)	Neural	Mes, epith	Ca <sup>2+</sup> , PKC	Eicos
UTP/UDP (S97)	Neural	Mes, epith	cAMP	Eicos
5-HT (S98, S99)	EC, mast cell	Neural, epith	Ca <sup>2+</sup> , PKC	VIP and ACh
NT (S94, S100)	EC	Neural	Ca <sup>2+</sup> , PKC	Eicos, adeno, VIP, and ACh
Guanylin (39)	Goblet cells	Epith	cGMP	
PGs (13, S101)	Mes	Epith, neural	Ca <sup>2+</sup> , PKC; cAMP	
LTs, pre-LTs (S28, S102)	Mes	Epith, neural	Ca <sup>2+</sup> , PKC	
PAF (S22, S103)	Mes	Mes	Ca <sup>2+</sup> , PKC; cAMP	Eicos
Histamine (S104, S105)	Mast cell	Mes, neural	Ca <sup>2+</sup> , PKC; cAMP	Eicos, VIP, ACh
Bradykinin (S106)	Vascular	Mes	Ca <sup>2+</sup> , PKC; cAMP	Eicos
Adenosine (S107-S111)	Epith, lumen	Epith, mes	A1 R: Ca <sup>2+</sup> , PKC A2 R: cAMP	PGs (not LTs)
Endothelin-1 (S112)	Vascular	Mes	Ca <sup>2+</sup> , PKC; cAMP	PGs
<b>Antisecretory/Proabsorptive stimuli</b>				
Norepi (22, S32, S113)	Neural	Epith, neural	Activate G <sub>i</sub>	
NPY (S32, S114-S117)	Neural, EC	Epith, neural	?	? Norepi
SST (S26, S118, S119)	EC, neural	Epith, neural	Activate G <sub>i</sub> (SST R2)	
Enkeph (S120, S121)	Neural	Epith, neural	?	
12-HETE (S27)	Mes	Epith	Block BL K <sup>+</sup> channel	

Epith, epithelial; ACh, acetylcholine; mes, mesenchymal cell (fibroblast, neutrophil, eosinophil, lymphocyte, mast cell, etc.); SP, substance P; eicos, eicosanoids (prostaglandins, leukotrienes, and their precursors); 5-HT, 5-hydroxy-tryptamine (serotonin); EC, enterochromaffin or epithelial endocrine cell; NT, neurotensin; adeno, adenosine; PG, prostaglandin; LT, leukotriene; PAF, platelet-activating factor; R, receptor; norepi, norepinephrine; G<sub>i</sub>, inhibitory G protein; NPY, neuropeptide Y; SST, somatostatin; enkeph, enkephalins (opioids); 12-HETE, 12-hydroxyeicosatetraenoic acid; BL, basolateral. Numbers in parentheses indicate references.

**Table 1: Intestinal active molecules.** Taken from (2).

### 1.5.1 The endocrine / paracrine system

The adrenal glands can release the mineralocorticoid hormone aldosterone in response to dehydration and volume contraction and the glucocorticoid hormone cortisol in response to stress. In distal colon, aldosterone binds its receptor and stimulates electrogenic Na<sup>+</sup>

absorption (3). Cortisol increases NHE3-mediated electroneutral  $\text{Na}^+$  absorption (38) but also activates SGLT1 and thus glucose-coupled  $\text{Na}^+$  absorption (39).

Numerous endocrine cells, called enterochromaffin cells (EC cells), are found all along the gastrointestinal tract. They produce molecules that modulate ion transport via a paracrine effect. As an example, they secrete guanylin and uroguanylin in the intestinal lumen in response to salt intake. These short peptides bind an apical receptor for guanylate cyclase (GC-C) in epithelial cells; this increases cGMP levels leading through stimulation of  $\text{Cl}^-$  secretion through CFTR (40-42). Interestingly, the heat-stable toxin of E.Coli that causes travellers' diarrhea acts through the same mechanism (figure 8). Recently, one gain of function mutation and two loss of function mutations in the GC-C gene have been reported in patients with chronic diarrhea and meconium ileus respectively (43,44) (see later). The GC-C receptor may also have other intestinal functions such as modulation of the intestinal barrier and inflammation, and regulation of epithelial cell proliferation and apoptosis (45,46). Interestingly, extra-intestinal roles for this receptor have been proposed in renal electrolytes handling, satiety and metabolic syndrome, and attention deficiency and hyperactive behaviour (47-49).

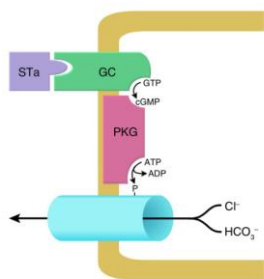


**Figure 8: Mechanism of action of heat-stable E.Coli enterotoxin (STa).** STa binds the GC-C receptor increasing cGMP levels and activating  $\text{Cl}^-$  channels such as CFTR. Taken from (2)

### *1.5.2 The neuroenteric system*

The gastrointestinal tract possesses a complex intrinsic nervous system called enteric nervous system (ENS). ENS is composed of two plexi, the myenteric plexus and the submucosal plexus. In particular, it has nerves that release factors with ion transport modulating activity on epithelial cells. Examples of such modulators include acetylcholine and vasoactive intestinal peptide (VIP), which inhibit electroneutral NaCl absorption and stimulate Cl<sup>-</sup> secretion, via the muscarinic M3 receptors (Ca<sup>2+</sup> as a second messenger) and the VIP receptors (via cAMP) respectively (50).

### *1.5.3. The immune system*

The immune system is able to release active molecules that regulate ion transport in epithelial cells. For instance, mast cells secrete histamine, which has secretory and anti-absorptive effects on epithelial cells probably indirectly through cholinergic enteric nerves (51). Cytokines secreted by T cells such as tumor necrosis factor  $\alpha$  (TNF $\alpha$ ) and interferon  $\gamma$  (INF $\gamma$ ) may also inhibit electroneutral NaCl absorption and increase Cl<sup>-</sup> secretion (52,53).

## **2. DIARRHEA**

Diarrhea is a very frequent disease around the world. According to the World Health Organization ([www.who.int](http://www.who.int)), 1.5 million children die every year because of diarrhea and about 2 billion of diarrheal diseases are diagnosed every year. Fortunately, most cases are self-limited and can be treated by conservative means, namely rehydration. However, in some cases, diarrhea may be intractable and may persist for a long time.

From the patient's point of view, diarrhea may be defined by the excretion of loose stools to watery stools, by an increase in stool mass and/or by an increase in stool frequency. More strictly, diarrhea is defined as a stool mass higher than 200-250 g/day, even though the passage of loose / watery stools more than three times a day is used in clinical practice.

Diarrhea occurs when the absorptive capacity of the small intestine and colon, although normally very efficient (up to 15 liters/day of fluid and 5 liters/day respectively), is overwhelmed or when intestinal motility is altered. Acute diarrhea lasts several days, whereas chronic diarrhea persists for weeks, months or years. Depending on the causal mechanism, diarrheal diseases can be classified into 5 groups (Robbins Basic Pathology, 7<sup>th</sup> edition, Kumar, Cotran and Robbins, 2005):

- 1) Secretory diarrhea: Intestinal fluid secretion exceeds absorption even during fasting. For instance, infection of the intestinal epithelial cells by viruses or bacteria can provoke a secretory diarrhea because of damages within the epithelium or of production of toxins by the microorganisms that activate fluid secretion or block fluid absorption (e.g Cholera toxin or E.coli toxin).
- 2) Osmotic diarrhea: Unabsorbed molecules exert osmotic forces driving fluid movement towards the intestinal lumen. This happens for example when taking lactulose to treat hepatic encephalopathy, Mg<sup>2+</sup> containing antacids or purgative agents.
- 3) Exudative diarrhea: Several bacteria or parasites such as Salmonella may cause extensive destruction of the mucosa resulting in purulent, bloody diarrhea. This also occurs with inflammatory bowel diseases (Crohn's disease and ulcerative colitis).
- 4) Malabsorption: Diarrhea occurs because of the presence of unabsorbed nutrients and fat in the intestinal lumen, e.g. due to a lack of digestive enzymes (pancreatic

insufficiency or genetic enzymatic defects), defective bile secretion, reduced intestinal surface area, lymphatic obstruction...

- 5) Altered motility: Increased motility as seen in hyperthyroidism for example may reduce the intestinal retention time necessary for absorptive processes.

Of course, multiple mechanisms may be present within the same individual. Thus, diarrheas are also grouped depending on the etiology of the diarrhea; e.g. infectious diarrhea, endocrine diarrhea, inflammatory diarrhea, neoplasia-induced diarrhea, drug-induced diarrhea...

### **3. CONGENITAL DIARRHEAL DISORDERS AND FAMILIAL DIARRHEA SYNDROMES**

#### **3.1. General considerations**

Congenital diarrheal disorders and familial diarrhea syndromes form a heterogeneous group of diarrheas sharing one common feature; they are all due to a known or putative gene defect (54,55). Although very rare, these pathologies are particularly interesting because they point out genes playing important roles in the gastrointestinal tract and thus provide in turn the possibility to better understand intestinal physiology and the pathophysiological mechanisms of more frequent intestinal diseases. In addition, studying such diseases may allow the identification of new pharmacological targets leading to the design of new drugs.

Clinical presentation can vary from a very severe and intractable diarrhea starting out immediately after birth (sometimes with prenatal onset), threatening life because of massive dehydration, alterations in pH, various metabolic disorders and failure to thrive, to milder

diarrhea appearing only later in life. The management of the disease depends on the genetic etiology; intravenous fluid replacement might be the only treatment in most cases, whereas some diarrheas can be treated by theoretically “simple” but practically complicated means such as removal of lactose from the diet in the case of congenital lactase deficiency (56) or pancreatic enzyme replacement for enterokinase deficiency (57). Interestingly, some spontaneous improvement, as children grow, has been reported for example in enterokinase deficiency suggesting that compensatory mechanisms may appear later in life or that some gene is important only during infancy and its function becomes no longer necessary during childhood or adult state (58).

Berni Canani et al have recently proposed to classify congenital diarrheal disorders into 4 categories (see also figure 9) (54):

1) Disorders with defects of digestion, absorption, and transport of nutrients and electrolytes. This category is further subdivided in:

- disaccharidase deficiencies: e.g. congenital lactase deficiency (59)
- ion and nutrient transport defects: e.g. congenital sodium diarrhea (60,61)
- pancreatic insufficiencies: e.g. enterokinase deficiency (58)
- lipid trafficking defects: e.g. chylomicron retention disease (62,63)

2) disorders with defects of enterocyte differentiation and polarization: e.g microvillous inclusion disease (63)

3) disorders with defects of enteroendocrine cells differentiation: e.g. enteric anendocrinosis (64)

4) disorders with defects of modulation of intestinal immune response: e.g. IPEX = immune dysregulation polyendocrinopathy (65).

Multiple congenital diarrheal disorders and familial diarrhea syndromes have been described and the list of such diseases is increasing rapidly, due to recent progress made in

molecular genetic tools. Therefore, it is not possible to review all of them. In the next chapter, the congenital sodium diarrhea, which is the main topic of this work, will be considered in details. Because of their close connection to this disease and/or to NaCl transport in the gut, the congenital chloride diarrhea, the glucose-galactose malabsorption and a recent familial diarrheal syndrome related to mutations in the GUCY2C gene will also be discussed.

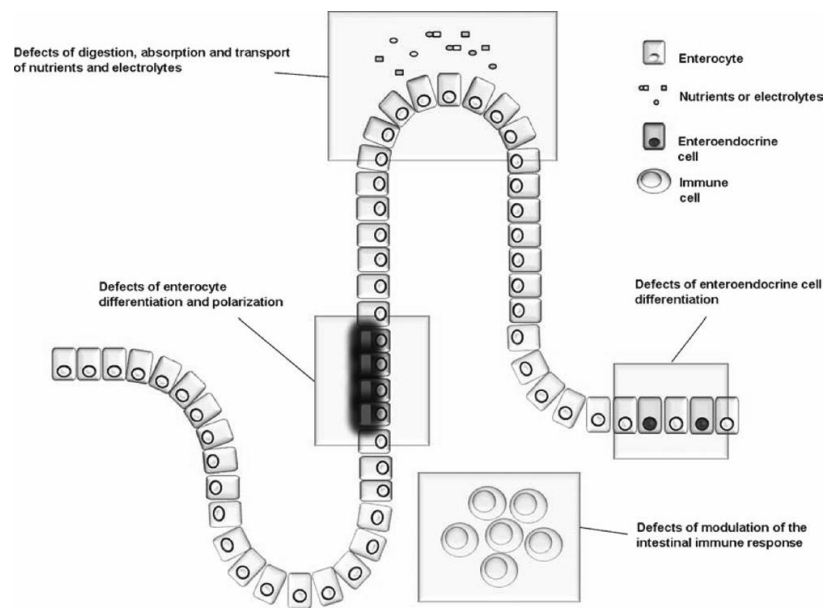


**Figure 9: Mechanisms involved in the pathogenesis of congenital diarrheas.** From (54)

### 3.2. Congenital chloride diarrhea

This rare secretory diarrhea was first reported in 1945 (66,67). The disease is characterized by a chronic, very profuse diarrhea with a specific faecal loss of chloride (>90mmol/l) resulting in severe dehydration, hypochloremic and hypokaliemic metabolic alkalosis that may threaten life unless treated with intravenous rehydration and salt substitution. Poorly treated patients may present impaired renal function and nephrocalcinosis (68). Other problems related to this diarrhea include intestinal inflammation, hyperuricemia, inguinal hernias, spermatoceles, and male subfertility (69,70). Mutations in the Slc26A3 gene



have first been identified in Finnish patients in 1996 (22). This gene, also known as DRA (for Down-Regulated in Adenoma), encodes a chloride-bicarbonate exchanger that play an important role in NaCl (re)absorption throughout the gut but mainly in ileum and large intestine (71). More than 50 different mutations of this gene have been reported so far, all predicting to lead to a loss of function of the exchanger (72). Slc26A3 deficient mice display a phenotype similar to the congenital chloride diarrhea, with high chloride content diarrhea, body weight loss, dehydration and hypochloremia (16).

### **3.3. Glucose-galactose malabsorption**

Glucose-galactose malabsorption was first reported in 1963 (73). This disease is characterized by a severe watery diarrhea in newborns. Removal of lactose, glucose and galactose from the diet results in a complete cessation of all symptoms, whereas diarrhea resumes upon reintroduction of those sugar molecules in the diet. Turk et al identified in a family with members affected by the glucose-galactose malabsorption one loss of function mutation in the SGLT1 gene, which had been cloned two years before (74-76). SGLT1 encodes a Na/Glucose co-transporter that is responsible for glucose-coupled Na<sup>+</sup> transport in intestinal and renal tissues (7).

### **3.4. Familial diarrhea syndrome and mutation of GUCY2C**

A group of Norwegian physicians has recently identified one family with 32 adult members suffering from a familial diarrhea syndrome (43). In opposite to congenital diarrheal disorders that are usually transmitted as autosomal recessive traits and are characterized by very severe diarrhea affecting infants, the transmission of this syndrome was autosomal dominant. Affected members of this family presented a mild chronic diarrhea associated with diverse intestinal problems such as irritable bowel syndrome, Crohn's disease, episodes of

bowel obstruction and esophagitis. One common gain of function mutation in the GUCY2C gene was detected in those patients. The GUCY2C gene encodes a transmembrane guanylate cyclase receptor expressed in epithelial intestinal cells (46). The heat stable toxin of E.Coli STa is a super agonist of this receptor and leads to secretory diarrhea by activating fluid secretion and inhibiting fluid absorption via an increase in cGMP levels. Endogenous ligands of this receptor include guanylin and uroguanylin that are secreted by epithelial intestinal cells into the lumen but also into the blood (45). Interestingly, recessive loss of function mutations of GUCY2C associated with meconium ileus have also been recently identified in 2 Bedouin families living in the desert (44). Therapeutic drug that targets this receptor are developed or are currently being tested in clinical trials for their efficacy to treat constipation or diarrhea (77,78).

## **4. THE CONGENITAL SODIUM DIARRHEA**

### **4.1. Description and pathophysiology**

The congenital sodium diarrhea is a rare congenital secretory diarrhea first described in 1985 (79,80). Only few cases have been reported in the literature (60,81-85).The diarrhea is characterized by a prenatal onset of disease with polyhydramnios, followed immediately after birth by large amounts of watery stools and faecal loss of sodium and  $\text{HCO}_3^-$ . Newborns suffer from hyponatremic dehydration with hypotension, secondary hyperaldosteronism and metabolic acidosis.

The management consists in parenteral nutrition, but patients die in the first year of life because of recurrent catheter-related infections or of liver failure due to parenteral nutrition. Anatomic defects or abnormalities are excluded by radiological examinations and no

anatomical or histopathological changes are observed except for some mild villous atrophy with slight crypt hyperplasia that are probably due to long term parenteral nutrition. Electron microscopy shows in villous cells lipid-negative vacuoles and membranous whorls in clear vacuoles, mitochondria and lysosomes (figure 10). Müller et al proposed that these changes may represent apical membrane breakdown products caused by instability and/or disordered configuration of a sodium/proton exchanger protein (60). Infectious and auto-immune origins for this diarrhea are excluded. Endocrine causes are also ruled out because of normal plasmatic levels of thyroid hormones, thyroid-stimulating hormone, vasoactive intestinal peptide, calcitonin, gastrin, and prostaglandin E2.

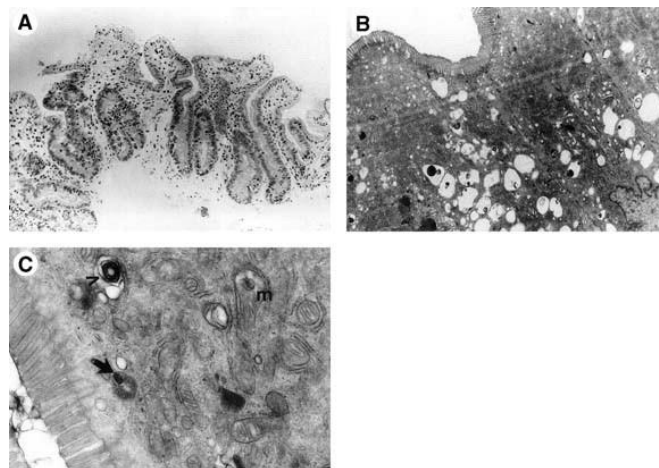


**Figure 10: Morphology of jejunal mucosa of a patient with the congenital sodium diarrhea.** (A) Light microscopy image of sections of jejunal mucosa showing abnormal crypt hyperplastic and villous atrophy, in which villus height equals crypt depth. (B) Transmission electron microscopic image of villous columnar epithelium showing marked vacuolation with slightly mounded apical membranes. (C) Transmission electron microscopic image of a villus tip epithelial cell from jejunal mucosa showing distinct membranous whorls within clear vacuoles (arrowhead), lysosomal bodies (arrow), and swollen mitochondria (m). From (60).

Affected children may also display dysmorphic features such as choanal atresia, anal atresia, corneal erosions and hypertelorism (figure 11). These changes associated with the sodium diarrhea constitute a syndromic form of the congenital sodium diarrhea. (61)



**Figure 11: Facial characteristics of patients with the congenital sodium diarrhea.** Note hypertelorism, long philtrum, sparse hair, and photophobia. From (61)

Jejunal perfusion studies in one patient and  $\text{Na}^+$ -transport analysis in brush border membrane vesicles of jejunal biopsies from two patients affected by the congenital sodium diarrhea showed a huge decrease in proton-gradient-dependent  $\text{Na}^+$  uptake, whereas  $\text{Na}^+$ -stimulated glucose uptake was normal, suggesting an important defect in Na-H-exchange in intestinal tissues (80,81).

#### 4.2. Mutations in the Spint2 gene

In 2000, Müller et al reported a family of consanguineous descent in Austria with 5 children affected by the congenital sodium diarrhea (figure 12) and concluded that the disease was not related to mutations in the genes encoding Na-H-exchangers known to be expressed in the gut, namely NHE1, NHE2 and NHE3 (60). More recently, this same laboratory has identified one common mutation in the Spint2 gene in the patients of this Austrian family (61). They also report 4 other mutations in several other families with members having the congenital sodium diarrhea.

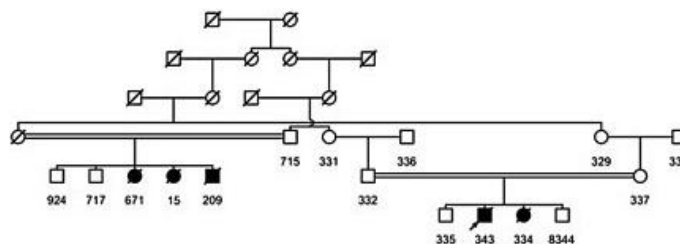


**Figure 12: Pedigree of the congenital sodium diarrhea family.** from (61)

Spint2 mutations associated with the congenital sodium diarrhea were detected in a splice acceptor site (c.593.1G>A) and in splice donor sites (c.337+2T>C, c.553+2T>A), which probably provoke an aberrant splicing and the loss of normal gene expression. Another mutation was identified in a highly conserved region of the protein (Y163C), which might hinder the correct folding of the protein or decrease the activity of the reactive site (figure 13). A fifth mutation involves the start codon and probably abolishes the expression of Spint2. Although not clearly demonstrated, these mutations are expected to result in a loss of function of Spint2.

**A**

163

SPINT2 (D2)	YEEYCTANAVTGPCRASFPWWYFDVERNSCNNFIYGGCRGNKNSYRSEACMLRC
SPINT2 (D1)	IHDFCLVSKVVGRCRASMPRWYVNTDGSQCFLVYGGCDGNSNNYLTKEECLKKC
APLP2	VKAVCSQEAMTGPCRAVMPRWYFDLSKGGKCVRFIYGGCGGNRNNFESDYCMAVC
APP	VREVCSEQAETGPCRAMISRWYFDVTEGKCAPFFYGGCGGNRNNDTEEYCMAVC
TFPI-2 (D1)	NAEICLLPLDYGPCRALLLRYRYRYTQSCRQFLYGGCEGNANNFYTWEACDDAC
TFPI-2 (D2)	IPSFCTSPKDEGLCSANVTRYFNPRYRTCDAFYGGCGGNDNFVSRREDCKRAC
TFPI-1 (D3)	GPSWCLTPADRGLCRANENRFYFNSVIGKCRPFKYGGCGGNENNFYSKQECLEAC
TFPI-1 (D1)	MHSFCAFKADDGPKAIMKRFFFNIFTRQCEEFIYGGCEGNQRFESLEECKRMC
TFPI-1 (D2)	KPDFCFLEEDPGICRGYITRYFYNNQTRQCEERFYGGCLGNMNFETLEECKNIC
HAI-1 (D1)	TEDYCLASNKVGRCRGSFPRWYDPTQICKSFVYGGCLGNKNNYLRBEECI LAC
HAI-1 (D2)	DKGHCVDLPDTGLCKESIPRWYYPFSEHCFARFYGGCYGNKNNFEEBQQCLESC
Kunitz consensus	---C-----G-C-----C--F---GC-----C--C

**B**

163

H. sapiens	DMFNYYEYCTANAVTGPCRASFPWWYFDVERNSCNNFIYGGCRGNKNSYRSEACM
P. troglodytes	DMFNYYEYCAAKAVTGPCRASFPWWYFDVERNSCNNFIYGGCRGNKNSYRSEACM
M. mulatta	DMFNYYEYCAAKAVTGPCRASFPWWYFDVERNSCNNFIYGGCRGNKNSYRSEACM
C. familiaris	DIFDYEEYCTAKAVTGPCRASFPWWYDVEKNSCDSFIYGGCRGNKNSYLSKEECM
B. taurus	DIFSYYEHCIAKAVTGPCRAAFPRWYFNAEENSNDNFIYGGCRGNKNNYRSEECM
O. cuniculus	DGFSYYEYCTAKAVTGPCRAAFPRWYFNAEENSNDNFIYGGCRGNKNSYPSQEACM
L. africana	DVFNYYEYCTAKAVTGPCRAAFPRWYFNAEENSNDNFIYGGCRGNKNSYRSEECM
R. norvegicus	EIFNYYEYCVPAKAVTGPCRAAFPRWYDVEKNSSSFIYGGCRGNKNSYLSQEACM
M. musculus	EIFNYYEYCVPAKAVTGPCRAAFPRWYDVEKNSSSFIYGGCRGNKNSYLSQEACM
M. domestica	NDFNYEDYCAAKAVTGPCRAAFPRWYFNAEENTCARFIYGGCRGNKNSYLTQEDCM

**Figure 13: Conservation of the SPINT2 p.Y163C mutation.** (A) Alignment of multiple human Kunitz domains from different proteins. The mutated tyrosine is invariantly conserved within the highly conserved catalytic Kunitz domain.(B) Alignment of known and predicted SPINT2 orthologs shows high evolutionary conservation of this mutated tyrosine residue. From (61)

Interestingly, mutations of Spint2 were associated with the syndromic form of the congenital sodium diarrhea, given that all patients affected exhibited the dysmorphic features mentioned above. Patients that only suffer from the congenital sodium diarrhea alone do not have any mutations in the Spint2 gene. Mutations in the NHE8 gene encoding for a  $\text{Na}^+/\text{H}^+$  exchanger, which might be important in  $\text{Na}^+$  handling in the gut in early life, have

recently been ruled out in those patients (86). How mutations of Spint2 result in the congenital sodium diarrhea or a dysmorphic phenotype is completely unknown.

## 5. **SPINT2**

### 5.1. Definition

The spint2 gene encodes a serine protease inhibitor of Kunitz-type 2, also called HAI-2 for Hepatocyte Growth Factor Activator Inhibitor-2, placental bikunin or kop for Kunitz domain containing protein overexpressed in pancreatic cancer. Its cloning or protein isolation was reported in 1997 from three different origins: (1) pancreatic cancer tissues, (2) a cDNA placental library and (3) from the condition medium of the human stomach carcinoma cell line MKN45 (87-89).

Spint2 is a protein that is 252 amino acid long and weighs around 30-35 kD.

It has the following structure (figure 14):

- 1 signal peptide on the N-terminus (Signal peptides are found in proteins that are targeted to the endoplasmic reticulum and eventually destined to be either secreted/extracellular/periplasmic/etc., retained in the lumen of the endoplasmic reticulum, of the lysosome or of any other organelle along the secretory pathway or to be I single-pass membrane proteins. Source: [www.uniprot.org](http://www.uniprot.org))
- 2 Kunitz domains, which are 60 amino acid long domains, with a characteristic highly conserved spacing of six cysteine residues forming three disulfide bonds, responsible for the inhibition of trypsin-like serine proteases.
- one 24 amino acid long hydrophobic segment at the C-terminal end as a putative transmembrane domain .

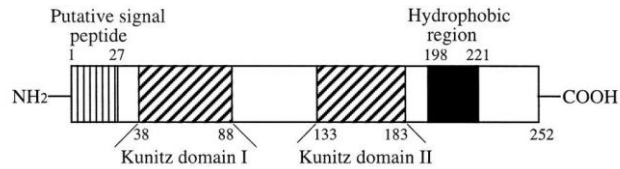


**Figure 14: Schematic structure of the Spint2 protein.** From (87,90)

## 5.2 Tissue distribution and expression of Spint2

Strong Spint2 mRNA expression is detected by Northern blot analyses in human placenta, kidney, pancreas, prostate, testis, thyroid and trachea with milder expression in thymus, ovary, small intestine, colon, lung and brain (87-89). In mouse, strong mRNA expression was seen in stomach, duodenum, jejunum, ileum, colon, liver, kidney, testis, ovary, and placenta, with weak expression in heart and esophagus, but no expression in brain (91).

Two isoforms have been described: a long isoform which consists in the full length inhibitor with its two Kunitz domains and a shorter isoform that lacks the N-terminal part Kunitz domain (91). At the mRNA level, the long isoform is the main isoform in human tissues whereas the small isoform is more predominant in mouse tissues. Recently, a mouse model with the LacZ gene inserted in the locus encoding Spint2 and thus driven by the promoter of Spint2 has been generated (92).  $\beta$ -galactosidase activity, supposed to reflect Spint2 protein expression, could then be shown in different epithelia including in kidney (mainly in the distal part of the renal tubules but also weakly in proximal tubules), gallbladder, sebaceous glands and hair follicles, trachea and bronchi/bronchioles, bladder, uterus, seminal glands and thymus. In the gut, activity was found in the small intestine and colon, both in cryptic and villous/surface cells (although villous expression was weaker) and also in goblet cells. Surprisingly, in pancreas,  $\beta$ -galactosidase activity was only detected in endocrine cells of islets of Langerhans but not in exocrine acinar cells. Finally, activity was

also seen in brain and ovary but not in liver, salivary glands, heart, skeletal muscle, spleen, vessels, mammary gland, oral cavity and esophagus. Globally, the tissue distribution of Spint2 is very similar to Spint1 and CAP3 expression (92).

The subcellular localization of Spint2 has been studied only in the Caco-2 cell line, which consists in epithelial cells of colonic carcinoma origin. In those cells, grown on filter as monolayers, endogenous Spint2 protein expression is thought to be mainly intracellular although it can be detected at the apical membrane (93).

### **5.3. Function of Spint2**

The function of Spint2 has been assessed only in cell-free in vitro assays using soluble recombinant proteins, so far. Spint2 has been to be a powerful inhibitor of several proteases including trypsin, plasmin, plasma kallikrein, pancreatic kallikrein, tissue kallikrein, HGFA (hepatocyte growth factor activator), chymotrypsin, factor XIa, but is a poor inhibitor of factors VIIa, IXa, Xa, XIIa (88,94). These proteases that are rather non-specific or involved in blood coagulation are likely not related to the congenital sodium diarrhea. Both domains present a similar inhibition capacity, although the first domain shows a small decrease capacity to block kallikrein and factor XIa. Qin et al generated mutants of Spint2 in which the P1 arginine residue of the reactive site of each Kunitz domain (see later) was mutated to a leucine residue (90). The mutation in the first Kunitz domain R48L significantly decreases the inhibitory activity of Spint2 on HGFA whereas the homologous mutation in the second Kunitz domain R143L was similar to the wild-type form of Spint2, suggesting that the first inhibitory domain of Spint2 is important for HGFA inhibition. These data were obtained using the human long isoform of Spint2 that has two Kunitz domains. Interestingly, the major mouse form of Spint2 that lacks the first Kunitz domain is also able to potently inhibit HGFA, as does a mouse construct with both Kunitz domains (95). Still in cell-free assays, Spint2 was



shown to be also a powerful inhibitor of the membrane bound-serine proteases Tmprss1 (also known as hepsin), CAP3 (also known as matriptase), CAP1 (also known as prostasin), Tmprss13 and matriptase-2 (92,96-99). Regarding the inhibition of CAP3, the first Kunitz domain of Spint2 seems to be more important than the second domain since the R48L mutant binds less efficiently to CAP3 than Spint2 wild-type and mutant R143L (93).

#### **5.4. Spint2 and cancers**

Spint2 may act as a tumor suppressor gene in medulloblastomas (100), gastric cancers (101), uterine leiomyosarcoma (102), prostate cancers (103), endometrial cancer (104), gliomas (105), hepatocellular carcinomas (106), renal cell carcinomas (107-109), breast cancers (110,111) cervical cancers (112) and ovarian cancers (113). In almost all these studies, low Spint2 expression was associated with poor clinical outcome. As a putative mechanism, it has been proposed that Spint2 might have, depending on the cancer cell line, anti-proliferative, pro-apoptotic, anti-migratory and anti-invasiveness properties presumably by regulating the HGF/met pathway via the inhibition of HGFA but also of CAP3 and Tmprss1 (114). The first inhibitory domain of Spint2 was shown to be more important than the second domain to mediate inhibition of migration and invasiveness of SMMC-7721 hepatocellular cancer cells (114). In contradiction to all studies mentioned above, one study showed that high Spint2 expression was associated with breast tumor aggressiveness (115). It is important to note that most of these studies report correlative findings and the role of Spint2 has been assessed only in vitro cancer cell lines via its overexpression. Furthermore, some studies are based on immunohistochemistry experiments done on tumor biopsies, although no good antibodies against Spint2 for such applications seem to be available (92). Experiments done in Spint2 KO or Spint2 transgenic mice are clearly required to confirm the role of Spint2 in carcinogenesis.

## 5.5. Spint2 in mouse models

Spint2 knockout mice show have a lethal phenotype in utero (116) due to early defects during the gastrulation stage, hypoplasia of the placental labyrinth with loss of epithelial polarity and reduction in vessels number, and non-closure of the neural tube as seen in figure 15 (117).

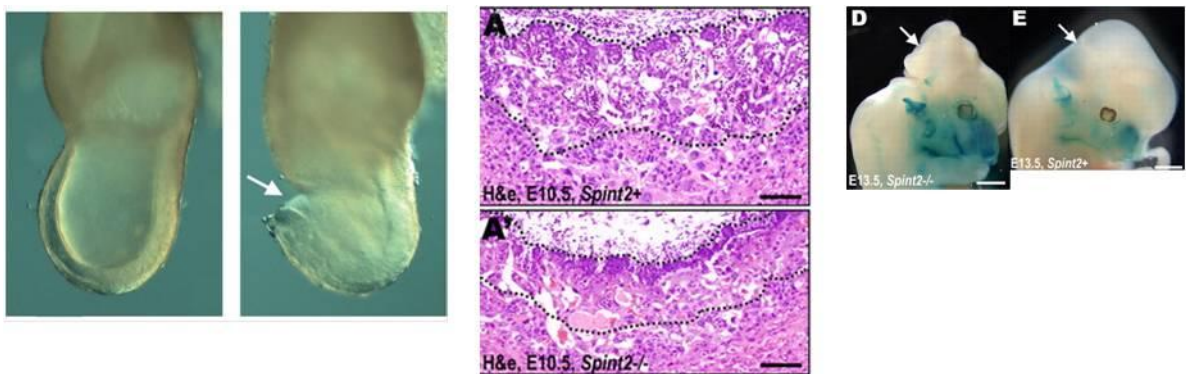


**Figure 15: Constitutive Spint2 KO mice display embryonic defects:** (left panel) abnormal clefting of the epiblast near the embryonic/extraembryonic junction (arrow) in KO embryo (right) compared to WT embryo (left), (middle panel) histological sections showing placental labyrinth hypoplasia (middle layer) in KO animals (lower image) compared to WT animals (upper image) and (right panel) defects of neural tube closure in KO embryos (left) compared to WT embryos (right). From (116,117)

This model can be rescued by disrupting the st14 gene encoding the membrane-bound serine protease CAP3, indicating that Spint2 controls crucial proteolytic pathways essential for embryonic development (117). Additional proteases are involved in such pathways since non-closure of the neural tube was still seen in  $Spint2^{-/-}$ ,  $st14^{-/-}$  double knockout mice, albeit at a lower frequency. Embryonic lethality of Spint2 knockout mice can also be avoided when the activity of the membrane-bound serine protease CAP1 is strongly decreased as seen in the Frizzy mice that have a point mutation in the CAP1 gene that reduces its function (118,119). Globally, these rescue experiments indicate that there is a genetic interaction between Spint2, CAP3 and CAP1 during development in utero. Whether the Spint2 protein directly interacts with CAP3 or CAP1 in cells remains unknown.

## **5.6. Putative roles of Spint2 in vivo**

A role of Spint2 in idiopathic pulmonary fibrosis has been proposed based on a work done in fibroblasts (120). Compared to fibroblasts from healthy donors, lung fibroblasts from patients with idiopathic pulmonary fibrosis display decreased HGFA expression and activity (HGFA has a protective effect in animal models of lung pulmonary fibrosis), which is associated with an increase in Spint2 expression.

A recombinant truncated form of Spint2, lacking the transmembrane domain, potentially decreases sodium transport when applied on primary cultures of human bronchial epithelial cells obtained from healthy subjects or from cystic fibrosis patients (121). This effect, also seen with serine protease inhibitor aprotinin but not with soybean trypsin inhibitor (SBTI) and alpha1-antitrypsin, can be reversed upon treatment with trypsin. Similarly, the same construct of Spint2 attenuated tracheal potential difference in vivo in trachea of guinea pigs (122,123).

It has been recently proposed that Spint2 could play a role in liver fibrosis occurring after cholangiopathies such as biliary atresia (124). This is based on the observation that Spint2 expression at the mRNA levels and at the protein level is increased in biliary atresia livers and in other cholangiopathies. This occurs in reactive cells of portal areas. Further experiments done on primary culture of fetal liver cells showed that several inflammatory molecules such as TNF- $\alpha$  and TGF- $\beta$  increase Spint2 expression and that Spint2 enhances fibrotic processes and affects hepatic differentiation possibly by inhibiting HGFA.

## 6. SPINT1/HAI-1

### 6.1. Definition

Spint1, better known under the name of HAI-1 for Hepatocyte Growth Factor Activator Inhibitor type 1 because of its isolation from a gastric cancer cell line based on its capacity to inhibit HGFA, is a homologous protein of Spint2 (125). HAI-1 has also two Kunitz domains that are responsible for serine protease inhibition and a putative transmembrane domain, but it is a longer protein (513 amino acids) than Spint2 and it has a LDL-receptor-like domain between both Kunitz domains (figure 16). The percentage of homology of the two Kunitz domain of Spint2 and HAI-1 is 54% and 36% respectively (87).

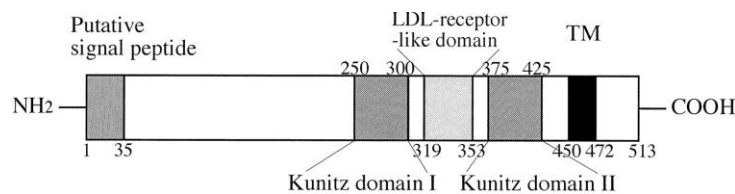


**Figure 16: Schematic structure of the HAI-1 protein.** TM=transmembrane domain. From (125).

### 6.2. Tissue distribution, expression and function of HAI-1

The tissue distribution of HAI-1 is very similar to Spint2 (92,125). At the subcellular level, HAI-1 is expressed predominantly on the basolateral membrane of epithelial cells and its expression is increased in injured or regenerative epithelia (126,127). In cell-free in vitro assay, HAI-1 inhibits HGFA and trypsin (125,128). The first kunitz domain of HAI-1 seems to be responsible for the inhibition of HGFA (128). Other proteases inhibited by HAI-1 include Tmprss1, CAP1, Tmprss13, HAT (97,99,129,130).

### 6.3. Interaction HAI-1-CAP3

HAI-1 also inhibits CAP3 in cell free assay and a complex CAP3-HAI-1 has been isolated in human milk, suggesting that HAI-1 is a physiologic inhibitor of CAP3 (131). Again, the first Kunitz domain of HAI-1 is likely responsible for this inhibition (132). In addition, several studies suggest that HAI-1 is necessary for the activation CAP3 (133-135) and it has been proposed that HAI-1 might transport CAP3 from the basolateral membrane to the apical membrane (136), where it might mediate the secretion of CAP3.

### 6.4. HAI-1 knockout mouse models

HAI-1 knockout mice display embryonic lethality due to failed placental development and function (137,138). As for *Spint2*, this model can be rescued by disrupting the *CAP3* gene (139). A highly hypomorphic mouse model of HAI-1 also avoid the embryonic lethality issue but these mice display strong growth retardation and die 16 days after birth (140). In particular, HAI-1 hypomorphic mice develop scaly skin with diminished barrier function due to altered filaggrin processing (figure 17).



**Figure 17: Scaly skin of hypomorphic HAI-1 mice.** From (112)

As for the placental failure, the postnatal mortality of HAI-1 mice can be totally rescued by knocking down the *CAP3* gene (141). Similar rescue can be obtained with a hypomorphic mutation in the *CAP1* gene (119). It is still unclear how HAI-1, *CAP1* and *CAP3* interact at the protein level. A putative cascade involving HAI-1, *CAP1* and *CAP3* has been proposed based on experiments performed in primary cultures of human keratinocytes or with Caco-2

cells. Here, CAP1 might be activated by CAP3, whose activity would be controlled by HAI-1 (142,143). In contrast to this model, Szabo et al suggested that in placental cells CAP1 activates CAP3 (119).

A HAI-1 gut-specific knockout mouse model has been generated using Cre-mediated recombination driven by the villin promoter (144). These mice are normal on gross examination but show in cryptic cells of their proximal colon mild alterations such as cryptic architecture modifications, increased apoptosis and enhanced permeability. They are also more sensitive to DSS-induced colitis.

As other putative roles of HAI-1, it has been shown that, in vivo, HAI-1 (but not Spint2) is increased in regenerative intestinal epithelium after chemical-induced colitis (145). Like Spint2, HAI-1 may act also as a suppressor tumor gene in many cancer cell types (146) and may also play a role in the pathogenesis of lung fibrosis (147).

## **7. PROTEASES AND THEIR INHIBITORS**

### **7.1 General considerations about proteases**

Unless otherwise specified, data of these chapters come from the following sources (148-154) and the textbook Biochemistry, Berg, Tymoczko and Stryer, 5th edition, 2002, W.H. Freeman.

Proteases are enzymes responsible for the catalytic breakdown of peptide bonds; a process called proteolysis. Their role in biological processes is very large. Proteases are involved in unspecific protein degradation, which is not only important at the level of the entire organism to obtain free amino acids from dietary proteins or peptides, but also at the cellular level to remove proteins that are no longer used and recycle amino acids for the synthesis of new proteins.

In addition to these effects, proteases have multiple other biological functions in which they only cleave their substrates at specific regions and in a tightly controlled manner; a process called limited proteolysis. Limited proteolysis is responsible for the activation or inactivation of enzymes, transcription factors, hormones and other proteins and peptides. For example, hormones and enzymes might be translated first in an inactive form called prohormones and proenzymes. Then, proteolytic removal of a short part of these immature molecules leads to their activation. This is the case for insulin or trypsin for instance that are synthesized as proinsulin or trypsinogen. Limited proteolysis may also occur in a cascade where one protease cleaves and activates another protease, which in turn cleaves and activates a third protease. This continues until the final effector is activated as seen in the coagulation cascade. Many important biological and physiological processes are regulated by limited proteolysis: cell proliferation and cell death, various signalling pathways, complement system, blood coagulation, fibrinolysis, immune system, tissue remodelling, wound healing, development ...

Because of this large diversity, proteases play an important role in diseases and are thus the targets of classical drugs such as inhibitors of the angiotensin-converting-enzyme used to treat hypertension and cardiovascular disease, inhibitors of coagulation factors for thrombosis or HIV protease inhibitors in the treatment of AIDS (149). Much effort is made towards the discovery of new therapeutics targeting proteases (155).

The human genome encodes 578 proteases ((156) / [www.sitedegradome.uniovi.es](http://www.sitedegradome.uniovi.es)), which are divided in subgroups according to their catalytic mechanism:

- aspartic proteases (21 members): e.g pepsin and renin.
- cysteine proteases (161): e.g. caspases
- metalloproteases (191): e.g matrix metalloprotease such as collagenases

- serine proteases (178): e.g. trypsin, chymotrypsin, membrane-bound serine proteases
- threonine proteases (27): e.g. proteasome subunits.

## **7.2. Mechanisms of proteolysis**

Substrate cleavage by chymotrypsin has been extensively studied and represents a good example of proteolysis by a serine protease. Cleavage of the peptide bond occurs in a small cleft of the rather spherical chymotrypsin called the active site. This active site contains three amino acids that are critical for proteolysis: serine at position 195, histidine at position 57 and aspartic acid at position 102. These amino acids form the so-called catalytic triad. Briefly, figure 18a shows that the histidine residue, with the help of the aspartate residue, deprotonates the hydroxyl group of the serine residue. The highly reactive serine makes a nucleophilic attack of the carbonyl carbon atom of the substrate and form with the latter a transient covalent bond to form the acyl-enzyme intermediate. Then hydrolysis occurs, releasing the cleaved substrate and regenerating the enzyme (figure 18a).

Cysteine proteases use a similar mechanism but here a cysteine residue is responsible for the nucleophilic attack of the peptide bond (no aspartic acid residue is involved in this reaction) (figure 18b). Aspartic proteases and metalloproteases use two aspartic acids residues and a metal ion (usually zinc) respectively in their active site to activate a molecule of water, which in turn performs the nucleophilic attack on the substrate (figure 18c and d).



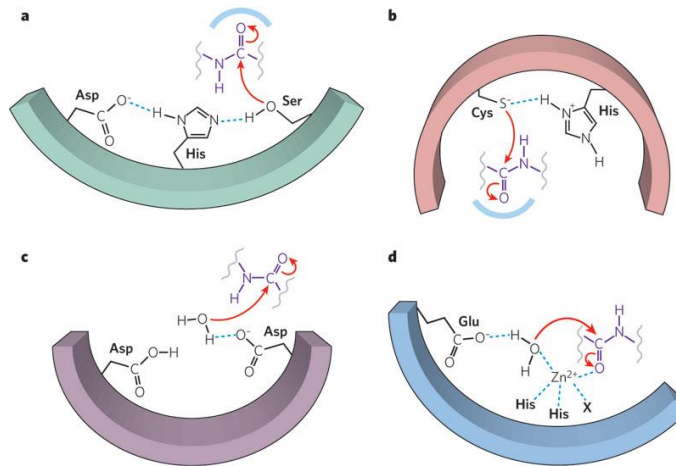


**Figure 18: Mechanisms of proteolytic activity of serine (a), cysteine (b), aspartic (c) and metalloproteases (d).** See text for explanations. From (157)

Chymotrypsin cleaves peptides bonds after amino acids residues such as tryptophan, tyrosine, phenylalanine (all are large hydrophobic residues), whereas trypsin cleaves after arginine or lysine. This specificity is related to the presence of a pocket, called S1 pocket, into which such residues can fit (figure 19). Further substrate specificity can be achieved by the presence, within the active site of the protease, of subsites that have to accommodate with side chain residues of the substrate located around the scissile bond. Such residues are labeled P1, P2, P3 and so forth or P'1, P'2, P'3 depending on their localization on the amino-terminal or carboxy-terminal side, respectively, of the scissile bond. Likewise, corresponding subsites in the protease are labeled S1, S2, S3 or S'1, S'2, S'3 (figure 20).

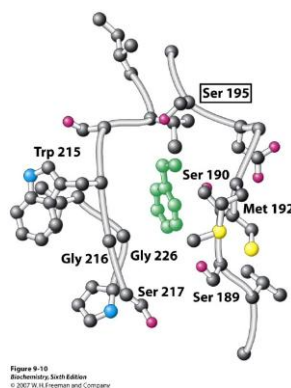


**Figure 19: S1 pocket of Chymotrypsin.** From Biochemistry, Berg, Tymoczko and Stryer, 5th edition, 2002, W.H. Freeman

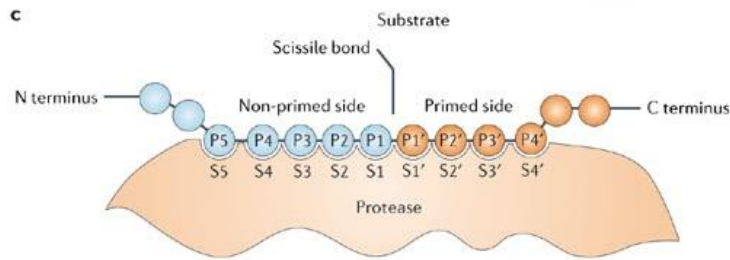


**Figure 20: Schematic representation of a protein substrate binding to a protease.** From (149)

### 7.3. General consideration about protease inhibitors

Excessive proteolytic activity might result in deleterious effects in tissues and cells. To avoid this problem, several mechanisms of defense exist. First, proteases are sometimes confined in very restricted and specialized area. For instance, cellular proteases involved in protein degradation are localized in lysosomes or proteasomes (158,159). Second, proteases are translated as inactive enzymes called zymogens. Zymogens are then converted in a controlled manner into active proteases by other proteases or sometimes via auto-activation (figure 21). A third line of defense consists in the inhibition of proteases by inhibitors (figure 21).

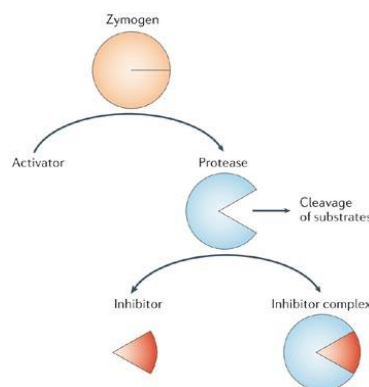


**Figure 21: Regulation of protease activity by inhibitors.** From (149)

Paradoxically, natural protease inhibition is performed only by proteins, except in some microorganisms, which can produce small non-peptidic compounds with the capacity to

inhibit proteases. The human genome is estimated to encode 156 protease inhibitors ((156) / [www.sitedegradome.uniovi.es](http://www.sitedegradome.uniovi.es)). This is clearly less than the numbers of genes encoding proteases (578, see above). One explanation for this difference would be that inhibitors are able to block multiple proteases. Alternatively, new inhibitors are to be found or already known proteins might have the capacity to inhibit proteolytic activity in addition to their initial function.

#### **7.4. Classifications of serine protease inhibitors**

Although it is clear that protease inhibitors avoid uncontrolled and thus excessive proteolysis, their physiological role in a more specific sense is poorly known. Indeed, most inhibitors were discovered and isolated based on their capacity to inhibit well-known proteases such as trypsin, chymotrypsin, elastase or subtilisin. The “true” physiological targets of most inhibitors remain to be found. Because of this lack, classification of protease inhibitors has been generating a lot of confusion in the field.

Laskowski and Kato were the first to propose a system to order protease inhibitors (148). Based on extensive homology, they introduced eight different families, whose name is the name of the most studied protease inhibitor of that family (e.g. *Streptomyces subtilisin* inhibitor family) or the name of the scientist who discovered it (e.g. Kunitz, Kazal or Bowman-Birk inhibitors). As an example, Kunitz inhibitors, first crystallized in 1945 by Moses Kunitz (160), are made of inhibitory domains of 58 amino acids that are highly stable (even to boiling) and show a conserved sequence and structure. In particular, the Kunitz consensus has 6 conserved cysteines that make three disulfide bonds in a specific manner (figure 22) with the P1 residue (scissile bond) close to the second cysteine (figure 23).

Today, around 78 families are listed in the Peptidase database MEROPS (161). These families are defined by homology in amino acid sequence. This database also groups protease

inhibitors into clans based on similarities in their tertiary structure. As mentioned in the database, « a clan of peptidase inhibitors contains all the modern-day inhibitors that have arisen from a single evolutionary origin of inhibitors ». One clan can include several families and one family may not belong to a clan. In spite of this broad diversity, common characteristics related to structure and function can be found, leading to a limited number of inhibition mechanisms.

HAI-2 (domain I)	34	IHDFCLVSKVVGR	CRASMPRWYNVTDGSCQLFVYGGCDGNSNNYLTKEECLKKCATVTEN	94
HAI-2 (domain II)	129	YEEYCTANAVTGPC	CRASFRWYFDVERNSCNNFIYGGCRGNKNSYRSEEAACMLRCFRQEN	189
HAI-1 (domain I)	246	TEDYCLASNKVGR	CRGSFPRWYDFTEQICKSFVYGGCLGNKNNVLRREEECILACRGVQGP	306
HAI-1 (domain II)	371	DKGHCVDLPDTGL	CKESI PRWYNNPFSEHCARFTYGGCYGNKNNFEEEQQCLESCRGISKK	431
APP	287	VREVCSEQAETGPC	RAMISRWYFDVTEGKCAPFFYGGCGGNRNNFDTEEYCMVAVCGSAIPT	347
APPH	306	VKAVCSQEAETGPC	RAVMPRWYFDLSKGRKCVRFIYGGCGGNRNNFSEEDYCMVAVCKAMIPP	366
I $\alpha$ TI (domain I)	227	KEDSCQLGYSAGP	CMGMTSRFYNGTSMACETFQYGGCMGNNGNPFVTEKECLQTCRT	283
I $\alpha$ TI (domain II)	284	VAAFCNLPIVRGP	CRAFIQLWAFDAVKGKCVLFPYGGCQGNNGNKFVSEKECKREYCGVPDGG	343
TFPI (domain I)	50	MHSFCAFKADDGP	CKAIMKRFFNIFTRQCEEFYGGCEGNQNRFSLEECCKKMCTRDNAN	108
TFPI (domain II)	121	KPDFCFLEEDPGI	CRGYITRYFYNNQTKQCEERFKYGGCLGNMNNFETLEECKNKICEDGPNG	179
TFPI (domain III)	213	GPSWCLTPADRGL	CRANENRFYNSVIGKCRPFKYGGCGGNENNFTSKQECCLRACKGFIQ	271
collagen $\alpha$ 3 chain	2874	ETDICKLPKDEGT	CRDFILKWYDPTKSCARFWYGGCGGNENKFGSQKECEKVCAPVLAK	2932
consensus		----	C-----G-C-----C--F--GC-----C--C-----	

Figure 22: **Alignment of the amino acid sequence of the Kunitz domains of Spint2 (=HAI-2)** with human homologous protein sequences (HAI-1, APP for Amyloid  $\beta$ A4 protein, APPH for Amyloid-like protein 2, I $\alpha$ TI for Inter- $\alpha$ -trypsin inhibitor, TFPI for Tissue factor pathway inhibitor). The consensus sequence is shown at the bottom with the 6 conserved cysteines. From (87)

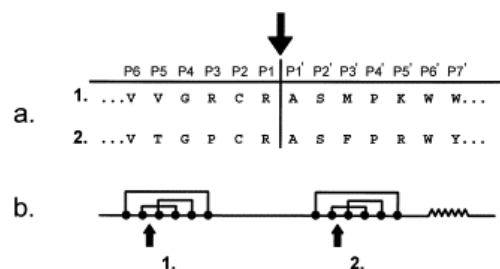


Figure 23: **Kunitz domains of Spint2:** (a) Amino-acid residues in the *Spint2* sequence surrounding the reactive sites (arrow) of the two Kunitz-domains (1, 2). (b) Scheme of the presumed topological structure of the disulfide bonds (solid circle, a half cystine residue; arrow, presumed reactive site). From (89).

## 7.5. Mechanisms of protease inhibition

### 7.5.1. General considerations

Proteases can be classified, based on the mechanism of proteolysis, into serine, cysteine, metallo-, aspartic and threonine proteases. Accordingly, protease inhibitors usually block specifically one of these classes of proteases. However, there are exceptions to this rule; for

instance, serpins (described later) can inhibit not only serine proteases but also cysteine proteases.

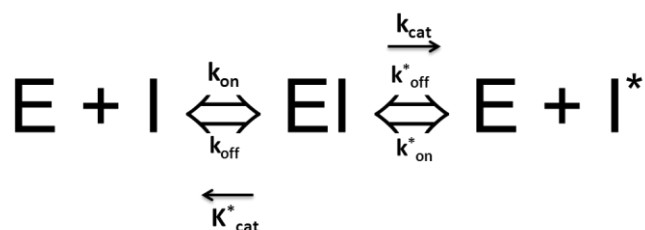
The region of the inhibitor that blocks protease activity is called the reactive site. From a general point of view, inhibition of the protease active site is achieved by the docking of the inhibitor reactive site, which can consist in defined structural elements such as a binding loop or an amino- or carboxy terminal ends of a protein (or both). This way, substrates can no longer have access to the active site of the protease.

Serine proteases inhibitors form the most studied family. Mechanistically, three different types of serine protease inhibitors can be distinguished that will be described in further detail in the next chapter:

- canonical inhibitors
- non-canonical inhibitors
- serpins.

#### *7.5.2. Canonical inhibition*

The canonical mechanism also called standard mechanism was first described by Laskowski and Kato (148). Most serine proteases inhibitors, including Kunitz-type inhibitors, use this mechanism. They interact with the target protease in a substrate-like and non-covalent manner. In fact, inhibitors serve as a substrate for the protease. Their reactive site should thus fit the active site and subsites of the protease. A nomenclature similar to real substrates (mentioned above) can be used to characterize the reactive site of inhibitors containing the peptide bond that can be cleaved by protease (e.g. scissile bond and subsites P1, P2, P3 / P'1, P'2, P'3) (see figure 23). However, in contrary to substrates, inhibitors form highly stable complexes with the proteases, and the scissile bond (between P1 and P'1) is cleaved very slowly. The reaction can be defined as follow:



where E is the enzyme (protease), I the inhibitor, EI the stable protease-inhibitor complex and I\* the modified inhibitor whose scissile bond has been cleaved.  $k_{\text{on}}$  and  $k_{\text{on}}^*$  are respective association rate constants and  $k_{\text{off}}$  and  $k_{\text{off}}^*$  are respective dissociation rate constants.  $k_{\text{cat}}$  and  $k_{\text{cat}}^*$  are the respective catalytic rate constants that indicate how much substrate (in mol) is converted into product per second per mole of enzyme. Several things are important to mention about this reaction:

- both the Michaelis-Menten constant  $K_m = (k_{\text{off}} + k_{\text{cat}}) / k_{\text{on}}$  and the catalytic rate constant  $k_{\text{cat}}$  are extremely low. In spite of this, the ratio  $k_{\text{cat}} / K_m$  is high indicating that I is a good substrate for E. In other words, the affinity of the inhibitor for the protease is very high but the efficiency of the protease to cleave the inhibitor is very low.
- the reaction is reversible. I\* can react with E and the cleaved peptide bond can be re-synthesized. I\* is very similar to I, except for minor modifications around the scissile bond. The ratio  $I / I^*$  is near unity, indicating that I and I\* form a complex with E with similar efficiency.

### 7.5.3. Structure of canonical inhibitors

Canonical inhibitors have a large variability in their global structure, which may comprise  $\beta$  sheets,  $\alpha$  helices or a mix of both, and usually contain disulfide bonds. This scaffold structure accounts for the multiple families described among serine protease

inhibitors such as Kunitz-type inhibitors, Kazal-type inhibitors or Bowman-Birk inhibitors. However, they share a common feature: the binding loop. This segment includes the scissile bond and interacts with the active site of the protease. In spite of the very diverse amino acid sequences, the binding loops of different inhibitors from different families display a strikingly similar canonical conformation characterized by a convex loop, complementary to the concave active site of the protease. Figure 24 shows the conserved binding loop despite the high variability of the scaffolding domain in several canonical inhibitors from different families. Figure 25 is a superimposition of the P3-P'3 segments of binding loops of OMSVP3 (ovomucoid inhibitor of Kazal-type), SSI (subtilisin inhibitor) and BPTI (bovine pancreatic trypsin inhibitor also known as aprotinin, Kunitz-type) inhibitors. The binding loop is a rather flexible segment in free inhibitors but become very rigid upon binding with the target protease. Minimal conformational changes take place upon formation of the enzyme-inhibitor complex; this is described as the classical lock and key interaction. The conformation of the binding loop is the results of disulfide bonds, hydrogen bonds and hydrophobic interactions occurring between residues both from the loop and the scaffold. For instance, inhibitors of Kunitz-type have 6 conserved cysteines forming disulfide bonds in a very specific manner. Interestingly, one study has shown that a mutant of BPTI with almost all residues in the binding loop mutated to alanines was still able to display a canonical binding loop, although less structured than the wild-type loop, and to interact with trypsin (162). This highlights the important role played by the inhibitor scaffold in the generation of the binding loop.

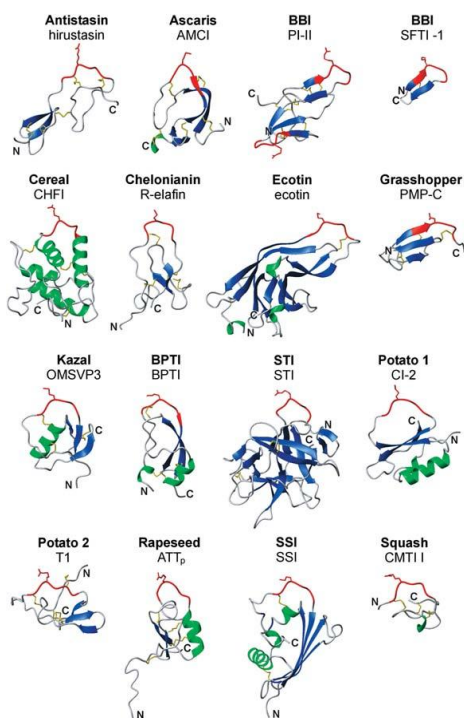


**Figure 24: Representative set of canonical inhibitor structures.** Binding loop and P1 side chain residue are marked in red, secondary-structure elements are colored in blue ( $\beta$  sheets) and green ( $\alpha$  helices), disulfide bonds are in yellow. Name of inhibitor family (in bold) and name of representative are indicated. From (151)

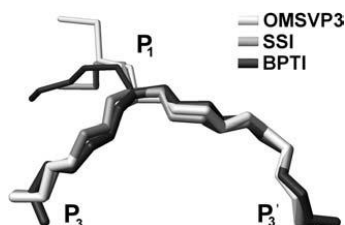


**Figure 25: Superimposition of main chain P3-P3 of binding loops of: OMSVP3, light gray; SSI, gray; BPTI, dark gray.** From (151)

The P1 residue of the binding loop is fully exposed in all inhibitors and interacts tightly with the S1 pocket of the protease. Its nature is therefore important for protease inhibition specificity. Arg and Lys residues confer specificity towards trypsin-like proteases, Tyr, Phe, Trp, Leu and Met residues towards chymotrypsin-like proteases and Ala and Ser towards elastase-like proteases respectively. Thus, mutating this P1 key residue does not necessarily abolish the inhibition activity but rather changes the substrate specificity. Since the subsites



(P2, P3, P'2, P'3 and so forth) are also important for proper function of the binding loop, P1 mutant inhibitors may still exhibit significant inhibition activity.

#### 7.5.4. Examples of canonical inhibition

##### I) Complex trypsin-CMTI1 inhibitor

Figure 26 shows, as an example of canonical inhibition, the interaction between trypsin and CMTI1 inhibitor (Potato I family). Trypsin is the larger protein seen in the upper part of the complex with its active site in the bottom bound to the small inhibitor CMTI (lower part of the complex). The canonical binding loop and the P1 side chain residue are depicted in red. The interaction is shown in further detail in figure 27. Here, P3 to P'3 residues of the binding loop interact with the active site of trypsin. In particular, P1-P3 residues (Arg5-Cys3) form an anti-parallel  $\beta$  sheet with residues 214-216 of the protease. In addition, the P1 residue (Arg5) is in close contact with the oxygen atom from the hydroxyl group of catalytic Ser195.

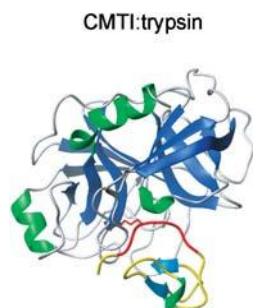


**Figure 26: Complex Trypsin-CMTI.** From (151)

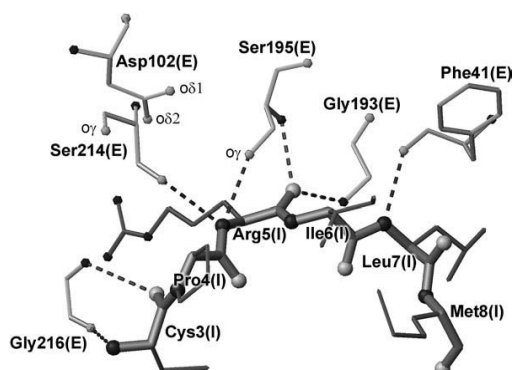


**Figure 27: Schematic representation of canonical inhibition based on the structure of the CMTI I-trypsin complex.** The inhibitor [dark gray, residues marked as (I)] binds to the protease [light gray, residues marked as (E)] in a manner similar to that of a typical substrate. Several characteristic interactions are shown: (i) antiparallel  $\beta$  sheet formed between residues P1-P3 of the inhibitor and residues 214–216 of the protease; (ii) sub-van der Waals contacts between Ser195 Og and P1 carbonyl carbon. From (151)

## II) Complex HGFA-Kunitz domain 1 of HAI-1

The complex formed by the serine protease Hepatocyte Growth Factor Activator HGFA and the first inhibitory domain of Kunitz-type of HAI-1 (Hepatocyte Growth Factor Activator Inhibitor-1), an inhibitor homologous to Spint2 is shown in figure 28 (163,164). In Fig.28A, the first Kunitz domain of HAI-1 is in purple with side chains in magenta, and the catalytic domain of HGFA is in beige with its active site in orange. This complex follows the rules of canonical inhibition. HAI-1 residues P1 R260, C259-C283 and R258 make contacts with subsites S1 (S195), S2 and S4 of HGFA in a substrate-like manner, forming an anti-parallel  $\beta$  sheet. In Fig28 B and C, all residues (in green) of HGFA (catalytic H57 and S195 are in yellow) that interact with residues of HAI-1 (side chains in blue) are shown. The P1 residue R260 of the first domain of HAI-1 (KD1) is highly exposed to allow deep insertion into the S1 pocket.

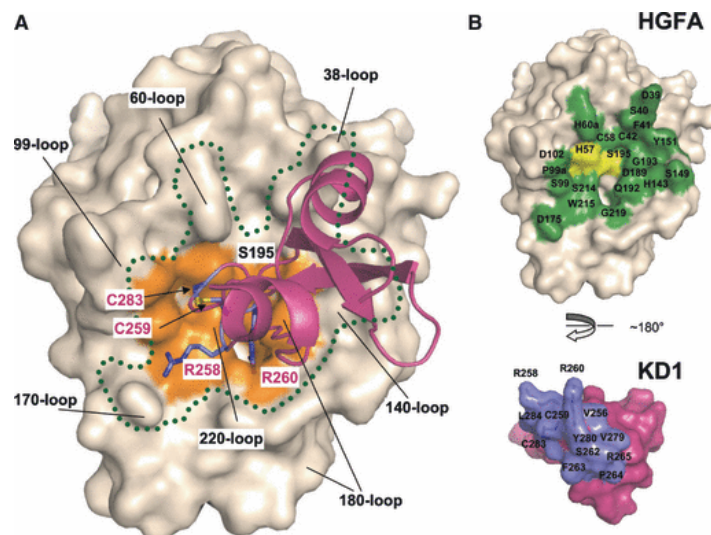


**Figure 28: Interaction of HGFA protease domain with HAI-1-derived Kunitz domain 1 (KD1).** (A) KD1 (magenta) interacts with HGFA (beige) in a substrate-like manner by occupying subsites S4, S2 and S1 (in orange) with Arg258, Cys259–Cys283, and Arg260 (P1 residue), respectively (side chains in blue). The binding region is delineated by the dotted line, and corresponds to the green surface in (B). (B) Open book representation of the HGFA–KD1 interaction. Residues on HGFA (green) and KD1 (blue) with an atom within 4.0Å of the

other protein (=binding region) are indicated. KD1 uses the protruding P1 Arg260 for insertion into the deep S1 pocket. The catalytic His57 and Ser195 are also within 4.0Å of KD1 and are in yellow. From (163).

### III) Complex CAP3-Aprotinin

A final example of canonical inhibition is represented in figure 29, which shows the interaction between the catalytic domain of the membrane-bound serine protease matriptase (in red), also known as CAP3, with the bovine pancreatic trypsin inhibitor aprotinin (BPTI, Kunitz-type) in blue. The classical contacts between P3-P1 residues of the binding loop (Pro13I and Ly15I) with the S1 pocket and subsites can be easily recognized. Moreover, this structure also shows a secondary binding segment (Gly36I-Arg39I). The presence of this additional binding segment indicates that protease-substrate or protease-inhibitor interactions involve more residues than those of the binding loop. This may add more specificity in such interactions.

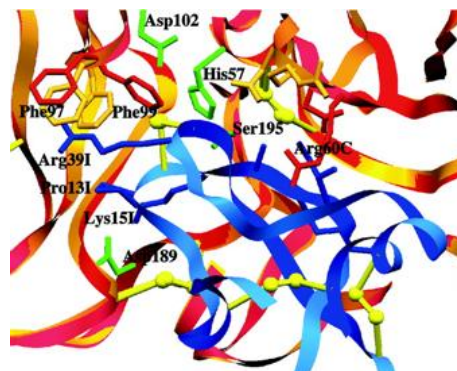


**Figure 29: Section of the complex formed between Aprotinin (blue color) and CAP3 (red-orange).** See text for description. From (165)

#### *7.5.5. Non-canonical inhibition*

Beside the canonical inhibition, some serine proteases can also be inhibited via a non-canonical mechanism. This is the case for selective thrombin inhibitors such as hirudin or ornithodorin. The anticoagulant properties of hirudin have been known for a long time. This 65 amino acid long peptide was isolated from salivary gland of medicinal leech and shown to be a powerful inhibitor of thrombin (166). The crystal structure of the thrombin-hirudin

complex solved in 1990 shows that the N-terminal part of hirudin is inserted into the narrow cleft of the active site of thrombin, partially blocking it by forming a parallel  $\beta$  sheet (167,168). In addition to this contact, hirudin makes a second contact via its long C-terminal tail with the exosite of thrombin usually recognized by fibrinogen (figure 30); this further hinders substrates to have access to the active site. Ornithodorin, isolated from a blood sucking soft tick, is a two-domain inhibitor. Although a canonical inhibition of thrombin would be anticipated since the structure of these two domains resemble to BPTI inhibitor (Kunitz-type), their binding loops are a bit distorted (169). Thus, they inhibit thrombin via a non-canonical mechanism similar to hirudin. The N-terminal domain binds the active site, while the C-terminal domain binds the fibrinogen recognition exosite.

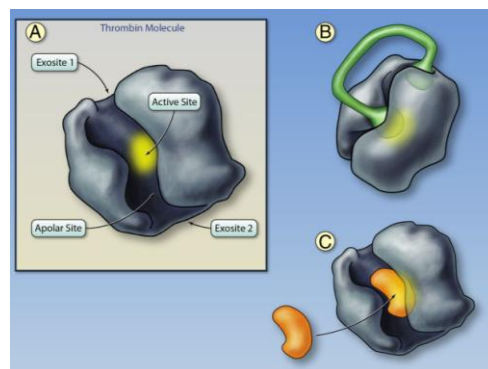


**Figure 30: Structure of thrombin and thrombin-inhibitor complexes.** **A**, The active site of the thrombin molecule is highlighted in yellow; the binding site is located at the base of the cleft. Adjacent to the binding site is the apolar binding site for fibrinogen. Exosites I and II are located on opposite sides of the thrombin molecule. Exosite I functions as a substrate docking site, enhancing the affinity of the interaction between thrombin and fibrinogen. Exosite II binds to heparin. **B**, Thrombin bound to the bivalent direct thrombin inhibitor hirudin. The C-terminus tail of hirudin binds to exosite I and the N-terminus partly obstructs the active site. After binding, bivalirudin is cleaved by the thrombin active site, which partly restores thrombin activity. **C**, Thrombin bound to a univalent, small-molecule direct thrombin inhibitor. Univalent direct thrombin inhibitors (argatroban, melagatran, dabigatran) fit into the cleft on thrombin and bind to both the active and apolar sites. From (166)

#### 7.5.6. Mechanism of inhibition used by serpins

Serpins stands for serine proteases inhibitors. They form a large family of inhibitors with more than 1500 members identified in various species (170). The name might lead to some confusion by implying that all serine protease inhibitors are serpins, which is not the

case. Serpins constitute a well-defined family among other families of serine protease inhibitors (e.g. canonical inhibitors). Moreover, serpins can also block other types of proteases such as cysteine proteases (171). Unlike other serine protease inhibitors, which are usually small proteins, serpins are large inhibitors of about 350-500 amino acids. Examples of serpins in human include antithrombinIII,  $\alpha$ 2-antiplasmin and  $\alpha$ 1-antitrypsin, which play important roles in the coagulation cascade, fibrinolysis and lung physiology respectively (172).

Their mechanism of inhibition is also different from the canonical inhibition (173). The process is irreversible as opposed to canonical inhibitors, which form thermodynamically stable but reversible complexes with their targets. The initial contact between serpin and enzyme is similar to canonical inhibitors based on a binding loop (called the reactive center loop RCL) inserted into the active site of the protease (figure 31). Then, the enzyme attacks the P1-P'1 peptide bond of the serpin to form an acyl-enzyme intermediate. At this point, unlike the very rigid canonical inhibitors, which exhibit little conformational changes, serpins fully incorporate the cleaved RCL into the core domain ( $\beta$  sheet A) and the covalently bound protease undergoes a pole-to-pole movement related to the inhibitor. In this complex, the inhibitor remains mostly intact. This is not the case for the protease, which is deformed over one third of its structure, including the catalytic site.

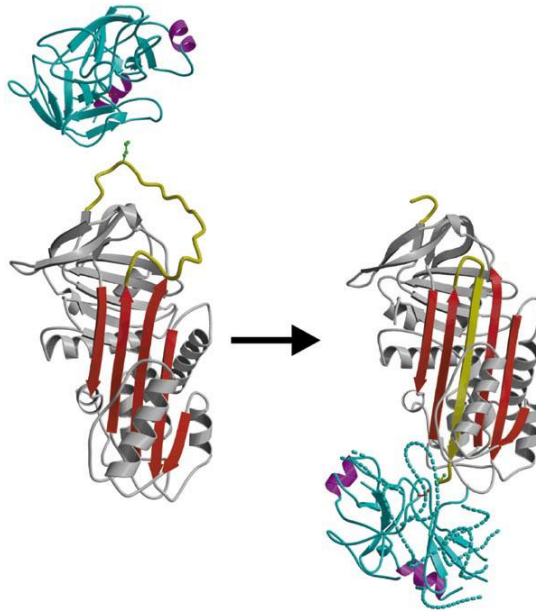


**Figure 31: Mechanism of trypsin inhibition by the serpin  $\alpha_1$ -antitrypsin.** Ribbon depictions of native  $\alpha_1$ -antitrypsin with trypsin aligned above it in the docking orientation (left), and of the complex showing the 71Å shift of the P1 methionine of  $\alpha_1$ -antitrypsin, with full insertion of the cleaved reactive-centre loop into the A-sheet (right). Regions of disordered structure in the complexed trypsin are shown as interrupted coils projected from the native structure of trypsin. Red,  $\alpha_1$ -antitrypsin  $\beta$ -sheet A; yellow, reactive-centre loop; green ball-and-stick, P1 Met; cyan, trypsin (with helices in magenta for orientation); red ball-and-stick, active serine 195. from (173)

## **8. MEMBRANE-BOUND SERINE PROTEASES AS POTENTIAL PARTNERS OF SPINT2**

### **8.1. General considerations**

Spint2 is an inhibitor of serine protease that contains a transmembrane domain. Putative partners of Spint2 could thus belong to a recently identified new subfamily of serine proteases composed of 20 members, called membrane-bound (or membrane-anchored) serine proteases (174). All these proteases share a similar catalytic domain of the S1 peptidase family (same as trypsin) and can have several accessory domains in the stem region (figure 32). They can be classified into two groups based on their membrane anchorage. Proteases have either a transmembrane domain in the C-terminus (as for tryptase- $\gamma$ 1) or are anchored to the

membrane via GPI-anchor (as for prostatic and testis). They are known as type-I transmembrane proteases. Alternatively, proteases have a transmembrane domain located on the N-terminus. They are called type-II transmembrane serine proteases. This group can be further phylogenetically divided into four smaller groups.

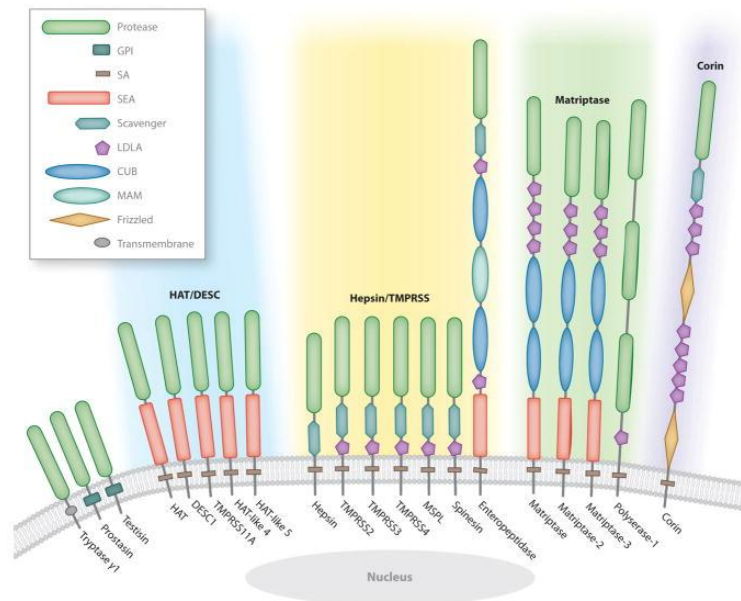


**Figure 32: The human complement of membrane-anchored serine proteases.** The single serine protease domain of tryptase  $\gamma$ 1, prostatic, and testis is attached to the membrane by a C-terminal type I transmembrane domain or glycosylphosphatidylinositol (GPI) anchor. Type II transmembrane serine proteases are attached to the membrane by a signal anchor (SA) located close to the N terminus. The stem region between the SA and the C-terminal serine protease domain contains an assortment of domains including low-density lipoprotein receptor class A (LDLA); sea urchin sperm protein, enteropeptidase, and agrin (SEA); C1s/Clr, urchin embryonic growth factor, and bone morphogenic protein-1 (CUB); meprin, A5 antigen, and receptor protein phosphatase  $\mu$  (MAM); frizzled; and group A scavenger receptor. From (174)

## 8.2. Physiological role of membrane-bound serine proteases

Some of these proteases have been shown to be involved in various physiological processes. For instance, CAP1/prostatic and CAP3/matriptase play an important role in the maintenance of the epidermal barrier integrity (175-177) and, only for CAP3, in intestinal barrier integrity (178,179). They are also known, with Tmprss3 and CAP2/Tmprss4 to regulate ENaC activity in vitro (47,180,181), although in vivo implication of membrane-

bound serine proteases in the regulation of ENaC has only been shown for CAP1 so far (118,182). Physiological roles have been defined for Tmprss3 and Tmprss1/hepsin in auditory development and deafness (183-185), for Corin in the processing of proANP to ANP in heart (186) and in remodeling of spiral arteries in placenta (187), for Tmprss6/matriptase-2 in iron metabolism (188), for Tmprss15/Enterokinase in the intestinal activation of pancreatic trypsinogen into trypsin (58), and for testisin in fertility (189). All these data are inferred from experiments done in knockout mice. Human mutations have been reported for CAP3, Tmprss3, Tmprss6 and Tmprss15 leading to autosomal recessive ichthyosis with hypotrichosis, hearing loss, iron-refractory iron-deficiency anemia and intestinal enterokinase deficiency with diarrhea and hypoproteinemic edema respectively (58,183,188,190). No biological role has been defined for Trypsinase  $\gamma$ 1, Tmprss11d/HAT, Tmprss11e/DESC1, Tmprss11a, Tmprss11f/HAT-like4, Tmprss11b/HAT-like5, Tmprss2, Tmprss4, Tmprss13/MSPL, Tmprss5/Spinesin, Tmprss7/Matriptase-3 and Tmprss9/Polyserase-1. Moreover, no phenotype could be ascribed to Tmprss2, Tmprss11a or Tmprss11d knockout mice (191,192).

### **8.3 Membrane-bound serine proteases and Spint2**

In vitro, Spint2 is a potent inhibitor of Tmprss1, CAP3, CAP1, Tmprss13 and matriptase-2 (92,96-99). Similar findings were found for HAI-1 who inhibits Tmprss1, CAP1, Tmprss13 and HAT (97,99,129,130). In particular, indirect evidence suggests that HAI-1 seems to be a physiological inhibitor of CAP3 since a complex CAP3-HAI-1 could be purified from human milk (131). In addition, in vivo studies performed in mice indicate genetic interactions between CAP1, CAP3, HAI-1 and Spint2 (see chapters about Spint2 and HAI-1). Briefly, the embryonic lethality of Spint2 and HAI-1 knockout mice can be rescued by the disruption of the CAP1 or CAP3 genes and the postnatal lethality of HAI-1 hypomorphic can be rescued by knocking down CAP3. These experiments demonstrate that



membrane-bound serine proteases, as well as membrane-bound serine protease inhibitors, play an important role in embryogenesis, fetal and placental development, and support that Spint2 and HAI-1 are inhibitors of membrane-bound serine proteases. In spite of these data, it is still unknown whether and how these proteins interact with each other in vivo.

## **9. NHE3 AS A CANDIDATE GENE IN THE CONGENITAL SODIUM DIARRHEA**

### **9.1. General considerations**

NHE3 is one of the nine isoforms of Na-H-exchangers that belongs to the mammal SLC9 family (193). This exchanger mediates the transport of one Na<sup>+</sup> ion into the cell and one proton out of the cell. NHE3 is abundantly located on the plasma membrane of intestinal epithelial cells (duodenum, jejunum, ileum, proximal colon) and tubular cells of the kidney (proximal tubule and thick ascending limb) (11). At the subcellular level, it is found at the plasma level but also has juxtannuclear localization. NHE3 cycles from one region to the other in a tightly regulated manner (194).

### **9.2. Physiological role of NHE3**

NHE3 is a major actor in Na<sup>+</sup> (re)absorption in the gastro-intestinal tract and in the kidney (11,195). NHE3 knockout mice show a phenotype very similar to the congenital sodium diarrhea, although the diarrhea is milder (196). These mice display absorptive defects fluid and bicarbonates in intestine and kidney, and consequently suffer from a mild diarrhea with alkaline stools and enlarged small intestine and colon, metabolic acidosis and hypotension. As compensatory mechanisms, aldosterone is increased, as is ENaC (epithelial

sodium channel) activity and H-K-ATPase mRNA expression. In the kidney, proximal fluid and bicarbonate absorption is reduced, whereas renin and AE1 (Cl-HCO<sub>3</sub> exchanger) mRNA expression is increased. These mice die quickly when fed with a low salt diet (197,198) and also suffer from spontaneous colitis (199). In the intestine, NHE3 is functionally linked to the Cl-HCO<sub>3</sub> exchangers SLC26A3 and SLC26A6 (DRA and PAT-1) to mediate electroneutral NaCl absorption (20,21). NHE3 is thus important for sodium absorption in the gut between the meals. In the kidney, it plays an important role in NaCl absorption but also bicarbonate absorption and ammonium secretion (200). Interestingly, NHE3 is also active when located inside the cell where it may mediate acidification of early endosomes (201,202).

### **9.3. Regulation of NHE3**

The expression, localization and activity of NHE3 are highly regulated by a wide group of molecules (table 2). Of note, the second messengers cAMP, cGMP and Ca<sup>2+</sup> can all decrease the abundance of NHE3 at the plasma membrane as well as its intrinsic activity. NHE3 is made of N-terminal domain of about 500 amino acids making 11 transmembrane domains that is responsible for the exchange of Na<sup>+</sup> and H<sup>+</sup> (203) and a large intracellular C terminal part, which is required for its regulation. Many molecules have been shown to bind this C-terminal loop (figure 33). These are reviewed in detail elsewhere (36,204).

	NHE1	NHE2	NHE3
Adenosine	—	—	S,I <sup>a,b</sup>
ATP Depletion	I	I	I
Albumin	—	—	S
Angiotensin II	S	—	S
ANP	—	—	I
cAMP	S	S	I
cGMP	—	—	I
Dopamine	I	—	—
EGF	—	—	S
Elevated [Ca <sup>2+</sup> ] <sub>i</sub>	S	—	I
Endothelin-1	—	—	S
Epinephrine	I	—	S
FBS	S	S	S
FGF	S	S	S
Glucocorticoids	S	—	S
Hyperosmolarity	S	S,I <sup>a</sup>	I
Insulin	—	—	S
LPA	—	—	S
Mineralocorticoids	—	S	—
Nitric oxide	—	—	I
Norepinephrine	—	—	S
PMA	S	S	I
PTH	—	—	I
Okadaic acid	—	S	S
Serotonin	S	—	I
Short chain fatty acid	—	—	S
Somatostatin	I	—	—
Thrombin	S	S	S

<sup>a</sup>S, stimulate; I, inhibit; —, not reported.

**Table 2: Molecules that acutely regulate NHE3.** From (11)

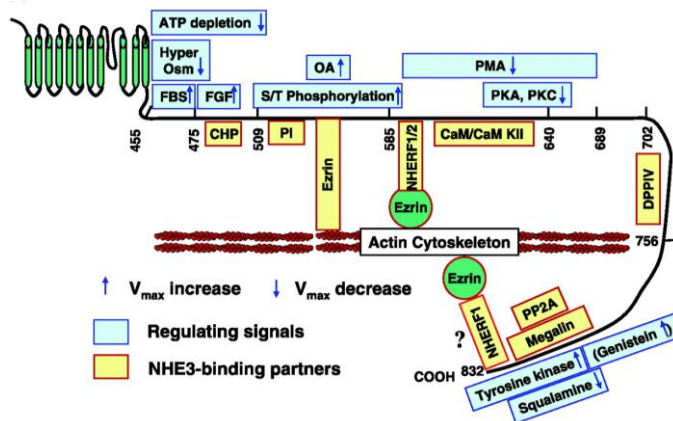


**Figure 33: NHE3 regulatory complexes.** NHE3 organization including COOH-terminal domains involved in acute regulation and binding partners. The NHE3 NH<sub>2</sub> and COOH termini are illustrated. Shown above the COOH terminus in blue are sites of action of regulatory stimuli defined by the truncations which abolish the specific regulatory effects. The direction of the arrow indicates acute stimulation (↑) or inhibition (↓) of NHE3 activity. Below the COOH terminus in yellow are listed associating proteins and the areas of their binding sites on NHE3. From (36)

#### **9.4. NHE3 and serine proteases**

Regulation of NHE3 by serine proteases is poorly unknown. Among the various regulatory proteins of NHE3, the serine protease dipeptidyl peptidase IV (DPPIV) has been shown to bind to NHE3 in Opossum kidney cells (205). This protease is a member of the prolyl oligopeptidase family, which specifically cleaved prolyl bonds of small peptides (161). It is a membrane-bound serine protease with a broad tissue distribution including the intestine, kidney, liver, pancreas, salivary glands and immune organs such as spleen, thymus and lymph node (206). DDPIV is well known for its capacity to cleave and inactivate incretin hormones glucagon-like peptide-1 (GLP-1) and glucose insulinotropic peptide (GIP) (207). These hormones are secreted in the gut after a meal and bind receptors in many organs including in pancreas, where they regulate glucose metabolism. Inhibitors of DDPIV are now used as therapeutic tools in diabetes mellitus (208). DDPIV play also an important role in immune function (206). Regarding NHE3, inhibition of DDPIV reduces NHE3 activity in opossum kidney cells (a model of proximal tubular cells) and in proximal tubules of rats (209,210). DDPIV inhibitors also decrease blood pressure in young spontaneous hypertensive rats (211). This is the sole example of regulation of NHE3 by serine protease and thus an interesting partner for Spint2. However, if we assume that Spint2 mutations linked to the congenital sodium diarrhea are loss of function mutations, unopposed DDPIV activity would lead to an increase in NHE3 activity and thus to Na<sup>+</sup> hyperabsorption in the gut, not to a diarrhea with a Na<sup>+</sup> loss.

# AIMS OF THE PROJECT

Mutations in the Spint2 gene, which encodes a transmembrane serine protease inhibitor, have been associated with the congenital sodium diarrhea. How Spint2 is involved in the pathogenesis of this rare disease is currently unknown and the physiological role of Spint2 remains elusive.

Based on the clinical findings of the congenital sodium diarrhea mainly consisting in a specific loss of  $\text{Na}^+$  and  $\text{HCO}_3^-$  in the stools, and the known jejunal defect in Na-H-exchange, we hypothesize that Spint2 may be a novel regulator of ion transport in gastrointestinal tissues. Since the congenital chloride diarrhea, with a specific loss of  $\text{Cl}^-$  and  $\text{H}^+$  in the stools (a mirror finding of the congenital sodium diarrhea), is due to mutations of the Cl-HCO<sub>3</sub> exchanger Slc26A3 and because NHE3 knockout mouse model phenocopies the congenital sodium diarrhea (even though the phenotype is milder), the Na-H-exchanger NHE3 appears as a particularly interesting candidate transporter. Loss of function mutations of Spint2 could result in the loss of inhibition of a yet unknown target serine protease. The unopposed activity of this protease may lead, directly or indirectly via other proteases or substrates, to the inhibition of NHE3. In consequence of this inhibition,  $\text{Na}^+$  and  $\text{HCO}_3^-$  are poorly (re)absorbed throughout the gut, as seen in the congenital sodium diarrhea.

Spint2 might also regulate other intestinal transporters such as the  $\text{Cl}^-$  channel CFTR or the electrogenic  $\text{Na}^+$ - $\text{HCO}_3^-$  cotransporter NBC1. Increased activity of CFTR, as observed during *Vibrio Cholerae* infections, results in a very severe watery diarrhea with important loss  $\text{Na}^+$ ,  $\text{Cl}^-$ ,  $\text{K}^+$  and  $\text{HCO}_3^-$  (212). NBC1 is responsible for  $\text{HCO}_3^-$  reabsorption in renal proximal tubules and loss of function mutations of NBC1 have been reported in patients suffering from proximal tubular acidosis (213,214). NBC1 KO mice showed profound metabolic acidosis

and hyponatremia (215). These mice do not display any diarrhea but intestinal impactions (like CFTR knockout mice (216)), suggesting that, in contrary to its role in kidney, NBC1 plays a role in intestinal anion secretion. Thus, an increase in NBC1 activity might be present in congenital sodium diarrhea patients.

Alternatively, ion transport via the paracellular route could be altered in the congenital sodium diarrhea. For instance, mutations in the tight junction forming proteins claudin 16 and 19 have been reported to cause renal  $Mg^{2+}$  wasting in humans (217,218). Other claudins, such as claudin-2, -10 and -15 have been shown to mediate specific  $Na^+$ -transport (219-221). Interestingly, the membrane-bound serine protease CAP3 has been proposed to regulate intestinal barrier in mice via the modulation of claudin-2 expression (179).

No in vivo targets of Spint2 have been identified so far. As mentioned above, rescue experiments in Spint2 knockout mice strongly suggest that the membrane-bound serine proteases CAP1 and CAP3 are potential partners of Spint2 (117,119,179). The Spint2 protein has a transmembrane domain and there is growing evidence that HAI-1 (the homolog of Spint2) is an in vivo partner of CAP3 (222). Thus, we hypothesize that in vivo partners of Spint2 may belong to the membrane-bound serine proteases family. Of course, we cannot exclude serine proteases from other families as potential targets of Spint2.

Spint2 has two inhibitory domains of the Kunitz type. How these two domains mediate serine protease inhibition is unknown. Answering this question has been difficult since no in vivo partners have been attributed to Spint2. In vitro studies suggest that both domains can inhibit serine proteases such as trypsin, plasmin, plasma kallikrein, pancreatic kallikrein, tissue kallikrein, chymotrypsin, factor XIa (see chapter about Spint2). Using site-directed mutagenesis, one study showed that the first domain Kunitz is mainly responsible for the inhibition of HGFA (90).

Mutations of the Spint2 gene associated with the congenital sodium diarrhea are probably loss-of-function mutations. This is based on three observations: 1) the congenital sodium diarrhea is transmitted as an autosomal recessive trait, 2) the Spint2 mutant Y163C shows a reduced inhibitory activity on trypsin and 3) start codon or intronic mutations of Spint2 lead to the absence of Spint2 protein detection when transfected in COS cells (61). However, the functional consequences of mutations in the Spint2 gene, particularly the Y163C missense mutation, have not been carefully assessed.

The aims of this research project are:

- 1) To perform a structure-activity study to determine the impact of the Spint2 mutation Y163C on its inhibitory activity. This also intends to identify partners of Spint2 among the subfamily of membrane-bound serine proteases and to provide a better understanding of serine protease inhibition by the two Kunitz domains of Spint2.

Approach: functional assay in *Xenopus* oocytes to study both functional and biochemical interactions between Spint2 and membrane-bound serine proteases.

- 2) to understand the physiological role of Spint2, mainly assessing its putative involvement in the regulation of ion transporters (such as NHE3) in gastrointestinal tissues via the inhibition of membrane-bound serine proteases.

Approaches:

- A) Generation of a Spint2 knockout mouse model and analysis of its intestinal phenotype.
- B) Establishment of a polarized intestinal epithelial cell line to study the repercussions of Spint2 knock-down and overexpression, and

candidate protease overexpression on Na<sup>+</sup> transport and epithelial barrier integrity.

- C) Study of the potential regulation of NHE3 by membrane-bound serine proteases in *Xenopus* oocytes.



# MATERIAL AND METHODS

*cDNA clones.* cDNA clones of Tmprss3 and rat NHE3 (wt and mutant E213I) were gift from Bernard Rossier (University of Lausanne) and Daniel Fuster (University of Bern) respectively. cDNA clones of human CAP1, CAP3, Tmprss2, DPPIV and human NHE3 were obtained from the Mammalian Gene Collection (MGC). All cDNA were subcloned into the pSD(BS)easy vector (for expression in *Xenopus* oocytes) or into the pcDNA3.1 vector (for expression in Caco-2 cells). A FLAG-tag sequence was added to Spint2 using a single BstEII restriction site located in a sequence encoding the region between both Kunitz domains. PCR amplification was performed to add a tag HA-tag to NHE3 (rat and human forms, both in C-terminal part), a GFP tag in the C-terminal part of Spint2, a histidine-tag to CAP3 and DPPIV.

*Site directed mutagenesis.* Spint2 mutants (R48L, R143L, Y163C) were created using the Stratagene's QuickChange protocol.

*cRNAs.* pSD(BS)easy plasmids (including  $\alpha$ ,  $\beta$ , and  $\gamma$  subunits of rat ENaC) were linearized using restriction enzymes with single site located after the poly(A) tail and capped cRNAs were in vitro synthesized by SP6 polymerase.

*Expression in Xenopus oocytes.* Stage V and VI healthy oocytes were isolated from ovarian tissue of *Xenopus laevis* and pressure-injected with 100nl of cRNA solution as indicated in the legends of the figures. For the functional assay, oocytes were injected with the  $\alpha$ ,  $\beta$  and  $\gamma$  rat subunits of ENaC cRNAs (0,11ng of each subunit per oocyte) and with cRNAs of membrane-bound serine proteases and Spint2 (wild-type and mutants) as indicated. Oocytes were kept at 19° C in a low Na<sup>+</sup> (for the functional experiments with ENaC) modified Barth solution (MBS) containing (mM): 10 NaCl, 0.82 MgSO<sub>4</sub>, 0.41 CaCl<sub>2</sub>, 0.33 Ca(NO<sub>3</sub>)<sub>2</sub>, 80 N-methyl-D-glucamine (NMDG), 2 KCl and 5 HEPES or a normal Na<sup>+</sup> (for all other experiments) modified Barth solution (MBS) containing (mM): 85 NaCl, 1 KCl, 2.4 NaHCO<sub>3</sub>, 0.82 MgSO<sub>4</sub>, 0.41 CaCl<sub>2</sub>, 0.33 Ca(NO<sub>3</sub>)<sub>2</sub>, and 10 HEPES, 4.08 NaOH

*Electrophysiology.* Electrophysiological measurements were made 12 hours after injection. The oocytes were studied using the standard two-electrodes voltage clamp technique using a Dagan TEV voltage clamp amplifier (Dagan, Minneapolis, MN), the Digidata 1322 digitizer, and the PClamp 9 data-acquisition and analysis package (Axon Instruments, Molecular Devices, Sunnyvale, CA). The two electrodes contained 1 M KCl solution. All electrophysiological experiments were performed at room temperature (22 °C).

The holding potential was -100 mV. The composition of the perfusion solution was (in mM) 120 NaCl, 2.5 KCl, 1.8 CaCl<sub>2</sub>·2H<sub>2</sub>O, and 10 HEPES-H<sup>+</sup>. Amiloride-sensitive Na<sup>+</sup> current ( $I_{Na}$ ) was defined as the difference between Na<sup>+</sup> current obtained in the presence (10  $\mu$ M) and in the absence of amiloride. As a positive control for ENaC activation by serine proteases, the oocytes were exposed to 5  $\mu$ g/ml trypsin (Sigma-Aldrich Chemie) in the perfusion solution for 2-3 minutes.

*<sup>22</sup>Na uptake in Xenopus oocytes.* Non-injected oocytes or NHE3-injected oocytes (taken 3-4 days after injection) were washed and incubated in a Na<sup>+</sup>-free solution (mM: 100 choline Cl, 2 KCl, 1 CaCl<sub>2</sub>, 1 MgCl<sub>2</sub>, 10 HEPES/Tris, pH 6.8) for 30 minutes at 18°C. Oocytes were then transferred in a <sup>22</sup>Na-uptake solution (mM: 99 choline Cl, 0.5 <sup>22</sup>NaCl, 2 KCl, 1 CaCl<sub>2</sub>, 1 MgCl<sub>2</sub>, 10 HEPES/Tris, pH 7.4) for 30 minutes at 18°C. Uptake was stopped by transferring the oocytes in an ice-cold stop solution (mM: 50 choline Cl, 50 NaCl, 2 KCl, 1 CaCl<sub>2</sub>, 1 MgCl<sub>2</sub>, 10 HEPES/Tris, pH 7.4). After extensive washing using the same solution, oocytes were lysed in 10% SDS and uptake was measured by scintillation counting.

*Antibodies.* Mouse monoclonal anti-Actin and anti-FLAG antibodies are from Sigma and were used at a 1:1000 and 1:500 dilutions respectively. Rabbit polyclonal anti-GFP antibody is from Sigma and was used at a 1:1000 dilution. Mouse monoclonal anti-HA antibody is from Covance and was at a 1:1000 dilution. Rabbit polyclonal Anti-His antibody is from Rockland and was used at a 1:1000 dilution. This antibody is conjugated to an infrared dye IRdye800 that allows protein detection using the *Li-Cor*® technology. Monoclonal antibodies were detected with an anti-mouse IRdye800 or 680 antibody.

*Pull-down assays.* 24 hours after injection, oocytes were lysed in lysis buffer (1 % triton X-100, 100 mM NaCl, 20 mM Tris-HCl pH 7.5, 10mM Imidazole, 1 mM PMSF and 10  $\mu$ g/ml of each Leupeptin, Pepstatin and Aprotinin). Lysates were then vortexed and centrifuged for 10 minutes at 12'000rpm. The intermediate phase was withdrawn and a sample of each lysate was kept as a control of "total lysate fraction". The rest of the lysate was incubated overnight with 50 $\mu$ l of Nickel-beads (Ni-NTA Agarose, Qiagen). Elution was performed with 50 $\mu$ l of 2x SDS-PAGE sample buffer (containing DTT 25mM and EDTA 50mM). All samples were heated at 95°C for 10 minutes before loading on the SDS-PAGE (5-15%).

*Cell surface biotinylation.* 24h hours after injection, oocytes were rinsed twice in MBS and then incubated in biotinylation buffer (mM: 10 triethanolamine, 150 NaCl, 2 CaCl<sub>2</sub>, pH 9.5) containing 1mg/ml NHS-SS-Biotin (Sigma-Aldrich Chemie) for 15 minutes at 4°C. Excess biotin was quenched in quench buffer (mM:192 glycine, 25 Tris-HCl, pH7.5 in MBS)

and oocytes were washed twice in MBS. After biotinylation, oocytes were lysed in lysis buffer and lysates were incubated with 50µl streptavidin beads overnight at 4°C. Beads were washed three times with lysis buffer, twice with a high salt buffer (same as lysis buffer but with 500mM NaCl) and once in 50mM Tris-HCl pH7.4 or only three times with lysis buffer as indicated. Elution was performed with 50µl of 2x SDS-PAGE sample buffer (containing DTT 25mM). All samples were heated at 95°C for 10 minutes before loading on the SDS-PAGE (5-15%).

*Generation of Spint2 gut-specific and tamoxifen-inducible Knockout mice.* Embryonic stem cells with one allele of Spint2 trapped by the gene-trap construct rsFlipRosaCeo0 were obtained from the German Gene Trap Consortium (GGTC). These cells come from the 129P2 (formerly 129/Ola) mouse strain. The presence of the gene trap construct in the first allele of Spint2 was verified by PCR analysis and sequencing. ES cells were injected into the blastocoel cavity of C57/BL6-derived blastocysts and implanted into pseudopregnant females. Chimeric offsprings were crossed to C57/BL6 mice to obtain TRAP/+ mice. We were unable to obtain TRAP/TRAP mice by crossing TRAP/+ mice together because of embryonic lethality (see results). The orientation of the gene trap construct was inverted by crossing TRAP/+ mice with Gt(ROSA)26Sor-FLPe mice (kindly provided by Edith Hummler, University of Lausanne) to obtain Tinv/+ mice. Tinv/Tinv homozygous mice were crossed to Villin-Cre mice (kindly provided by Edith Hummler, University Of Lausanne) to obtain gut-specific Spint2 KO mice or to  $\beta$ -actin-Cre-ERtm mice (Jackson laboratory) to obtain Tamoxifen-inducible Spint2 KO mice. Genotyping of mice was performed by PCR on genomic DNA samples of tail or ear biopsies. The following primers were used to detect:

the spint2 wt allele:

mgS2\_18423F: GAAGTTCTTGGATTTGAGTGTTGG

mgS2\_18821R: CCCACTACCTTCGAAACTCC

the Spint2 trapped allele:

mgS2\_18423F: GAAGTTCTTGGATTTGAGTGTTGG

Cd2R: CAAGTTGATGTCCTGACCCAAG

the FLPe transgene:

FLIP\_anti: CTCGAGGATAACTTGTTTATTGC

FLIP\_sense: CTAATGTTGTGGGAAATTGGAGC

the VillinCre transgene:

Crevillin\_F: GTTCGCAAGAACCTGATGGAC

Crevillin\_R: CTAGAGCCTGTTTTGCACGTT

the CreERtm transgene:

CAGG\_CreERTM\_F: CTCTAGAGCCTCTGCTAACC

CAGG\_CreERTM\_R: CCTGGCGATCCCTGAACATGTCC

Quantitative PCR analysis. Total RNA was extracted from mouse tissues using the RNeasy kit from Qiagen according to the manufacturer's protocol. 1.5 µg RNA was reverse transcribed into cDNA with the M-MLV reverse transcriptase and random primers (Promega). RNA was treated with DNase I (Promega) to remove any possible traces of genomic DNA before the cDNA synthesis. The following primers and Taqman probes were used to detect:

Spint2 cDNA :

mSpint2\_exon3\_F: GAATGGAGCCGACTCTTCTG

mSpint2\_exon5\_R: GCCTTCGGGACACAGTATTC

mSpint2\_exon4\_Probe: AGAAAGCAGAGTGCTGAGGACCTGTCT

Actin cDNA:

mActin\_exon1\_F: GCTTCTTTGCAGCTCCTTCGT

mActin\_exon2\_R: CCAGCGCAGCGATATCG

mActin\_exon1-2\_Probe: CCCGCCACCAGTTCGCCATG

The qRT-PCR experiments were carried out on an ABI PRISM 7500 equipment (Applied Biosystems). PCR was performed in 96-well plates (Applied Biosystems) in 20-µl reactions that contained 10 µl of *TaqMan* Master Mix (Applied Biosystems), 250 nM of probe, 900 nM of each primer and 4 µl of cDNA (diluted 25 times).

*Tamoxifen-induced Spint2 ablation treatment.* 4 week-old *Tinv/Tinv*; *CreERTm+* or *Tinv/Tblocked*; *CreERTm+* mice (and littermates controls negative for the *Cre* transgene) were injected intraperitoneally with Tamoxifen (9mg or 3mg/40g of body weight, SIGMA) in peanut oil once day during 4 days or 10 days (see results).

*Metabolic cages.* 8 week-old mice were placed in individual metabolic cages to collect, after three days of adaptation, 24 hour urine and faeces and measure bodyweight water and food intake. Mice were fed a normal salt diet (>3.2% Na<sup>+</sup>, Sniff) for days and then a low-salt diet (0.18% Na<sup>+</sup>) for three days. At the end of the experiment, Mice were anesthetized with isoflurane and blood was collected by retroorbital plexus puncture. Mice were then sacrificed to collect tissues for qRT-PCR experiments. Urinary and plasma Na<sup>+</sup> and K<sup>+</sup> were measured using a flame photometer (Cole-Palmer Instrument).

*Cell culture.* Caco-2 cells were kindly provided by Blaise Corthésy (University of Lausanne). Cells were grown at 37°C in MEM (Gibco) supplemented with 10% FBS, 10 mM HEPES, 1% penicillin/streptomycin, 2mM glutamine, 1mM sodium pyruvate and 0.1% transferrin. Cells cultivated to 80% confluency were seeded on Snapwell filters (diameter, 12

mm; pore size, 0.4  $\mu\text{m}$ ; Corning Costar, Cambridge, MA) at a density of  $2.5\text{-}3.0 \times 10^5$  cells/ $\text{cm}^2$ . The culture medium was changed every 2-3 days. After 3 weeks, the formation of monolayers of polarized cells was assessed by measuring the transepithelial electrical resistance (TER) using a Millicell-ERS apparatus (Millipore, Bedford, MA). TER values of around 350-400 ohms  $\times \text{cm}^2$  were usually found. Cells were then washed three times with PBS and lysed in RLT-Buffer (from Qiagen RNeasy kit) by pipetting up and down. Before PCR-analysis, total RNA was extracted and then in vitro reverse transcribed into cDNA as described above. The following primers were used for PCR analyses:

Gene	Forward primer	Reverse primer
Spint2	ATCCTCCCCTGCCCTTGCC	GAGCTCCAGACGGTGCGCAG
Spint1	CTGCGGACCCAGGGCTTTGG	CCCCGCAGTAGGCGCCAATC
NHE3	AGGTCCATGTCAACGAGGTC	AGGACACTATGCCCTTCAAG
CFTR	AGCATTGTGCTGATTGCACAG	GAATCGTACTGCCGCACTTT
CAP1	AGCCAACGCCCTCCTCCCCA	TGCAGTGGCTTGGGCGTCAG
CAP3	GCACATGGAAACATTGAGGTG	CCCGTTGATCTCCACGTAGT
Tmprss2	CTTCCTCGTGGGAGCTGCGC	ATTCTCGTCTCCCGCCGG
Tmprss13	CTTGGTCTATGACAGTTACCTTACC	GTTGTTCTGCTCACAGACAAGAGG
GAPDH	TCTTTTGCCTCGCCAGCCGA	ACCAGGCGCCCAATACGACC

*Cell transfections.* Caco-2 cells grown on plastic were transfected using Lipofectamine2000 (Invitrogen) with pcDNA3.1 plasmids encoding Spint2 cDNA with FLAG-tag or GFP-tag or shRNA constructs targeting human Spint2 (Thermo Scientific, TRCN0000073578, -79, -80, -81 and -82). 48 hours after transfection, membrane preparation were performed or cells were lysed to collect total RNA.

*Membrane preparation.* All steps were performed at 4°C. Cells grown on plastic in 6 well-plates were scrapped in 300 $\mu\text{l}$  of lysis buffer (100 mM Tris-HCl pH 7.0, 300 mM NaCl, 10 mM MgCl<sub>2</sub>, 1 mM PMSF and 10  $\mu\text{g}/\text{ml}$  of each Leupeptin, Pepstatin and Aprotinin). Lysate were centrifuged at full speed for 30 minutes. The supernatant was kept as the cytosolic fraction. Pellets were resuspended in lysis buffer (same buffer as described in the pull-down assays section) and centrifuged at full speed for 15 minutes. The supernatant was kept as the membrane fraction. Both fractions were then used for SDS-PAGE.

# RESULTS

## **1. STRUCTURE-ACTIVITY STUDY OF SPINT2 WILD TYPE AND MUTANTS; A FUNCTIONAL ASSAY IN XENOPUS OOCYTES**

### **1.1. Functional assay in *Xenopus* oocytes**

The results of this project are found in a manuscript that is currently being in the reviewing process for publication in the Journal of Biological Chemistry (see manuscript at the end of this work).

### **1.2. Complementary data to the functional assay in *Xenopus* oocytes**

#### *1.2.1. Assessment of the Spint2 R48L and R143L mutations*

Qin et al generated mutants of Spint2 where the P1 residue (reactive site) at position 48 and 143 in each Kunitz domain is mutated from an arginine into a leucine (90). In cell-free in vitro assay using soluble recombinant proteins, the mutant in the first Kunitz domain, Spint2 R48L, showed a decreased inhibitory activity on HGFA (Hepatocyte Growth Factor Activator Inhibitor), whereas the mutant in the second Kunitz domain, Spint2 R143L, was still functional, suggesting an important role of the first domain for the inhibition of HGFA. Recently, the same mutants have been tested for their inhibitory activity on CAP3 in MDCK cells (93). The inhibition was only assessed on the capacity of Spint2 wild-type or mutants to “protect” the full length form CAP3 from (auto-?) proteolytic activation and degradation. In this aspect, Spint2 R48L showed a reduced capacity, whereas Spint2 R143L was still able to prevent the degradation of CAP3.

We assessed both mutants, together with the double mutant in our functional assay in *Xenopus* oocytes. As depicted in figure 1, Spint2 R48L showed a reduced capacity to block the activating effect of CAP3 on ENaC. Spint2 R143L displays a slightly decreased inhibitory activity although it is statistically significant. A more profound loss of function was seen with the double mutant Spint2 R48L/R143L, although its inhibitory capacity was not fully abolished.

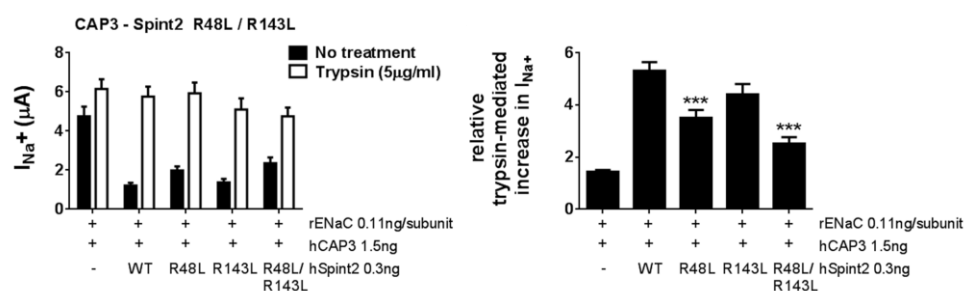


**Figure 1: Inhibitory effect of Spint2 R48L and Spint2 R143L on CAP3.** Oocytes were injected with 0.11 ng cRNA of each rENaC subunit, CAP3 and Spint2 (wild-type or mutants) cRNAs as indicated.  $n \geq 24$  measured oocytes. ENaC-mediated sodium currents  $I_{Na^+}$  are measured without (black bars) and with trypsin (5  $\mu$ g/ml) perfused extracellularly (white bars) as a positive control for ENaC activation. Left panel shows absolute values of  $I_{Na^+}$ . Right panel shows relative trypsin-mediated increase in  $I_{Na^+}$  as assessed by dividing for each oocytes  $I_{Na^+}$  after trypsin treatment by  $I_{Na^+}$  before trypsin treatment. Data are means  $\pm$  SEM. \*\*\*,  $p < 0.001$ , compared to ENaC + protease + Spint2 WT respectively after One-way ANOVA followed by Tukey's multiple comparisons test.

We also tested the effect of these mutations of Spint2 on Tmprss2. We did not observe any reduction of the inhibitory activity of Spint2 R48L and Spint2 R143L compared to Spint2 wild-type (figure 2). Only the double mutant Spint2 R48L/R143L showed a clear loss of function although it still had some inhibitory activity. These results confirm data from recent publications and suggest that the first inhibitory domain of Spint2 is more important for the inhibition of CAP3 but not for Tmprss2.

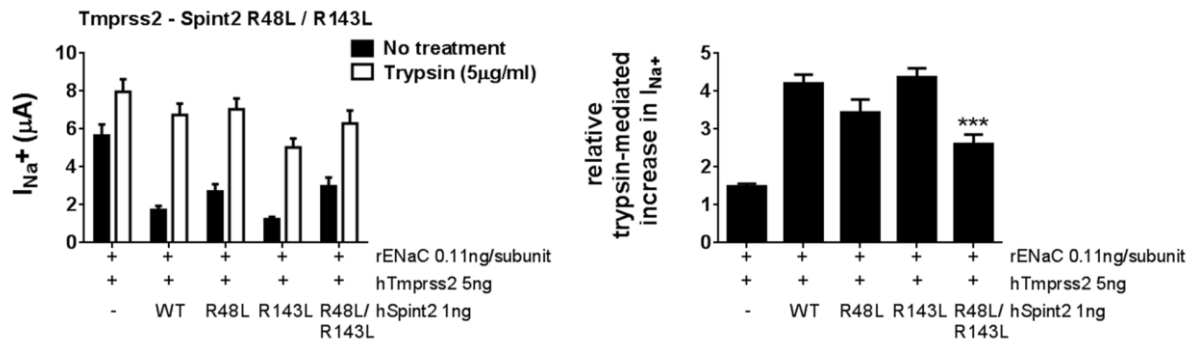


**Figure 2: Inhibitory effect of Spint2 R48L and Spint2 R143L on Tmprss2.** Oocytes were injected with 0.11ng cRNA of each rENaC subunit, Tmprss2 and Spint2 (wild-type or mutants) cRNAs as indicated.  $n \geq 20$  measured oocytes. ENaC-mediated sodium currents  $I_{Na}^+$  are measured without (black bars) and with trypsin (5 $\mu$ g/ml) perfused extracellularly (white bars) as a positive control for ENaC activation. Left panel shows absolute values of  $I_{Na}^+$ . Right panel shows relative trypsin-mediated increase in  $I_{Na}^+$  as assessed by dividing for each oocytes  $I_{Na}^+$  after trypsin treatment by  $I_{Na}^+$  before trypsin treatment. Data are means  $\pm$  SEM. \*\*\*,  $p < 0.001$ , compared to ENaC + protease + Spint2 WT respectively after One-way ANOVA followed by Tukey's multiple comparisons test.

We also compared the effect of Spint2 R48L to the effect of the congenital sodium diarrhea mutant Y163C on CAP3. Both mutants were tested during same experiments as was the double mutant R48L/Y163C. Figure 3 reports, as expected, a similar partial loss of function of both mutants with a residual inhibitory activity of about 40%. An additive effect of both mutations was observed using the double mutant Spint2 R48L/Y163C but the function was not totally abolished. These results imply that, in opposite to previous experiments, both domains might play a role in the inhibition of CAP3 by Spint2.

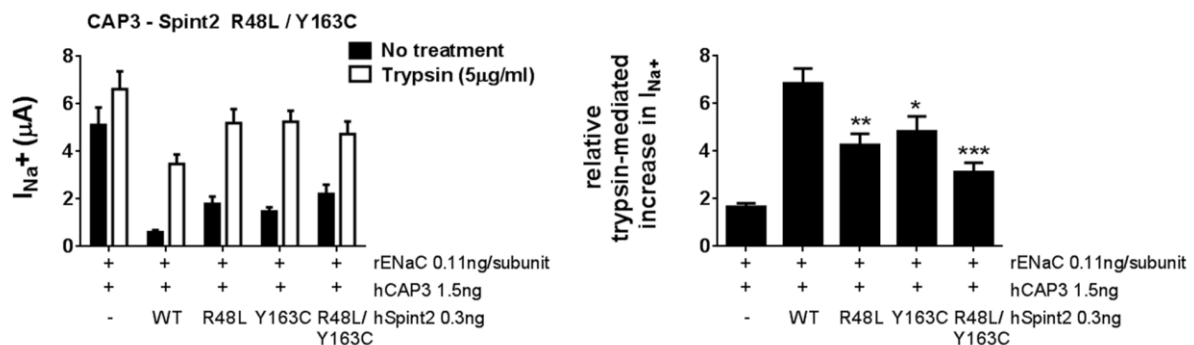


**Figure 3: Inhibitory effect of Spint2 R48L and Spint2 Y163C on CAP3.** Oocytes were injected with 0.11ng cRNA of each rENaC subunit, CAP3 and Spint2 (wild-type or mutants) cRNAs as indicated.  $n \geq 24$  measured oocytes. ENaC-mediated sodium currents  $I_{Na}^+$  are measured without (black bars) and with trypsin (5 $\mu$ g/ml) perfused extracellularly (white bars) as a positive control for ENaC activation. Left panel shows absolute values of  $I_{Na}^+$ . Right panel shows relative trypsin-mediated increase in  $I_{Na}^+$  as assessed by dividing for each oocytes  $I_{Na}^+$



after trypsin treatment by  $I_{Na}^+$  before trypsin treatment. Data are means  $\pm$  SEM. \*,  $p < 0.05$ , \*\*,  $p < 0.01$ , \*\*\*,  $p < 0.001$ , compared to ENaC + protease + Spint2 WT respectively after One-way ANOVA followed by Tukey's multiple comparisons test.

### 1.2.2. Dipeptidyl peptidase IV as putative target of Spint2

Dipeptidyl peptidase IV, DPPIV, is the only serine protease that has been proposed in the literature to act as a regulator of the Na-H-exchanger NHE3 (see introduction, chapter about NHE3). We tested the potential interaction between DPPIV and Spint2 in our functional assay in *Xenopus* oocytes. DPPIV, although a membrane-bound serine protease, belongs to the S9 family and is thus functionally and structurally different from the other membrane-bound serine protease studied in this project (CAP1, CAP2, CAP3, Tmprss1, Tmprss2, ...) that belong to S1 family. DPPIV is not able to stimulate the activity of the epithelial sodium channel ENaC (figure 4). This makes it difficult to use ENaC as reporter gene to test an interaction between DPPIV and Spint2.

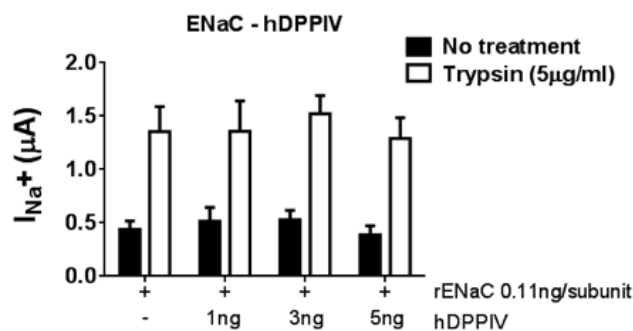


**Figure 4: Effect of DPPIV on ENaC in *Xenopus* oocytes.** Oocytes were injected with 0.11ng cRNA of each rENaC subunit and increasing amount of DPPIV cRNA as indicated. N=8 measured oocytes. ENaC-mediated sodium currents  $I_{Na}^+$  are measured without (black bars) and with trypsin (5  $\mu g/ml$ ) perfused extracellularly (white bars) as a positive control for ENaC activation.

We thus tried to make a competitive assay where ENaC, DPPIV, CAP3 and Spint2 are all co-injected in oocytes. If Spint2 binds DPPIV with a high affinity, CAP3 should not be inhibited anymore by Spint2 and could thus activate ENaC. Figure 5 shows that it is not case, because increases in injected DPPIV cRNA amounts did not prevent the inhibition of CAP3 by Spint2 as seen by the absence of activation of ENaC and its intact sensitivity to trypsin. The gradual

decrease in  $I_{Na^+}$  with and without trypsin seen when co-injecting CAP3, Spint2 and DPPIV is likely due to a decrease in the translation of ENaC because of a competition for the translational machinery.

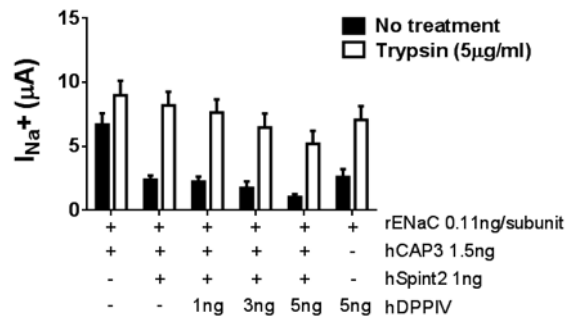


**Figure 5: Competition between CAP3 and DPPIV as substrate for Spint2.** Oocytes were injected with 0.11ng cRNA of each rENaC subunit, CAP3, Spint2 and increasing amount of DPPIV cRNAs as indicated.  $n \geq 10$  measured oocytes. ENaC-mediated sodium currents  $I_{Na^+}$  are measured without (black bars) and with trypsin (5µg/ml) perfused extracellularly (white bars) as a positive control for ENaC activation.

Pull-down experiments were performed to assess biochemically whether DPPIV and Spint2 interact. For this purpose a His-tag was introduced in the N- or C-terminal end of DPPIV to allow affinity purification of DPPIV using nickel-beads. As positive control, figure 6A shows the co-purification of Spint2-FLAG with CAP3 that has a His-tag in its N-terminal end. In contrary, in the same experiment, Spint2-FLAG could not be co-purified with DPPIV, even if DPPIV was affinity-purified using either the His-tag on the N- or C-terminal part (figure 6B). All these results from both functional and biochemical experiments suggest that Spint2 is not an inhibitor of DPPIV.

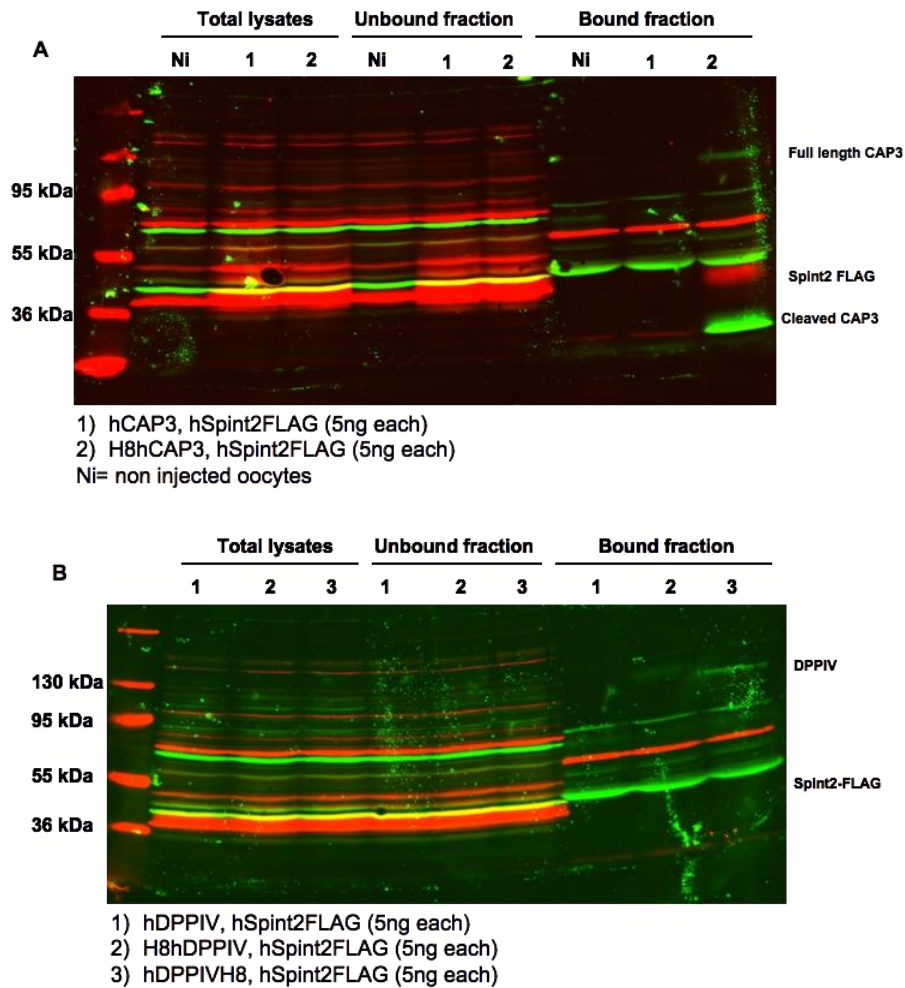


**Figure 6: Biochemical interaction between Spint2 and DDPIV in *Xenopus* oocytes.** A) Western blot performed using oocytes coexpressing tagged His-CAP3 and Spint2-FLAG as indicated. B) Western blot performed using oocytes coexpressing tagged His-DDPIV and Spint2-FLAG as indicated. Bound fraction contains proteins eluted after incubation onto nickel beads. Membranes were blotted with anti-FLAG (red) and anti-His (green) antibodies.

## 2. GENERATION OF A SPINT2 KNOCKOUT MOUSE MODEL

### 2.1. The gene-trap approach

A constitutive Spint2 mouse model has already been generated using a gene-trap approach (116,117). In opposite to the classical gene-targeting approach that specifically alters the expression of one selected gene by removing one or more critical exons based on homologous recombination (223), the gene-trap approach consists in the random insertion of

a gene trap vector construct into the genome of mouse embryonic stem (ES) cells (224). When inserted into an intronic or coding region of a gene, this construct is supposed to alter the expression of this gene and may even abolish it when present in one of the first introns of the gene or in a critical region.

Spint2 knockout mice unfortunately display embryonic lethality due to early defects during the gastrulation stage, abnormal placental labyrinth development and non-closure of the neural tube (116,117). To circumvent this issue, we planned to generate a conditional knockout mouse model of Spint2 using the Cre/lox technology (225).

In 2005, Schnütgen et al described two gene trap vector constructs combined with the Cre/lox system and generate more than 1000 ES cells clones with one gene trapped by one of their constructs, among them the Spint2 gene (226). We thus ordered from the German Gene Trap Consortium ES cells with the FlipRosaCeo construct inserted in the first intron of Spint2. Figure 7 shows how this construct abolishes gene expression when inserted within the first intron of a gene.

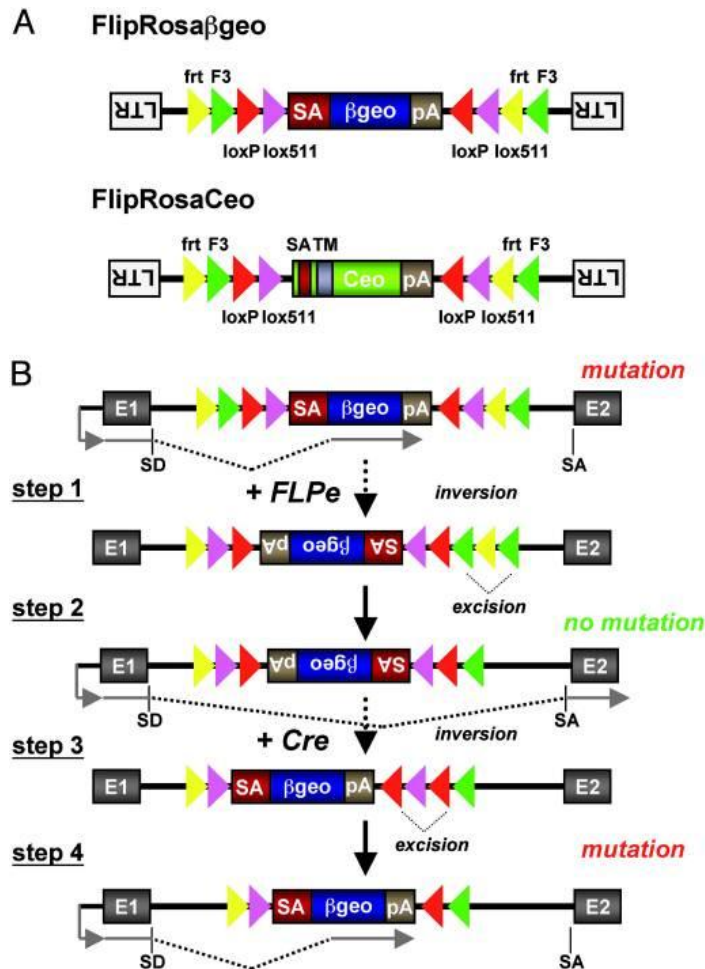


**Figure 7: Conditional gene trap vectors and mechanism of gene inactivation.** (A) Schematic representation of the retroviral gene trap vectors. LTR, long terminal repeat; frt (yellow triangles) and F3 (green triangles), heterotypic target sequences for the FLPe recombinase; loxP (red triangles) and lox511 (purple triangles), heterotypic target sequences for the Cre-recombinase; SA, splice acceptor;  $\beta$ geo,  $\beta$ -galactosidase/neomycin phosphotransferase fusion gene; pA, bovine growth hormone polyadenylation sequence; TM, human CD2 receptor transmembrane domain. (B) Conditional gene inactivation by a SA $\beta$ geo pA cassette. The SA $\beta$ geo pA cassette flanked by recombinase target sites (RTs) in a FIEx configuration is illustrated after integration into an intron of an expressed gene. Transcripts (shown as gray arrows) initiated at the endogenous promoter are spliced from the splice donor (SD) of an endogenous exon (here, exon 1) to the SA of the SA $\beta$ geo pA cassette. Thereby the  $\beta$ geo reporter gene is expressed and the endogenous transcript is captured and prematurely terminated at the cassette's pA causing a mutation. In step 1, FLPe inverts the SA $\beta$ geo pA cassette onto the antisense, noncoding strand at either frt (shown) or F3 (not shown) RTs and positions frt and F3 sites between direct repeats of F3 and frt RTs, respectively. By simultaneously excising the heterotypic RTs (step 2), the cassette is locked against reinversion because the remaining frt and F3 RTs cannot recombine. This inversion reactivates normal splicing between the endogenous splice sites, thereby repairing the mutation. Cre-mediated inversion in steps 3 and 4 repositions the SA $\beta$ geo pA cassette back onto the sense, coding strand and reinduces the mutation. Note that the recombination products of steps 1 and 3 are transient and transformed into the stable products of step 2 and 4, respectively. From (226)

## 2.2. Constitutive and conditional Spint2 knockout mice

We first generated mice having one allele of the Spint2 gene containing the FlipRosaCeo gene trap vector construct inserted within the first intron. In this configuration (that we called TRAP), the construct is supposed to abolish Spint2 expression because only a truncated mRNA and thus protein (made of the first exon of Spint2 and the reporter cassette Ceo) is produced when the Spint2 gene is active. No further exons should be expressed since the reporter cassette has a polyadenylation signal that terminates transcription prematurely (i.e. before transcription of exon 2). When crossing heterozygous mice together, we did not observe any mice homozygous for the trapped allele of Spint2 (Spint2 TRAP;TRAP) as shown by PCR genotyping in figure 8a. These results indicate that Spint2 expression is sufficiently altered to cause embryonic lethality as for the constitutive knockout model previously reported.

As shown in figure 6, recognition sites for the FLPe recombinase and Cre recombinase flank the FlipRosaCeo gene trap vector construct. There are two pairs of sites for each recombinase. Each pair can only recombine with itself; e.g. LoxP sites cannot recombine with Lox51 sites. Moreover, the sites are arranged in a specific manner that blocks the construct in its new configuration once recombination mediated by one recombinase has occurred.

To repair the mutation induced by the presence of the gene trap construct and thus rescue the embryonic lethality, TRAP/+ mice were crossed with transgenic mice expressing the FLPe recombinase under the Gt(ROSA)26Sor promoter (227). This promoter allows FLPe expression in all cells starting already during the preimplantation stage. FLPe-mediated recombination inverts the reporter cassette. In this configuration (called inverted trap = inv TRAP), the cassette is “inactive” and normal splicing of the Spint2 gene occurs thus repairing the mutation and allowing normal Spint2 expression (see Step 2 in figure 7). This step was correctly achieved as seen in figure 8b that shows three weaned mice being homozygous for

the inverted trapped allele (=inv TRAP), indicating that enough Spint2 expression is restored to avoid embryonic lethality. These mice are viable and are on gross examination undistinguishable from wild-type mice.

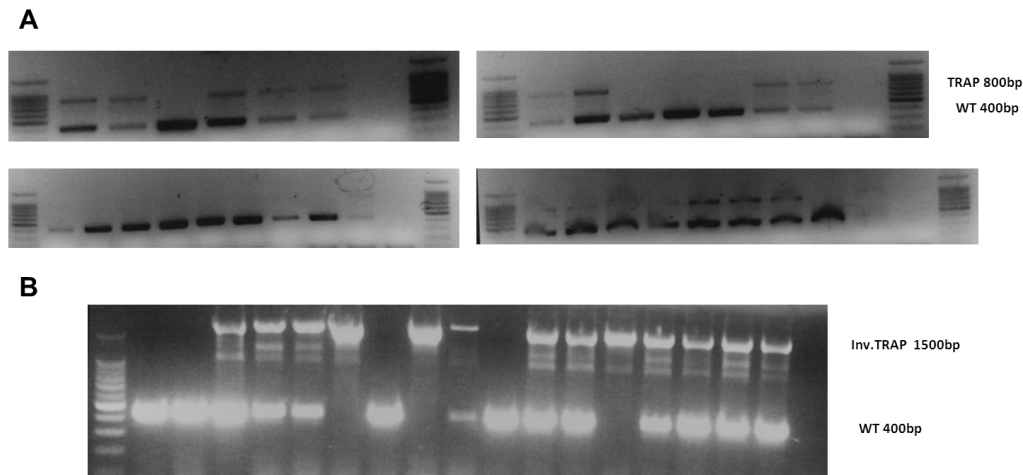


**Figure 8: PCR-genotyping.** **A**, Genotyping of pups born from the breeding between heterozygous mice. None of the pups are homozygous for the trapped allele (=TRAP, 800bp). WT allele is the product at 400bp. **B**, recombination with the FLPe. Mice no 6,8,13 are homozygous for the inverted trapped allele (Inv. TRAP 1500bp).

The final step consists in reactivating the mutation to abolish Spint2 expression in selected tissues, in our case epithelial cells of the small intestine and colon. We crossed inv TRAP / inv TRAP homozygous mice with transgenic mice expressing the Cre recombinase driven by the villin promoter. The villin promoter ensures Cre expression only in epithelial cells of the small intestine and colon (228). In this step (see Step 3 in figure 7), Cre-mediated recombination is supposed to occur only in those cells. This recombination repositions the reporter cassette back to its initial orientation. In this configuration, the mutation is reactivated and Spint2 expression should be abolished specifically in intestinal epithelial cells. Unfortunately, qRT-PCR experiments done using fractions of cells enriched in epithelial cells of the ileum (where both Spint2 and Cre expression is supposed to be high) showed that inv TRAP homozygous, Villin-Cre positive mice have a similar Spint2 mRNA expression than inv TRAP homozygous, Villin-Cre negative mice (figure 9).

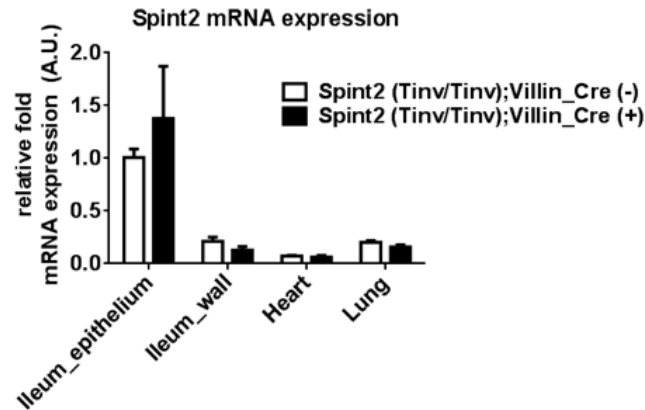


**Figure 9: Spint2 mRNA expression levels in selected organs.** Spint2 mRNA expression was assessed in mice homozygous for the inverted trapped allele expressing or not the Cre driven by the villin promoter. n=3 mice per genotype. Mucosa of the ileum was scrapped to obtain a fraction enriched in epithelial cells and another enriched in intestinal wall cells. Ileum was assessed here because both Spint2 and Cre expressions are expected to be abundant.

Furthermore, inv TRAP homozygous, Villin-Cre positive mice do not exhibit any phenotype on gross examination such as diarrhea. Analyses from experiments done in metabolic cages with mice fed a normal salt or a low salt diet do not show any difference between inv TRAP homozygous, Villin-Cre positive mice and controls (Table 1). These results indicate that the system used here failed to generate a conditional gut-specific Spint2 knockout mouse model. Mutations in the LoxP and Lox51 sites that are recognized by the Cre recombinase were excluded by sequencing (data not shown).

Metabolic cages	Standard diet (4 days)		Low salt diet (3 days)	
	Control (n=7)	“KO” (n=5)	Control (n=7)	“KO” (n=5)
Body weight (g)	27.2 ± 0.43	27.4 ± 1.01	27.4 ± 0.49	27.6 ± 1.16
Food intake (g/24h/gBW)	0.135 ± 0.006	0.138 ± 0.008	0.124 ± 0.005	0.129 ± 0.005
Water intake (g/24h/gBW)	0.16 ± 0.01	0.179 ± 0.007	0.167 ± 0.015	0.172 ± 0.005
Stool (g/24h/gBW)	0.019 ± 0.001	0.021 ± 0.001	0.019 ± 0.001	0.019 ± 0.001
Urine volume (g/24h/gBW)	0.057 ± 0.006	0.075 ± 0.005	0.054 ± 0.006	0.064 ± 0.007
Plasma Na <sup>+</sup> (mmol/l)	N.D.	N.D.	147.7 ± 2.4	144.9 ± 1.5
Plasma K <sup>+</sup> (mmol/l)	N.D.	N.D.	5.1 ± 0.3	4.9 ± 0.1
Urinary Na <sup>+</sup> excretion (μmol/24h/gBW)	7.15 ± 0.75	7.52 ± 0.6	1.47 ± 0.3	1.27 ± 0.3
Urinary K <sup>+</sup> excretion (μmol/24h/gBW)	22.75 ± 2.03	24.89 ± 1.44	35.99 ± 2.03	38.00 ± 2.5

**Table 1: Data of experiments in metabolic cages.** 7 inv TRAP/inv TRAP Cre negative (control) mice and 5 inv TRAP/inv TRAP Cre positive (“KO”) mice were fed first a standard diet (4 days) and then a low salt diet (3 days). Mice were housed in individual metabolic cages during the whole experiment.



Since Villin-Cre-mediated recombination was inefficient, we used another transgenic mouse model expressing in every cell-type a tamoxifen-inducible Cre as developed by Hayashi and McMahon (called Cre ERTM) (229). Tamoxifen-induction of this Cre driven by the  $\beta$ -Actin/CMV enhancer promoter is depicted in figure 10.

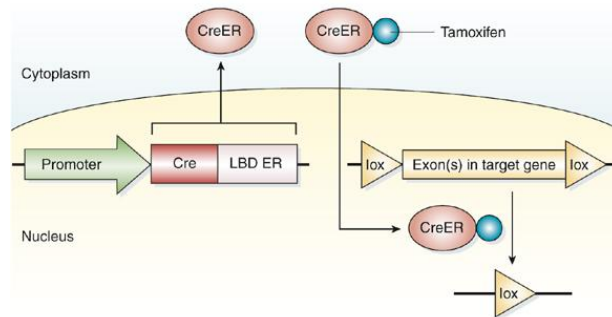


**Figure 10: Mechanism of action of Cre fused to the ligand-binding domain of the estrogen receptor.** The Cre protein is maintained in the cytoplasm because of its fusion to the estrogen-receptor (ER). Upon tamoxifen treatment, CreER translocates into the nucleus where Cre-mediated recombination occurs. From (230)

Inv TRAP homozygous mice were bred with transgenic mice Cre ERTM and 4 weeks old pups were treated with tamoxifen (9mg/40g of body weight intraperitoneally) once a day for 4 days. This time, we observed a 50% decrease in Spint2 mRNA expression in the distal part of the small intestine and colon (fig. 11) but on gross examination, these mice showed no diarrhea and no weight loss (data not shown).

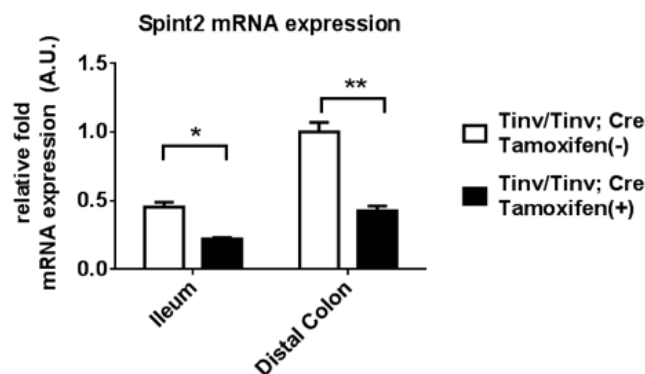


**Figure 11: Spint2 mRNA expression levels in selected organs.** Spint2 mRNA expression was assessed in mice homozygous for the inverted trapped allele expressing or not the Tamoxifen-inducible Cre driven by the  $\beta$ -Actin promoter. Mice were injected i.p. with Tamoxifen (9mg/40g body weight) once a day for 4 days. n=2 mice per genotype.

Since a 50% decrease is likely insufficient to observe any phenotype, we tried to improve the protocol. The tamoxifen-inducible Cre is expressed in every cell including in germ cells where Cre-mediated recombination also occurs upon tamoxifen. Thus, it is possible to generate heterozygous mice that have one Spint2 allele trapped by the gene-trap construct in the inverted position (repaired mutation, Step 2 in figure 7) and the other allele with the construct in its initial position (active mutation Step 4 in figure 7). In the latter configuration, the construct cannot further recombine because all pairs of homotypic recognition sites for the Cre are destroyed (this allele is called Tblock). In such heterozygous mice, only one allele should recombine to get both alleles with the gene trap active (Step 4 in figure 1). Tamoxifen treatment was increased to 10 days (3mg/40g of body weight). qRT-PCR analyses revealed again a 50% reduction in Spint2 mRNA expression in proximal colon and jejunum (figure 12). Interestingly, Tinv/Tblock heterozygous Cre-negative mice that are supposed to have only one functional allele (Tinv) show a similar Spint2 mRNA expression than Tinv/Tinv homozygous mice that have two functional alleles, suggesting that the functional allele can completely compensate for the reduced or abolished function of the non-functional allele (Tblock). This compensation was seen only in the proximal colon and jejunum, but not in the kidneys and lungs. In spite of this lack of compensatory mechanisms, no further decrease in Spint2 mRNA expression could be obtained in the kidneys and lungs upon tamoxifen treatment, suggesting that Cre-mediated recombination is inefficient to obtain a larger reduction in Spint2 mRNA expression. In conclusion, the strategy used here based on a gene-trap approach combined with the Cre/lox system is not suitable to get a gut-specific or a tamoxifen-induced Spint2 knockout mouse model.

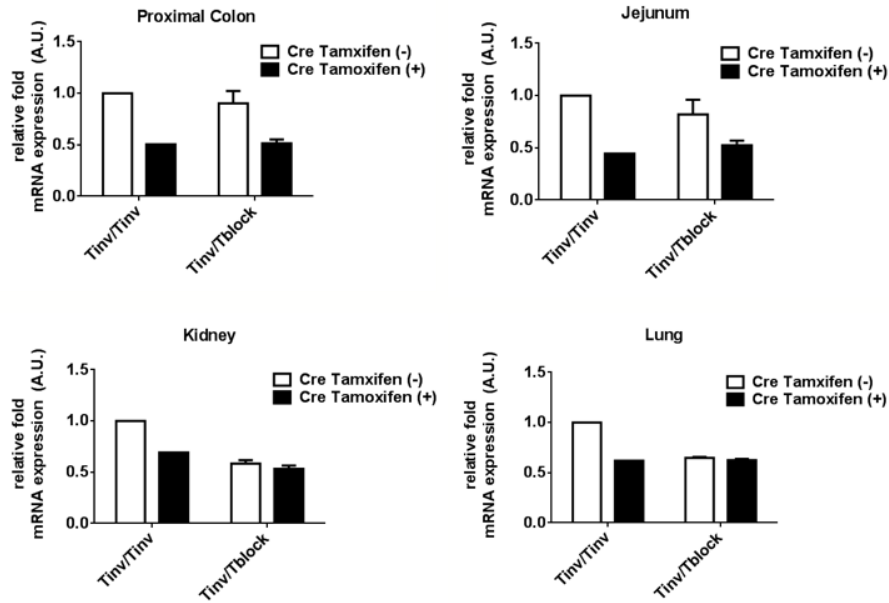


**Figure 12: Spint2 mRNA expression levels in selected organs.** Spint2 mRNA expression was assessed in mice homozygous for the inverted trapped allele or heterozygous (with one trapped blocked allele) expressing or not the tamoxifen-inducible Cre driven by the BetaActin promoter. Mice were injected i.p. with tamoxifen (3mg/40g body weight) once a day for 10 days.

### 3. AN EPITHELIAL CELL MODEL FOR SPINT2

#### 3.1. Characterization of Caco-2 cells

Animal models and particularly genetically modified mouse models are very useful tools to understand in vivo the physiological role of genes of interest. Since our strategy did not allow us to generate a viable Spint2 knockout mouse model, we planned to establish an epithelial cell model for Spint2.

We used the Caco-2 cell line, which is an intestinal epithelial cell line of colonic adenocarcinoma origin (231). These cells can be grown on filter where they form monolayers of polarized cells resembling villous cell of the small intestine called enterocytes. Caco-2 cells were cultured on Snapwells during 3 weeks to obtain monolayers with a transepithelial

electric resistance of around 350-400  $\Omega\text{cm}^2$ , which is consistent with recent publications (232,233).

In order to characterize these cells in more detail, mRNA gene expression analysis was performed on Caco-2 cells grown on plastic and on filters as a monolayer. Figure 13 shows that mRNA of Spint2 and its homolog Spint1 (HAI-1) can be easily detected in those cells. Candidate transporters for the congenital sodium diarrhea such as NHE3 and CFTR are also expressed. As expected, the mRNA expression of NHE3 increases when the cells differentiate into polarized enterocytes on filter. mRNA of several membrane-bound serine proteases such as CAP1, CAP3 and Tmprss2 can be detected, but not Tmprss13.

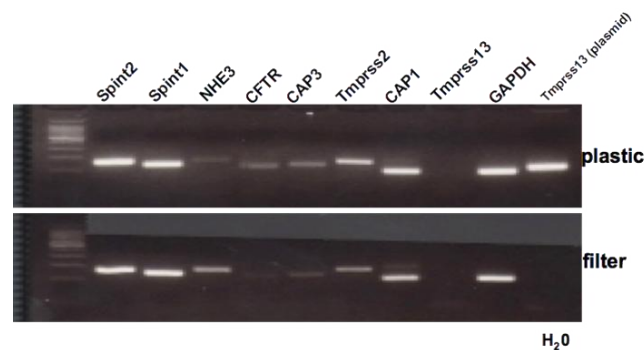


**Figure 13: mRNA gene expression analysis in Caco-2 cells.** RT-PCR was performed using total RNA extracted from Caco-2 cells grown on plastic (upper panel) or on filter to form a monolayer of polarized cells (lower panel). Plasmid cDNA of Tmprss13 was used as a control for Tmprss13 amplification.

### 3.2. Overexpression of Spint2 in Caco-2 cells

In order to overexpress Spint2 in Caco-2 cells, we generated two tagged constructs of Spint2. In one construct, a FLAG-tag was added in the putative extracellular region of Spint2 between the two Kunitz domains and in the other construct, a GFP-tag was fused to the C-terminal part of Spint2 (the putative cytosolic region). Both constructs are as functional as the wild-type untagged form of Spint2, as assessed by their capacity to inhibit the activating effect of CAP1 or CAP3 on the epithelial sodium channel (ENaC) in *Xenopus* oocytes (figure 14). Spint2-FLAG and Spint2-GFP cDNA constructs were transfected into Caco-2 cells

grown on plastic. Both constructs could be detected at the protein level by western blotting after membrane preparation (figure 15).

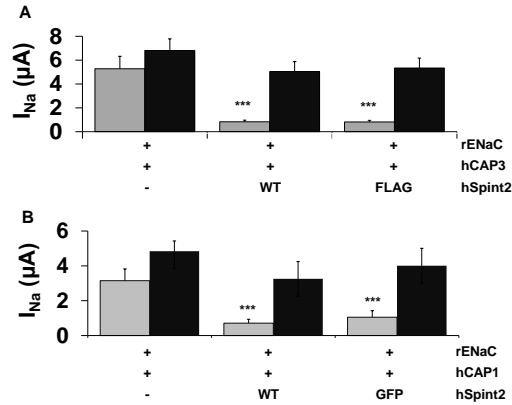


**Figure 14: Inhibitory activity of FLAG-tagged and GFP-tagged Spint2 on CAP3 and CAP1 as assessed by modulation of ENaC activity in *Xenopus* oocytes.** Oocytes were injected with 0.11ng cRNA of each rENaC subunit and CAP1, CAP3 and Spint2 cRNA as indicated. **A**, Inhibition of CAP3 by Spint2wt and Spint2FLAG. **B**, Inhibition of CAP1 by Spint2wt and Spint2GFP.  $n \geq 6$  measured oocytes. ENaC-mediated sodium currents  $I_{Na^+}$  are measured without (grey bars) and with trypsin ( $5 \mu g/ml$ ) perfused extracellularly (black bars) as a positive control for ENaC activation. \*\*\*  $P < 0.001$  compared to oocytes injected with rENaC and CAP3 or CAP1.

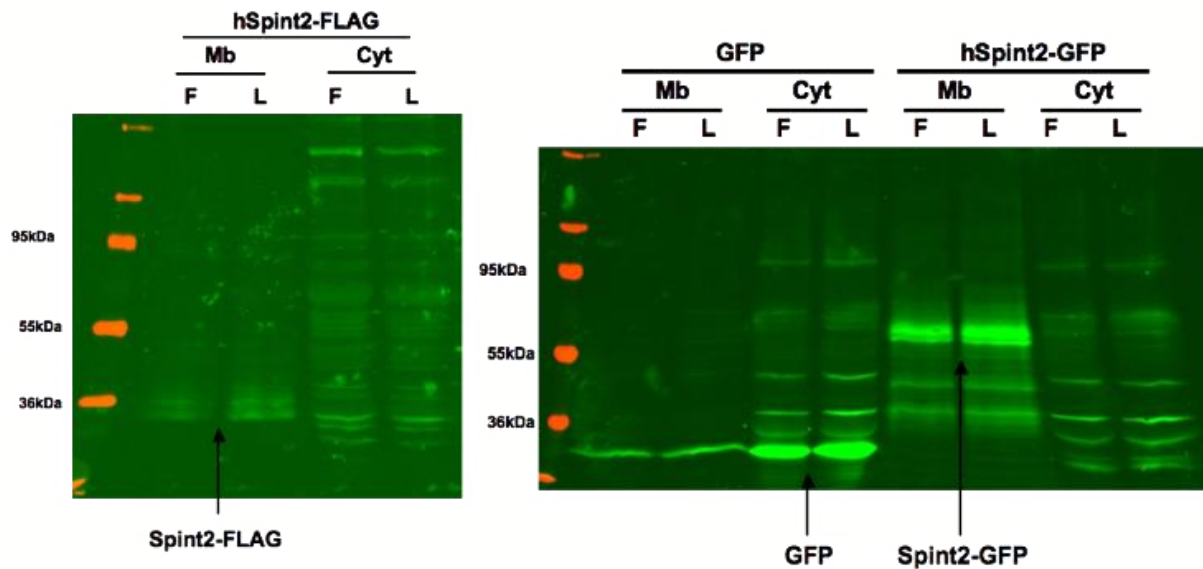


**Figure 15: Spint2-FLAG and Spint2-GFP protein expression in Caco-2 cells.** Caco-2 cells grown on plastic were transfected using Lipofectamine (=L) or FuGene (=F) with hSpint2-FLAG (left panel) or hSpint2-GFP (right panel). A membrane preparation was performed 18h after transfection (Mb=membrane fraction, Cyt=cytosolic fraction). Left panel: immunoblot with the anti-FLAG antibody. Right panel: immunoblot with the anti-GFP antibody. GFP was transfected as a positive control.

### **3.3. Knocking down Spint2 in Caco-cells**

In addition to overexpressing Spint2 in Caco-2 cells, we had also planned to knock-down endogenous expression of Spint2 and ordered 5 different shRNA constructs that target the Spint2 gene. After transfection into Caco-2 cells, a 50% reduction in Spint2 mRNA levels (figure 16). Since Caco-2 cells are known to be difficult to transfect and are usually transduced using lentiviruses, the reduction observed here suggests that all shRNA construct potently knock down Spint2 expression in cells that are readily transfected.

The efficiency of the shRNA construct 1 (shRNA 1 in figure 16) is further demonstrated in figure 17, where Spint2-FLAG protein levels are strongly decreased in Caco-2 cells transiently transfected with Spint2-FLAG cDNA and shRNA construct 1. We could not assess endogenous protein expression levels of Spint2, because we do not have any anti-Spint2 antibody.

### **3.4. Stably transfection of Caco-2 cells**

Caco-2 cells grown on filter require 3 weeks to form monolayers of well-differentiated and polarized cells. The effect of transient transfection performed before culturing the cells on filter is therefore lost when monolayers are formed. A second issue is that Caco-2 cells on filter are even more difficult to transfect than Caco-2 cells grown on plastic. One solution would be to use a retroviral-based transduction system to infect monolayers. Another possibility would be to generate stably transfected clones.

To do so, Caco-2 cells were transfected with Spint2-FLAG, Spint2-GFP or shRNA 1 and 2 against Spint2 and cells were then selected by adding puromycin in the culture medium. In a first attempt, serial dilution was done to get single stably transfected clones. Unfortunately, no clone could be obtained. In a second try, no serial dilution was performed in order to get a polyclonal population of cells. This time, transfected cells grew in the

presence of puromycin, albeit slowly. However, neither any overexpression of Spint2-FLAG and Spint2-GFP nor any reduction in endogenous Spint2 mRNA expression levels could be detected in cells transfected with Spint2-FLAG, Spint2-GFP or shRNA-1 respectively (data not shown).

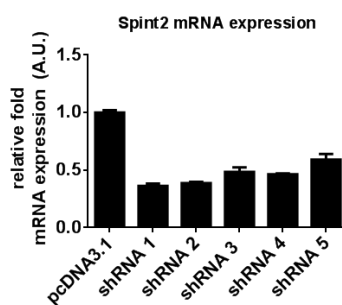


**Figure 16: Effects of shRNA constructs on Spint2 mRNA expression in Caco-2 cells.** Caco-2 cells were transiently transfected with 5 shRNA constructs that targets Spint2. 48 hours after transfection, Spint2 mRNA expression levels were assessed by qRT-PCR. Each condition was analyzed in duplicate.

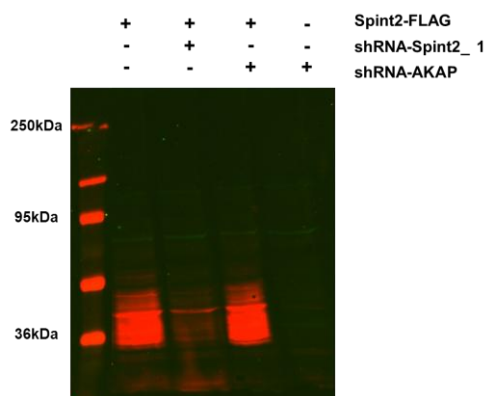


**Figure 17: Effect of shRNA construct 1 on Spint2-FLAG protein expression in Caco-2 cells.** Caco-2 cells were transiently transfected with Spint2-FLAG, shRNA 1 against Spint2, or shRNA against AKAP (unrelated protein used here as a negative control) as indicated. Immunoblot using the Anti-FLAG antibody (in red) was performed on membrane preparation.

## **4. THE NA-H-EXCHANGER NHE3 AND MEMBRANE-BOUND SERINE PROTEASES**

### **4.1. Cleavage of NHE3 by Tmprss3**

As mentioned in the introduction, the Na-H-exchanger NHE3 represents an interesting ion transporter potentially involved in the pathogenesis of the congenital sodium diarrhea. We showed that Spint2 is a powerful inhibitor of membrane-bound serine proteases (see introduction and functional assay in *Xenopus* oocytes). Based on this, we made the hypothesis that NHE3 might be regulated by membrane-bound serine proteases that can then be blocked by Spint2. To address this hypothesis, we also used *Xenopus laevis* oocytes, because we succeed to express functional intestinal membrane-bound serine proteases in this heterologous expression system (see functional assay in *Xenopus* oocytes).

The  $\alpha$  and  $\gamma$  subunits of the epithelial sodium channel ENaC are known to be cleaved in the presence of several serine proteases (234). Similarly, we first used a biochemical approach to look for the presence of any cleaved fragment of NHE3 when co-expressed with serine proteases. cRNA of human NHE3 with a HA-tag in its C-terminal part was co-injected in *Xenopus* oocytes with cRNAs of all intestinal membrane-bound serine proteases used in our functional assay with Spint2 (see functional assay in *Xenopus* oocytes). Figure 18 shows that NHE3 can be expressed in oocytes and detected at the protein level via the HA-tag as a monomer around 90kDa and as a dimer around 200kDa as expected. The significance of the dimer is unknown (36,204). 24 hours after injection, no cleaved form of NHE3 or any change in its expression could be seen when co-injected with membrane-bound serine proteases except in the presence of Tmprss3 where a faint band of lower molecular weight (around 65kDa) could be observed. This band is better seen when NHE3 expression is increased by incubating the oocytes for 48 hours as seen in a second experiment (figure 19).



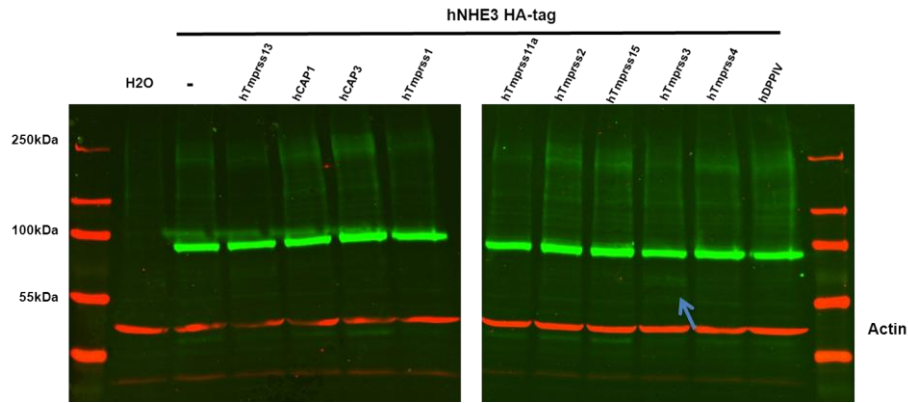


**Figure 18: Effect of membrane-bound serine proteases on NHE3 protein expression (24 hours after injection).** *Xenopus* oocytes were co-injected with 5ng of hNHE3-HA-tag cRNA and 5ng of membrane-bound serine proteases cRNAs as indicated. 24 hours after injection, oocytes were lysed and western blot were performed using anti-HA antibody (in green). Blue arrow indicates the putative cleaved form of NHE3. Actin control is in red.

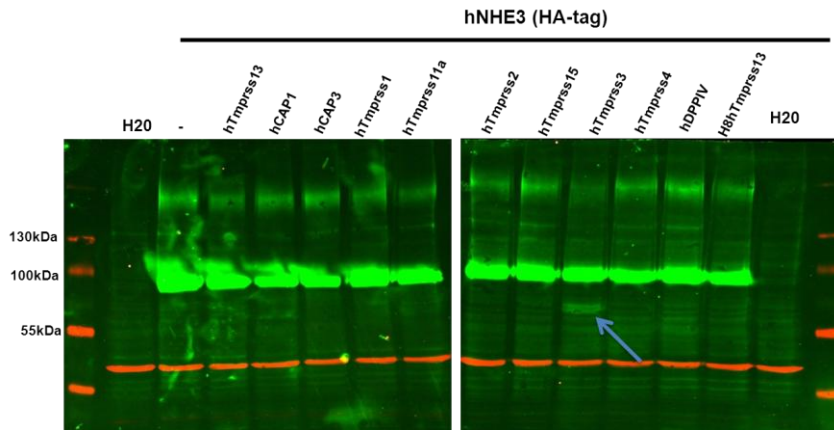


**Figure 19: Effect of membrane-bound serine proteases on NHE3 protein expression (48 hours after injection).** *Xenopus* oocytes were co-injected with 5ng of hNHE3-HA-tag cRNA and 5ng of membrane-bound serine proteases cRNAs as indicated. 48 hours after injection, oocytes were lysed and western blot were performed using anti-HA antibody (in green). Blue arrow indicates the putative cleaved form of NHE3. Actin control is in red.

This extra band, which can be easily detected in every experiment we performed ( $n > 7$ ), was not observed in oocytes injected with Tmprss3 alone, but only in the presence of NHE3, strongly suggesting that this signal represent a cleaved form a NHE3 as seen in figure 20.

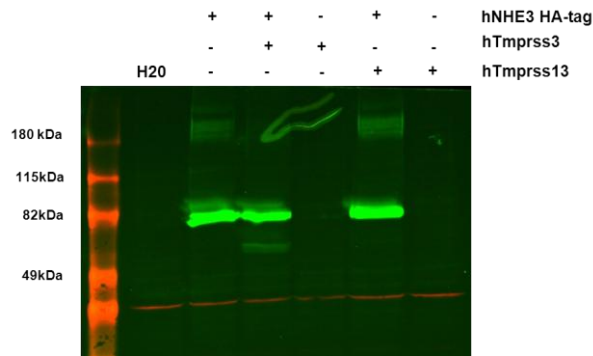


**Figure 20: NHE3 protein expression in *Xenopus* oocytes.** *Xenopus* oocytes were injected with 5ng of hNHE3-HA-tag cRNA and 5ng of Tmprss3 or Tmprss13 cRNAs as indicated. 48 hours after injection, oocytes were lysed and western blot were performed using anti-HA antibody (in green). Actin control is in red.

These experiments were performed using a human construct of NHE3. We were also able to detect this cleaved form of NHE3 using a rat form of NHE3 (figure 21). In this particular experiment, two extra bands were seen for the rat construct but also for the human construct, although the signal is weaker for the human construct.

For all these experiments, 5ng of Tmprss3 cRNA were used. Since it represents a rather high amount of cRNA and this might lead to non-specific and toxic effect on NHE3, we tested whether it was possible to observe the cleaved fragment of NHE3 with lower amounts of Tmprss3 cRNA. Indeed, in oocytes injected with 3ng of NHE3 cRNA, an effect of Tmprss3 was still seen when Tmprss3 cRNA amounts as low as 0.375ng were injected (figure 22). No clear dose-dependent effect was identified; it seems rather that Tmprss3 acts in an all-or-nothing manner because the cleaved form was abruptly lost in another experiment when using Tmprss3 cRNA amount lower than 0.4ng (figure 23). Similarly, very low Spint2 cRNA amounts (0.01ng!) should be injected to prevent the effect of Tmprss3 (figure 23).

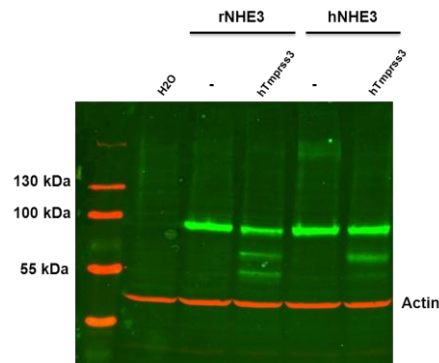


**Figure 21: Effect of Tmprss3 on rat NHE3.** *Xenopus* oocytes were injected with 5ng of rat or human NHE3-HA-tag cRNA and 5ng of as indicated. 48 hours after injection, oocytes were lysed and western blot were performed using anti-HA antibody (in green). Actin control is in red.

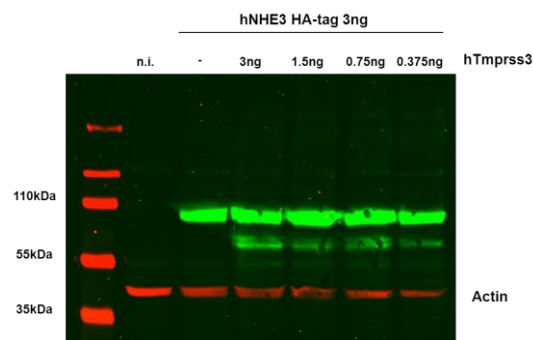


**Figure 22: Effect of injecting decreasing amounts of Tmprss3 on NHE3 expression pattern.** *Xenopus* oocytes were injected with 3ng hNHE3-HA-tag cRNA and decreasing amounts of Tmprss3 cRNA as indicated. 48 hours after injection, oocytes were lysed and western blot were performed using anti-HA antibody (in green). Actin control is in red.

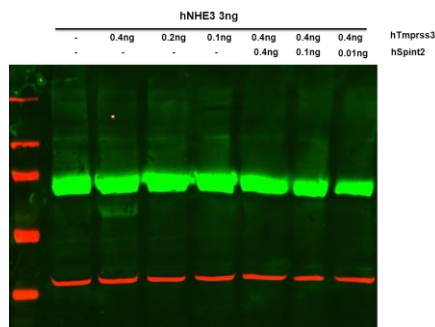


**Figure 23: Inhibition by Spint2 of the Tmprss3-dependent cleavage of NHE3.** *Xenopus* oocytes were injected with 3ng hNHE3-HA-tag cRNA and decreasing amount of Tmprss3 and Spint2 cRNA as indicated. 48 hours after injection, oocytes were lysed and western blot were performed using anti-HA antibody (in green). Actin control is in red.

To assess whether the putative Tmprss3-mediated cleavage of NHE3 occurs at the cell surface, we co-injected oocytes with NHE3 and Tmprss3 and incubate them with extracellular aprotinin, a serine protease inhibitor of Kunitz-type. The cleaved fragment of NHE3 was still

detected even in the presence of extracellular aprotinin (figure 24). This suggests that the effect of Tmprss3 on NHE3 does not occur at the cell surface. However, it is also possible that aprotinin does not inhibit Tmprss3. To address this question, we observed the capacity of extracellularly added aprotinin to block the activating effect of Tmprss3 and CAP1 on the epithelial sodium channel ENaC in *Xenopus* oocytes. Although the activation of ENaC by CAP1 could be fully prevented by extracellular aprotinin, Tmprss3 was only slightly inhibited by aprotinin, whereas full inhibition could be achieved with Spint2 (Figure 25). Thus no clear conclusion can be drawn from these experiments.

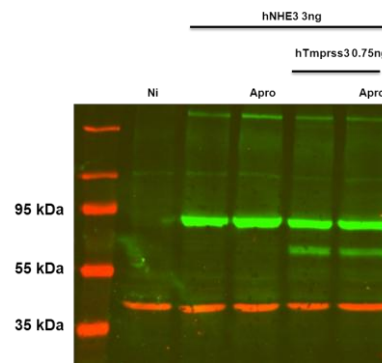


**Figure 24: Effect of aprotinin on Tmprss3-dependent cleavage of NHE3.** *Xenopus* oocytes were injected with 3ng hNHE3-HA-tag cRNA and 0.75ng Tmprss3 cRNA as indicated and then incubated in 100 $\mu$ g/ml aprotinin. 48 hours after injection, oocytes were lysed and western blot were performed using anti-HA antibody (in green). Actin control is in red.

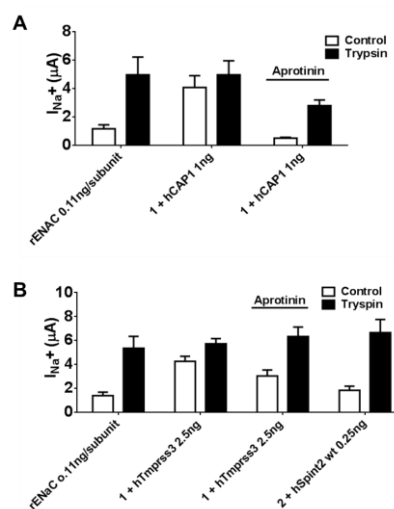


**Figure 25: Inhibitory activity of extracellular aprotinin on CAP1 and Tmprss3.** *Xenopus* oocytes were injected with 0.11ng cRNA of each rENaC subunit and CAP1, Tmprss3 and Spint2 cRNA as indicated and incubated with 100 $\mu$ g/ml aprotinin. **A**, effect of aprotinin on CAP1. **B**, effect of aprotinin on Tmprss3. n $\geq$ 8

measured oocytes. ENaC-mediated sodium currents  $I_{Na^+}$  are measured without (grey bars) and with trypsin (5 $\mu$ g/ml) perfused extracellularly (black bars) as a positive control for ENaC activation.

#### 4.2. Functional consequence of the Tmprss3-dependent cleavage of NHE3

The putative cleavage of NHE3 by Tmprss3 was only examined using a biochemical approach. We thus assessed the potential consequences of such cleavage on the function of NHE3. Since biochemical data were obtained in *Xenopus* oocytes, we used the same heterologous expression system to study the function of Spint2.  $Na^+$  fluxes using  $^{22}Na$  were measured as done in the laboratory of O.W. Moe and R.J. Alpern (235,236). Briefly, oocytes are incubated in a Na-free solution pH 6.8 for 30 minutes, then  $^{22}Na$  uptake is performed by transferring the oocytes into a  $^{22}Na$ -containing solution pH 7.4 for 30 minutes and uptake is terminated using an excess volume of ice-cold stop solution (50mM NaCl).

A first experiment was done with non-injected oocytes. Figure 26 shows that some  $^{22}Na$  transport occurs in non-injected oocytes, which can be inhibited by high dose of amiloride (10 $^{-5}$ M). This amiloride-sensitive  $^{22}Na$  uptake suggests that the protocol used here works and that some endogenous NHE activity is present, probably mediated by the ubiquitous NHE1.

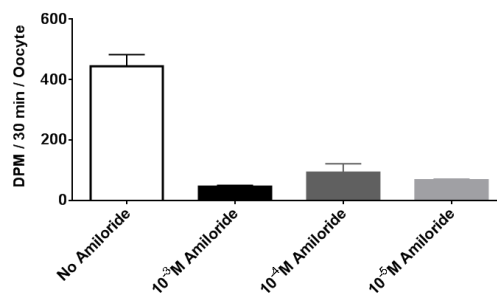


**Figure 26: Amiloride-sensitive  $^{22}Na$  uptake in non-injected *Xenopus* oocytes.** Non-injected oocytes were incubated in  $^{22}Na$  uptake solution to measure NHE activity in the absence or presence of amiloride. n=3 groups of 5 oocytes per condition.

The inhibition constant ( $IC_{50}$ ) of NHE1 and NHE3 for amiloride is around 1 $\mu$ M and 100 $\mu$ M respectively (237). We thus determined in another experiment that a concentration of 5x10 $^{-6}$ M amiloride might be high enough to block any NHE1 endogenous activity but not exogenous activity of NHE3 (figure 27).

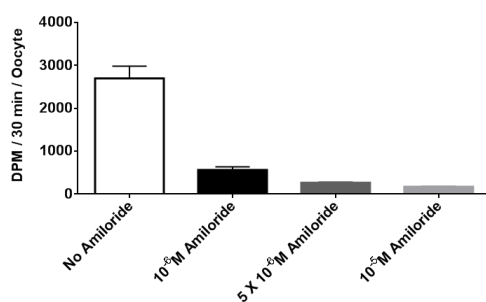


**Figure 27: Inhibition by amiloride of <sup>22</sup>Na uptake in non-injected *Xenopus* oocytes.** Non-injected oocytes were incubated in <sup>22</sup>Na uptake solution to measure NHE activity in the absence or presence of amiloride. n=3 groups of 5 oocytes per condition.

Having set good conditions, <sup>22</sup>Na uptake was next assessed in oocytes injected with human NHE3 cDNA. Surprisingly, we did not observe any increase in <sup>22</sup>Na uptake in NHE3-injected oocytes compared to water-injected oocytes (figure 28), even though <sup>22</sup>Na uptake could be blocked in both condition by amiloride.

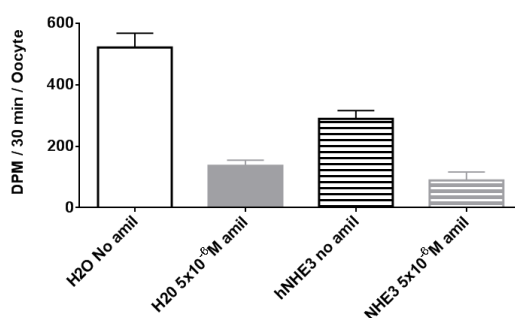


**Figure 28: human NHE3 activity in *Xenopus* oocytes.** Oocytes injected with H2O or 10ng human NHE3 cRNA were incubated (3 days after injection) in <sup>22</sup>Na uptake solution to measure NHE3 activity in the absence or presence of 5x10<sup>-6</sup>M amiloride (in grey). n=3 groups of 5 oocytes per condition.

It is possible that the concentration of amiloride used here inhibits exogenous NHE3 activity. To overcome this issue, we decided to block endogenous NHE activity with ethyl-isopropyl-amiloride (EIPA), which blocks Na-H exchangers more specifically. The IC<sub>50</sub> of human NHE3 for EIPA is around 6 μM, whereas the IC<sub>50</sub> of the putative endogenous NHE in *Xenopus* oocytes (a homolog of NHE1) is 25 nM (237,238). A dose-response experiment done in non-injected oocytes showed that endogenous NHE activity was inhibited by EIPA

with an  $IC_{50}$  of  $4 \times 10^{-7} M$  (figure 29), a value which is between the expected  $IC_{50}$  of the endogenous NHE and the human NHE3, suggesting the possibility that more than one type of NHE is expressed in *Xenopus* oocytes.

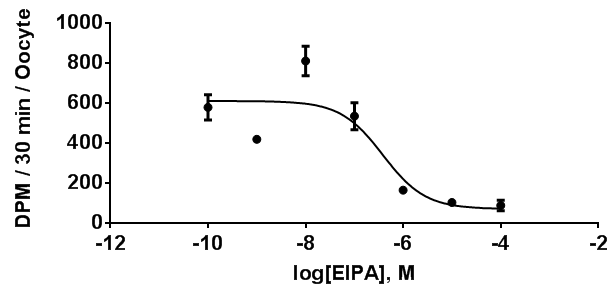


**Figure 29: Inhibition of endogenous NHE activity in non-injected oocytes.** Non-injected were incubated in  $^{22}Na$  uptake solution to measure NHE3 activity in the absence or presence EIPA.  $n=3$  groups of 5 oocytes per condition.

We first used  $10^{-6} M$  of EIPA, because it is supposed to inhibit most of the endogenous NHE activity while blocking only half of the human NHE3 activity. Despite this new protocol, similar results were obtained, namely no difference between water-injected oocytes and NHE3-injected oocytes in the presence or absence of  $10^{-6} M$  EIPA (figure 30). EIPA efficiently inhibited endogenous NHE activity as seen by the decrease in  $^{22}Na$  uptake in every condition.

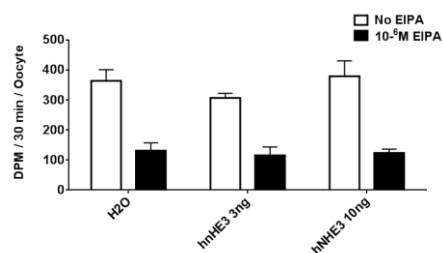


**Figure 30: human NHE3 activity in *Xenopus* oocytes.** Oocytes injected with H2O or human NHE3 cRNA (3ng or 10ng) were incubated (2 days after injection) in  $^{22}Na$  uptake solution to measure NHE3 activity in the absence or presence of  $10^{-6} M$  EIPA (in black).  $n=4$  groups of 5 oocytes per condition.

One explanation for this absence of exogenous human NHE3 activity could be that our construct is for some reason not functional. In another experience, we used a rat NHE3 cDNA

construct known to be functional (cDNA kindly provided by Daniel Fuster from the University of Bern). Oocytes were also injected with one mutant form of rat NHE3, which does not transport  $\text{Na}^+$  (NHE3 E213I). In addition, we also block any endogenous NKCC (Na-K-Cl-cotransporter) activity with  $100\mu\text{M}$  furosemide and the activity of the Na-K-ATPase pump with  $10\mu\text{M}$  ouabain. Unfortunately, there was again no difference in  $^{22}\text{Na}$  uptake in wild-type NHE3 and non-functional NHE3 E213I-injected oocytes, in the presence or absence of *Tmprss3* (figure 31A). However,  $10^{-6}\text{M}$  EIPA was able to block to decrease  $^{22}\text{Na}$  uptake in both conditions (figure 31B).

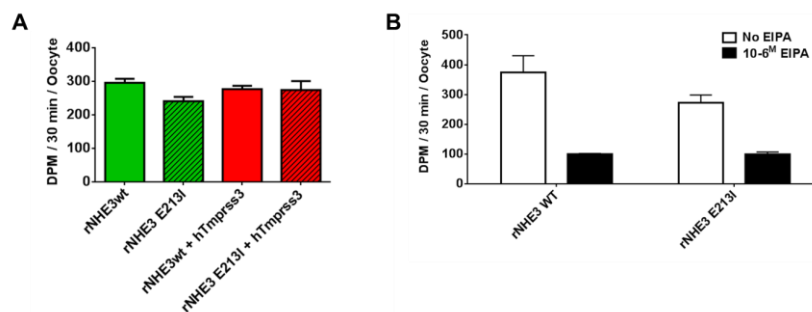


**Figure 31: rat NHE3 activity in *Xenopus* oocytes.** **A)** Oocytes injected with rat NHE3 cRNA (wild-type or mutant E213I) with or without h*Tmprss3* cRNA as indicated were incubated (4 days after injection) in  $^{22}\text{Na}$  uptake solution to measure NHE3 activity. **B)** Same protocol in the absence or presence of  $10^{-6}\text{M}$  EIPA. n=6-8 oocytes per condition measured individually.

The failure to measure any activity of exogenous rat NHE3 may be due to the fact that NHE3 proteins are not express at the cell surface in *Xenopus* oocytes. To answer this question, cell-surface biotinylation was performed. No conclusion could be drawn from this experiment since a lot of non-specific binding of NHE3 to the streptavidin beads as seen in lane 3 and 4 of the bound fraction where oocytes were not biotinylated (figure 32). Such binding could not be prevented by extensive washing steps (3 washes in Lysis Buffer, 2 in high salt buffer and 1 in low salt buffer).



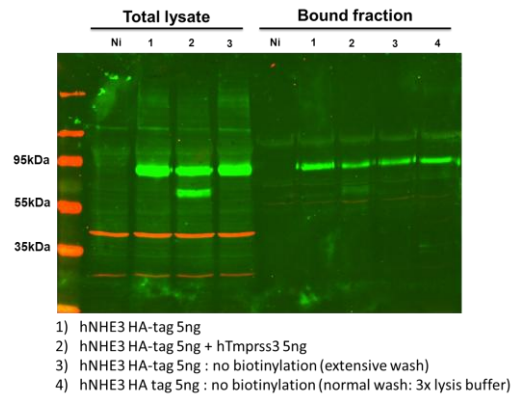


**Figure 32: Cell surface expression of NHE3 in *Xenopus* oocytes.** Oocytes were injected with human NHE3 HA-tag and human Tmprss3 cRNAs as indicated. 48 hours after injection, oocytes were biotinylated (except lane 3 and 4) and total lysate were mixed with streptavidin beads to purify cell surface protein (bound fraction). Anti-HA antibody (in green) is used to detect NHE3 and anti-actin (in red) antibody as negative control for intracellular protein.

# DISCUSSION

## 1. FUNCTIONAL ASSAY IN *XENOPUS* OOCYTES

This discussion is a complement to the discussion that can be found in the manuscript submitted to the Journal of Biological Chemistry. The focus is specifically related to the complementary data presented in the results section of this thesis manuscript.

### 1.1. The R48L and R143L Spint2 mutations

The canonical mechanism for serine protease inhibition involves a key and lock mechanism, where the inhibitor acts as a substrate of the protease that is only very slowly cleaved. In this aspect, the P1 residue in the reactive site of the inhibitor is of particular importance (see intro). We therefore tested functional consequences of mutations in the P1 residue involved in the reactive site of both Kunitz domains of Spint2. As done in two previous studies using a cell-free in vitro approach, we mutated the arginine residues at position 48 and 143 into a leucine residue (90,93). When tested for their inhibitory effect on CAP3, the mutant Spint2 R48L showed a partial loss of function, whereas the Spint2 R143L maintained its full inhibitory activity. A stronger loss of function was observed for the double mutant Spint2 R48L/R143L.

These results suggest that the first inhibitory domain of Spint2 plays an important role in the inhibition of CAP3, confirming the results obtained by Larsen et al in MDCK cells, although the loss of function observed in *Xenopus* oocytes is less dramatic (93). This discrepancy could be explained by the different heterologous expression system used (MDCK cells / *Xenopus* oocytes) and the different readouts used to monitor CAP3 activity; we used the epithelial sodium channel ENaC as reporter gene whereas Larsen et al assessed

biochemically the function of Spint2 as a “protector” of CAP3 from (auto-?) proteolytic activation and degradation. In both cases, an indirect mechanism where Spint2 in fact blocks another protease than CAP3 cannot be excluded. Qin et al have showed in a cell-free in vitro assay using soluble recombinant proteins and the proteolytic processing of HGF as a readout that Spint2 R48L have a strongly reduced capacity to inhibit HGFA compared to Spint2 R143L and wild-type, suggesting again an important role of the first Kunitz domain (90). Interestingly, both mutants were fully functional when assessed with Tmprss2, although this protease has an important homology with CAP3.

The P1 residue is highly conserved among Kunitz inhibitors. Inhibitors that have an arginine or a lysine residue in the P1 position usually inhibit trypsin, whereas a tyrosine, phenylalanine, tryptophane, leucine or methionine residue confers inhibition towards chymotrypsin (148). This highlights a very particular characteristic of serine protease inhibitors; mutating the conserved P1 residue of the reactive site usually does not abolish its function but rather change its capacity to block other types of substrates. Furthermore, residues other than the P1 residue in the inhibitory domain make contacts with the substrate. For these reasons, mutational approaches should be interpreted with caution and it is probably not possible to conclude that the first inhibitory domain is responsible for the inhibition of CAP3, HGFA or other protease based on the sole R to L mutation in the P1 position.

In addition, we showed that the loss of function of Spint2 R48L (first Kunitz domain) and Spint2 Y163C (second Kunitz domain) results in a similar reduced capacity of Spint2 to inhibit CAP3. The double mutant Spint2 R48L/Y163C displays even a larger loss of function than the single mutants. All these results suggest a complex interaction of both Kunitz domains of Spint2 in serine protease inhibition.

## **1.2. Dipeptidyl peptidase IV as putative partner of Spint2**

We also tested in our functional assay the hypothesis that Spint2 could be an inhibitor of the dipeptidyl peptidase IV, DPPIV, a putative regulator of NHE3. DPPIV did not activate ENaC. This might be expected since ENaC is very sensitive to trypsin- or chymotrypsin-like serine protease of the S1 family. DPPIV belongs to the S9 family and is known to cleave proline-containing small peptides, hence its name (161). Despite this issue, we still tried to use ENaC as a reporter gene by co-expressing CAP3 and DPPIV together with ENaC and Spint2. We did not observe any competition between CAP3 and DPPIV for the binding to Spint2 in the competition experiment, suggesting that Spint2 does not inhibit DPPIV. To support this result, no interaction could be detected at the protein level between Spint2 and DPPIV in a pull-down assay. It is thus unlikely that DPPIV plays a role in the pathogenesis of the congenital sodium diarrhea. Moreover, inhibition of DPPIV has been shown to reduce NHE3 activity in rat (210). If we assume that mutations of Spint2 associated with the congenital sodium diarrhea are loss-of-function mutations, increased Na<sup>+</sup> absorption mediated by NHE3 should occur. For all these reasons, we can reasonably rule out DPPIV as a candidate protease in the congenital sodium diarrhea.

## **2. GENERATION OF A SPINT2 KNOCKOUT MOUSE MODEL**

A Spint2 knockout mouse model has already been generated, but display an embryonic lethal phenotype (116,117). To solve this problem, we tried in this work to generate a gut-specific and a tamoxifen-inducible Spint2 knockout mouse model. A gene-trap approach combined with the Cre/lox technology was used here.

In its initial configuration (mutation is active), the conditional gene trap vector construct used in this project reproduced the embryonic lethal phenotype of the constitutive Spint2 knockout mouse model already known from the literature (116,117). We were then able to rescue this embryonic lethality with the overexpression of the FLPe recombinase driven by a ubiquitous promoter that invert the orientation of the construct and thus inactivate the lethal mutation. Reactivation of the mutation was done with the overexpression of the Cre recombinase, either specifically in intestinal cells using the villin promoter or in a tamoxifen-inducible manner in all cells. However, our strategy did not result in the generation of a gut-specific knockout or a tamoxifen-inducible knockout.

No decrease in Spint2 mRNA expression was observed in the gut-specific Villin-Cre model. Absence of Cre expression might explain this very low or even absent recombination rate with the Cre. However, other members of our department have used these Villin-cre expressing mice successfully, suggesting that Cre is correctly expressed in our mice.

Regarding the tamoxifen-inducible model, we observed a maximal reduction in Spint2 mRNA expression of only 50% using two different protocols. This indicates that the system works, namely recombination occurs within the gene trap vector construct and reactivation of the mutation is possible. However, this was not sufficient to completely abolish Spint2 expression. In both models, no clear phenotype could be observed as expected with this modest (or absent) decrease in Spint2 expression.

Assuming that the Cre expressing mice used in this project are functional, the failure of generation of conditional Spint2 knockout mice could be due to the inefficiency of the gene-trap system as designed by Schnutgen et al to abolish Spint2 expression in conditional manner (226). The reasons of this lack of efficiency are multiple.

First, the Cre recombinase may have a limited access to the Spint2 locus resulting in a low recombination rate. To address this hypothesis, it would be necessary to generate a

conditional Spint2 knockout using the classical gene-targeting method. A failure of such an approach would strongly suggest intrinsic problems of the Spint2 locus, while the successful generation a conditional Spint2 knockout mouse model would exclude that the Spint2 locus is somehow “inaccessible” to the Cre.

Second, Cre- or FLPe- mediated recombination is supposed to occur only once since the recognition sites for both recombinases are present as two pairs of sites for each recombinase that cannot recombine together. For example, both LoxP and Lox511 sites are recognized by the Cre but one LoxP site cannot recombine with one Lox511. In addition, sites are arranged in a specific manner so that the system is blocked once the orientation of the gene trap construct has been changed after successful Cre- or FLPe-mediated recombination. However, heterotypic (between LoxP and Lox511 sites for example) recombination has been reported, albeit at low but significant levels (239,240). Thus, if the system cannot block itself as described above, the gene trap construct can recover its initial configuration after one single recombination because of heterotypic recombination. This might easily cause a decrease in efficiency of this conditional gene-trap approach.

Third, the capacity of the gene trap vector construct to recombine in the presence of the FLPe and the Cre recombinases as reported in the original paper was only demonstrated in cell culture. In that study, embryonic stem cells that have one gene trapped by the gene trap vector construct were electroporated with plasmids encoding the Cre or FLPe recombinases and treated with antibiotics to select sublines with strong recombinase expression or very high/very low (depending on the configuration of the gene trap construct) reporter gene cassette expression. In addition to this drastic selection step, they provide data for only two genes. Both genes are localized on the X chromosome. Male derived ES cells were thus used so that analyses were performed on a haploid background, where only one allele has to recombine. Even with these strategies aimed to get maximal efficiency of the system, trapped

gene expression was not completely abolished in one case. Finally, no experimental evidence demonstrated that the system works in mice. To our knowledge, no published article has reported the successful recombination of this conditional gene trap vector construct in vivo, particularly in mice since 2005. Only one group showed in September 2012 that this mechanism was efficient in zebrafish, however (241). This group used a different construct but Cre and FLPe-mediated recombination was based on the same strategy.

Since all these explanations are not mutually exclusive, it becomes likely that the conditional gene trap approach used in our work results in a lack of efficiency to generate a conditional Spint2 knockout mouse model, although it seemed at first to be promising with the rescue of the embryonic lethality with the FLPe recombinase.

It is also important to mention that a classical gene trap-vector construct without Cre/lox technology-based conditional potential may be “leaky”. Indeed, to fully abolish Spint2 normal expression, the gene trap construct requires two important properties. It should have a strong polyadenylation signal leading to premature termination of transcription so that exons of Spint2 located downstream of the construct are not transcribed. Second, the gene trap vector is present in an intronic sequence and contains a splice acceptor site. In our case, the construct was present within the first intron of Spint2. Thus, correct splicing within the first intron is necessary to incorporate the gene trap transcript into the final mRNA. When the mutation is active, correct splicing and premature transcription termination downstream of the gene-trap construct result in the production of a truncated mRNA made of the first intron of Spint2 and the gene-trap reporter cassette. If one of these two properties is not 100% efficient, it may lead to the production of a “normal” mRNA containing all exons of Spint2 without the reporter cassette. To support the relative inefficiency of the gene-trap system, the group of Thomas Bugge generated two KO mouse models of CAP3, one using a classical gene targeting approach and one using a gene trap approach. The “gene-targeting” model was

lethal two days after birth whereas the gene trapping” model was viable and showed a milder phenotype (176,242) suggesting that the “gene trapping” model is not a constitutive KO with a completely abolished expression of CAP3 but a hypomorphic model with some residual expression of CAP3. For example, the authors observed that the newborn mice still have 1% CAP3 mRNA expression in skin compared to wild-type controls and adult mice have up to 12% CAP3 mRNA expression. Kidney and lung of newborn mice already showed a residual mRNA expression of around 10%. Other groups have reported this hypomorphic state of mouse models (243-246). In some situations, a hypomorphic and thus viable mouse model might be an advantage when for example embryonic or early postnatal lethality of the constitutive knockout model hinder biological analyses or experiments. However, expression should be low enough to still observe a phenotype as it is the case for CAP3 but not for Spint2.

Finally, a last problem related to this gene-trap approach is the fact that alternative splicing might interfere with the splicing event that is supposed to integrate the transcript of the reporter cassette to produce a final truncated mRNA molecule. Two isoforms of Spint2 have been described: a full-length isoform with both Kunitz domains and a shorter isoform that lacks the first inhibitory domain (91). The latter is thought to be the major form in mouse, the opposite occurring in human. Since the first Kunitz domain is encoded in the second exon and the gene trap vector construct is found in the first intron (between exon 1 and exon 2), it is possible that alternative splicing may skip the transcription of the gene trap reporter cassette so that transcription of the short isoform occurs and not of a truncated mRNA as expected (247). This provides another explanation for the low efficiency of the gene trap approach used in this work.

In conclusion, based on what has been said above, we recommend avoiding using a gene trap approach for the generation of knockout mouse models. This is particularly true for



gene trap vector constructs with conditional potential based on the Cre-lox technology, for which a successful use in mice still requires a well-demonstrated validation. Classical gene-targeting approaches, although more time-consuming, are more efficient and should be therefore preferred.

### **3. AN EPITHELIAL CELL MODEL FOR SPINT2**

In order to study the physiological role of Spint2 in epithelia, we used the Caco-2 cell line. These cells spontaneously form a monolayer of polarized cells showing enterocytic characteristics when grown on filter. Such monolayers have been widely used as a model for intestinal epithelial barrier either for pharmacological studies or for physiological experiments (248,249).

We showed here that transcripts of Spint2 as well as its homolog Spint1 can be amplified from Caco-2 cells total RNA. These cells also express at the mRNA level several membrane-bound proteases such as CAP1, CAP3 and Tmprss2. Tmprss13, a potential partner of Spint2, is apparently not expressed in Caco-2 cells. But Tmprss13 transcripts have already been detected in small intestine and colon of mice and humans (250). Caco-2 cells also express the sodium-hydrogen exchanger NHE3 and the chloride channel CFTR. Endogenous NHE3 and CFTR activity can be measured in Caco-2 cells (251,252). We also observed a stronger signal of NHE3 expression in polarized cells grown on filter. But CFTR expression was decreased in the same cells. In vivo, NHE3 expression is more abundant in the villous cells, whereas CFTR expression is mainly detected in crypts (37). It is probable that Caco-2 cells, when grown on filter, differentiate into cells that are more similar to villous cells than

cryptic cells, thus explaining the opposite findings about NHE3 and CFTR expression observed in this study.

We have also generated two tagged constructs of Spint2 for protein detection in overexpression studies: one with a FLAG-tag (in the putative extracellular part) and another with a GFP-tag (in the cytosolic region). Both constructs are functional and can be detected at the protein level in Caco-2 cells. Finally, 5 Spint2 shRNA constructs can be used to efficiently knock-down Spint2 in Caco-2 cells.

It is unfortunately difficult to use transfection for experiments with monolayers since effect of transfection is surely lost during the three weeks required for the differentiation of Caco-2 cells. To circumvent this issue, one approach would consist in transfecting the cells just before plating them on filter. Such approach was used to study the formation of tight junctions (253), in particular by Buzza et al to assess the consequence of knocking down the CAP3 gene in the formation of intestinal barrier (179). In such studies, experiments were carried out up to 7 days after transfection. However, this approach is inefficient for physiological experiments done after three weeks of differentiation.

Another approach is to generate stably transfected clones and let them grow on filter in the presence of the selection medium. Our strategy using the transfection reagent Lipofectamine2000 and puromycin for the selection failed to generate either monoclonal or polyclonal populations of stably transfected cells. This could be due to low amounts of transfected cells when starting the selection, the long doubling time of the Caco-2 cells (~ 60 hours) or altered proliferation/differentiation mediated by Spint2 overexpression or knockdown.

To overcome these problems, introduction of foreign cDNA material into caco-2 cells should be done using lentiviral-based transduction system (232). This approach is very

efficient and results in a high proportion of transduced cells so that selection done on cells that are in the majority of cases transduced is much easier.

A last possibility, which seems to be very efficient and relevant for the study of Spint2 in the regulation of ion transport in intestinal tissues is reported by the group of Mark Donowitz (254). In that study, Caco-2 cells are infected with lentiviral particules aimed to knock-down NHERF1, a regulator of the Na-H-exchanger NHE3. Transduced cells are selected with puromycin for 2 or 3 passages. Cells are then plated on filter and during differentiation an adenoviral-based approach is used to transduce polarized cells with NHE3 cDNA, so that the effect of knocking-down NHERF1 on NHE3 activity can be assessed in monolayers of Caco-2 cells.

We cannot exclude that the difficulties we had to get stably transfected clones are a consequence of an efficient knock-down or overexpression of Spint2. Spint2 is thought to play a role in cell proliferation and differentiation. It is thus possible that altering Spint2 expression in Caco2-cells might for example decrease cell proliferation and/or increase cell differentiation so that the culture of such cells becomes very tricky.

#### **4. THE NA-H-EXCHANGER NHE3 AND MEMBRANE-BOUND SERINE PROTEASES**

The Na-H-exchanger NHE3 is a particularly interesting candidate that could be involved in the pathogenesis of the congenital sodium diarrhea. Since, we showed using our functional assay in *Xenopus* oocytes that Spint2 is a potent inhibitor of several intestinal membrane-bound serine proteases, we tested whether theses proteases might regulate the activity of NHE3.

In biochemical experiments, we observed on western blot a specific band that could potentially correspond to a cleaved form of NHE3 that appears when co-expressed with the serine protease Tmprss3. This cleaved form of NHE3 was observed using both the rat and the human form of NHE3 and was not seen with all other proteases used in this assay suggesting a specific Tmprss3-mediated cleavage of NHE3. This is also highlighted by the fact that very small amounts of Tmprss3 cRNA were sufficient to generate the cleaved fragment.

It is still not clear whether this cleavage occurs at the cell surface since both the experiments with extracellular aprotinin and the cell surface biotinylation were non-conclusive. One reason is that NHE3 proteins extracted from non-biotinylated oocytes bind in a non-specific manner to the streptavidin beads even when extensive washing steps are done. This is surprising since there is an abundant literature reporting the successful study of cell surface expression of NHE3 using cell surface biotinylation. It is important to note in every case that cell surface biotinylation was performed in fresh tissues or heterologous expression system other than *Xenopus* oocytes. This raises the possibility that NHE3 expressed in *Xenopus* oocytes can show non-specific binding to the streptavidin beads because of different post-translational modifications occurring in oocytes for example. Such non-specific binding to the streptavidin beads has already been observed for the alpha subunit of ENaC (255,256).

The HA-tag used to reveal NHE3 protein expression in injected oocytes is located at the C-terminal end of NHE3 composed of a large cytosolic region. The cleaved fragment has a molecular weight that is only 10-15kDa lower than the full length NHE3. This indicates that the cleavage occurs in the N-terminal part of NHE3, a region containing the 12 transmembrane segments involved in Na-H-exchange, suggesting that this cleavage could alter the transporting activity of NHE3.

Unfortunately, NHE3 activity could not be detected in *Xenopus* oocytes. We faithfully followed a protocol reported by the laboratories of Moe and Alpern (235,236), which

successfully allows them to observe a significant increase (5 fold in average) in  $^{22}\text{Na}$  uptake in NHE3-injected oocytes compared to water-injected oocytes. Furthermore, these experiments were carried out without the pharmacological inhibition of endogenous Na-H-exchange by EIPA or other blockers. We did not detect any increase in  $^{22}\text{Na}$  uptake in NHE3-injected oocytes likely because of the very high endogenous Na-H-exchange mediated by NHE1 in *Xenopus* oocytes (238). No improvement could be obtained even when using carefully defined concentrations of amiloride and EIPA. We made the observation that endogenous NHE activity varied from batch to batch. The laboratories of Moe and Alpern reported only individual experiments and not pooled data from several independent experiments, raising the possibility that some batches, although rare, might have endogenous NHE activity sufficiently low to measure activity of exogenous NHE3. To avoid issues due to endogenous NHE activity, NHE-deficient cell lines, such as AP1 cells or PS120 cells, are usually used to study the activity of NHE3 (257,258).

Another explanation for this lack of detectable activity of exogenous NHE3 in oocytes could be that only a very small fraction of NHE3 proteins do insert into the plasma membrane. For example, in fibroblast cell lines such as AP1 cells and PS120 cells, only 15%-20% of NHE3 proteins are found at the cell surface (11,259,260). Thus, very low exogenous NHE3 expression at the plasma membrane in the presence of high endogenous NHE activity might easily explain the problems encountered in this project.

Tmprss3 is a membrane-bound serine protease for which loss of function mutations that lead in deafness in humans have been reported (183,184). Tmprss3 is expressed at low levels in stomach, kidney, lung, small intestine, colon and thymus (181,183). Our qPCR data on mouse gastro-intestinal tissues confirmed a low but significant expression of Tmprss3 in the gut with an increased expression in stomach and jejunum (see functional assay in *Xenopus*

oocytes). Interestingly, the role of NHE3 in Na<sup>+</sup> absorption in the gut occurs throughout the gastro-intestinal tract but is particularly important in jejunum.

Proteolytic regulation of NHE3 has never been described so far. The significance of the cleavage of NHE3 observed in *Xenopus* oocytes in the presence of Tmprss3, although consistent, remains elusive. NHE3 has been intensively studied, notably during diarrheal states where its activity is inhibited. In spite of this, a cleaved fragment of NHE3 as seen in our experiments has never been reported so far. Given that we do not know the functional repercussions, if any, of such cleavage, it is difficult to speculate about its physiological role. Although Spint2 is able to potently inhibit Tmprss3 (see functional assay in *Xenopus* oocytes), the mutant associated with the congenital sodium diarrhea Spint2 Y163C still conserve an inhibitory activity on Tmprss3 of about 50% compared to the wild-type form of Spint2. It seems thus unlikely that Tmprss3 plays a role in the congenital sodium diarrhea, even though we cannot rule out any involvement of Tmprss3 solely on these findings. One hypothesis would be that Tmprss3 and Spint2 appear as members of a novel pathway that regulates NHE3 activity in the gut. Alternatively, the physiological role of Tmprss3 in intestinal tissues might not be related to ion transport at all and it is only when Tmprss3 is no longer efficiently inhibited by Spint2, possibly indirectly via a Spint2-CAP1/Tmprss13-Tmprss3 cascade, that uncontrolled proteolytic activity could result in off-targets toxicity such as undesired cleavage of NHE3 leading to a decrease Na-H-exchange in the gut. Such a toxic effect of unopposed proteolytic activity is suggested in our functional assay in *Xenopus* oocytes, where high amounts of membrane-bound serine protease cRNA led to a paradoxical decrease in ENaC-mediated sodium currents (see the case of Tmprss13 for example). All these ideas are pure speculations and work done in Spint2 knockout mouse models and epithelial cell lines are clearly necessary.

# GENERAL CONCLUSIONS AND PERSPECTIVES

In this work, we established a functional assay in *Xenopus* oocytes that allows us to study interactions between Spint2 and gastro-intestinal membrane-bound serine proteases. With this approach, we identified Tmprss13 and CAP1 as potential partners of Spint2 because they were no longer inhibited by the congenital sodium diarrhea mutant Spint2 Y163C. We propose that the highly conserved tyrosine at position 68 and 163 in the first and second Kunitz domains respectively may play a role in the regulation of the binding of Spint 2 to the target protease whereas the mutation of this residue into a cysteine may alter the scaffold of the Kunitz domain. Depending on the serine protease to be blocked, this reduces the inhibitory activity of Spint2 to different extent. How both Kunitz domains of Spint2 participate in membrane-bound serine protease inhibition remains elusive. To better understand how Spint2 inhibits serine proteases, crystallographic studies on Spint2-target complexes could be particularly interesting. In our assay, the expression of the Spint2-Tmprss13 complex was quite abundant. It would be therefore possible to use this data as a basis to elaborate a strategy for a crystallographic approach. Crystals of complex formed by intact membrane-bound serine proteases and inhibitors have never been solved. Only complexes with truncated proteins (catalytic domain of the protease bound to one Kunitz domain) have been studied (164,165). Consequently, crystallographic data of full-length Tmprss13 bound to full-length Spint2 wild-type and mutants (Y68C and Y163C) would be unique and would provide a lot of useful data regarding various aspects such as the interaction between both Kunitz domains and their involvement in Tmprss13 inhibition, the effects of

mutations on the structure of Kunitz domains and the binding to Tmprss13 or the role of the accessory domains of membrane-bound serine proteases that may play a role in protein-protein interaction (261,262). In addition, it may give explanations about how the mutant Spint2 Y163C shows an almost complete loss of inhibitory activity on Tmprss13 in spite of increased binding to the protease.

In this work, we also showed that a gene trap approach combined with the Cre/lox technology was inefficient to generate a conditional Spint2 knockout mouse model. An animal model deficient of Spint2 expression and activity constitutes the best tool to decipher the physiological role of Spint2, provided that Spint2 plays a significant role in mice. In particular, Spint2-deficient animals could be used to identify the ion transporter that is defective in the congenital sodium diarrhea.

A last attempt that should be performed with our gene trap model is to cross Spint2 TRAP mice (homozygous are embryonic lethal) with Frizzy mice (loss-of-function point mutation in the CAP1 gene), since Szabo et al demonstrated that the Frizzy background enables to rescue the embryonic lethality of Spint2 knockout mice and allows postnatal survival (at least up to one day after birth as indicated in their publication) (119). As an alternative to the gene trap approach described in this project, a classical gene-targeting approach should be preferred to generate such animals. Although more time-consuming, gene-targeting has been widely and successfully used to generate knockout mouse models. The Spint2 gene is 28kb long, but critical exons (exon 2 and exon 6) coding for both Kunitz domains are found in region of around 6kb. Thus, it seems feasible to flank this region with lox sites in order to remove almost all exons of Spint2 upon Cre-mediated recombination. Alternatively, it would be also interesting to flank the first exon of Spint2 with lox sites to remove the start codon and the peptide signal, but this approach predicts the putative



existence of an open reading frame encoding a protein truncated in the N-terminal part containing the second Kunitz domain and the transmembrane domain.

New technologies for the generation of genetically modified animal models have arisen recently. Among them, the TALEN (for transcription activator-like effector nucleases) technology looks promising, in particular because it avoids manipulation of embryonic stem cells and thus allows genetic modifications in animals other than mouse such as rats (263,264). Regarding Spint2, several differences exist between mouse and human: 1) constitutive Spint2 knockout mice display embryonic lethality, whereas Spint2 is probably dispensable for human development in utero, 2) the major isoform of Spint2 in mouse lacks the first Kunitz domain, while the major isoform in human has both Kunitz domains. In addition, knockout mouse model do not always recapitulate human genetic diseases, for example CFTR knockout mice do not develop any pulmonary phenotype as seen in patients with cystic fibrosis (216,265). Knockout rats appear therefore as very interesting models. Generating mouse models that overexpress in the gut membrane-bound serine proteases such as Tmprss13 or CAP1 that have been identified in the functional assay in *Xenopus* oocytes as potential targets of Spint2 could also be of great interest.

We started to use Caco-2 cells as an epithelial cell model for Spint2 and showed endogenous expression of Spint2, overexpression of tagged constructs of Spint2 (FLAG and GFP tags) and efficient knock down of Spint2. Because these cells are rather resistant to transfection, a lentiviral-based approach should be used to overcome this problem. The possibility to study the activity of NHE3 and thus its putative regulation by Spint2 in monolayers of polarized and differentiated Caco-2 cells makes this model very useful as an alternative to animal models. Other ion transporters such as the CFTR could be tested in this model, as could be assessed paracellular transport and transepithelial resistance.

We also studied the potential involvement of membrane-bound serine proteases in the regulation of NHE3 in *Xenopus* oocytes and identified a putative cleavage of NHE3 in the presence of Tmprss3. The functional repercussion and physiological relevance of this cleavage is unknown. Since it seems difficult to measure the activity of NHE3 in *Xenopus* oocytes because of high endogenous Na-H-exchange, NHE-deficient cells such AP1 cells or PS120 cells could be used as an alternative model. Finally, it would be interesting to verify whether this cleavage also occur in more physiological models such as Caco-2 cells.

## REFERENCES

1. Kato, A., and Romero, M. F. (2011) Regulation of electroneutral NaCl absorption by the small intestine. *Annu Rev Physiol* **73**, 261-281
2. Field, M. (2003) Intestinal ion transport and the pathophysiology of diarrhea. *J Clin Invest* **111**, 931-943
3. Kunzelmann, K., and Mall, M. (2002) Electrolyte transport in the mammalian colon: mechanisms and implications for disease. *Physiological reviews* **82**, 245-289
4. Kiela, P. R., and Ghishan, F. K. (2009) Ion transport in the intestine. *Current opinion in gastroenterology* **25**, 87-91
5. Ghishan, F. K., and Kiela, P. R. (2012) Small intestinal ion transport. *Current opinion in gastroenterology* **28**, 130-134
6. Schultz, S. G., Fuisz, R. E., and Curran, P. F. (1966) Amino acid and sugar transport in rabbit ileum. *J Gen Physiol* **49**, 849-866
7. Wright, E. M., Loo, D. D., and Hirayama, B. A. (2011) Biology of human sodium glucose transporters. *Physiological reviews* **91**, 733-794
8. Ruxin, J. N. (1994) Magic bullet: the history of oral rehydration therapy. *Medical history* **38**, 363-397
9. Turnberg, L. A., Bieberdorf, F. A., Morawski, S. G., and Fordtran, J. S. (1970) Interrelationships of chloride, bicarbonate, sodium, and hydrogen transport in the human ileum. *J Clin Invest* **49**, 557-567
10. Turnberg, L. A., Fordtran, J. S., Carter, N. W., and Rector, F. C., Jr. (1970) Mechanism of bicarbonate absorption and its relationship to sodium transport in the human jejunum. *J Clin Invest* **49**, 548-556
11. Zachos, N. C., Tse, M., and Donowitz, M. (2005) Molecular physiology of intestinal Na<sup>+</sup>/H<sup>+</sup> exchange. *Annu Rev Physiol* **67**, 411-443
12. Schild, L. (2010) The epithelial sodium channel and the control of sodium balance. *Biochim Biophys Acta* **1802**, 1159-1165
13. Rossier, B. C., Pradervand, S., Schild, L., and Hummler, E. (2002) Epithelial sodium channel and the control of sodium balance: interaction between genetic and environmental factors. *Annu Rev Physiol* **64**, 877-897
14. Schweinfest, C. W., Henderson, K. W., Suster, S., Kondoh, N., and Papas, T. S. (1993) Identification of a colon mucosa gene that is down-regulated in colon adenomas and adenocarcinomas. *Proc Natl Acad Sci U S A* **90**, 4166-4170
15. Lohi, H., Kujala, M., Kerkela, E., Saarialho-Kere, U., Kestila, M., and Kere, J. (2000) Mapping of five new putative anion transporter genes in human and characterization of SLC26A6, a candidate gene for pancreatic anion exchanger. *Genomics* **70**, 102-112
16. Schweinfest, C. W., Spyropoulos, D. D., Henderson, K. W., Kim, J. H., Chapman, J. M., Barone, S., Worrell, R. T., Wang, Z., and Soleimani, M. (2006) slc26a3 (dra)-deficient mice display chloride-losing diarrhea, enhanced colonic proliferation, and distinct up-regulation of ion transporters in the colon. *J Biol Chem* **281**, 37962-37971
17. Soleimani, M. (2006) Expression, regulation and the role of SLC26 Cl<sup>-</sup>/HCO<sub>3</sub><sup>-</sup> exchangers in kidney and gastrointestinal tract. *Novartis Foundation symposium* **273**, 91-102; discussion 103-106, 261-104
18. Wang, Z., Petrovic, S., Mann, E., and Soleimani, M. (2002) Identification of an apical Cl<sup>-</sup>/HCO<sub>3</sub><sup>-</sup> exchanger in the small intestine. *Am J Physiol Gastrointest Liver Physiol* **282**, G573-579

19. Wang, Z., Wang, T., Petrovic, S., Tuo, B., Riederer, B., Barone, S., Lorenz, J. N., Seidler, U., Aronson, P. S., and Soleimani, M. (2005) Renal and intestinal transport defects in Slc26a6-null mice. *Am J Physiol Cell Physiol* **288**, C957-965
20. Walker, N. M., Simpson, J. E., Yen, P. F., Gill, R. K., Rigsby, E. V., Brazill, J. M., Dudeja, P. K., Schweinfest, C. W., and Clarke, L. L. (2008) Down-regulated in adenoma Cl/HCO<sub>3</sub> exchanger couples with Na/H exchanger 3 for NaCl absorption in murine small intestine. *Gastroenterology* **135**, 1645-1653 e1643
21. Seidler, U., Rottinghaus, I., Hillesheim, J., Chen, M., Riederer, B., Krabbenhoft, A., Engelhardt, R., Wiemann, M., Wang, Z., Barone, S., Manns, M. P., and Soleimani, M. (2008) Sodium and chloride absorptive defects in the small intestine in Slc26a6 null mice. *Pflugers Arch* **455**, 757-766
22. Hoglund, P., Haila, S., Socha, J., Tomaszewski, L., Saarialho-Kere, U., Karjalainen-Lindsberg, M. L., Airola, K., Holmberg, C., de la Chapelle, A., and Kere, J. (1996) Mutations of the Down-regulated in adenoma (DRA) gene cause congenital chloride diarrhoea. *Nat Genet* **14**, 316-319
23. De, S. N. (1959) Enterotoxicity of bacteria-free culture-filtrate of *Vibrio cholerae*. *Nature* **183**, 1533-1534
24. Dutta, N. K., Panse, M. V., and Kulkarni, D. R. (1959) Role of cholera toxin in experimental cholera. *J Bacteriol* **78**, 594-595
25. Gangarosa, E. F., Beisel, W. R., Benyajati, C., Sprinz, H., and Piyaratn, P. (1960) The nature of the gastrointestinal lesion in asiatic cholera and its relation to pathogenesis: a biopsy study. *The American journal of tropical medicine and hygiene* **9**, 125-135
26. Field, M. (1971) Ion transport in rabbit ileal mucosa. II. Effects of cyclic 3', 5'-AMP. *Am J Physiol* **221**, 992-997
27. Field, M., Fromm, D., al-Awqati, Q., and Greenough, W. B., 3rd. (1972) Effect of cholera enterotoxin on ion transport across isolated ileal mucosa. *J Clin Invest* **51**, 796-804
28. Kimberg, D. V., Field, M., Johnson, J., Henderson, A., and Gershon, E. (1971) Stimulation of intestinal mucosal adenyl cyclase by cholera enterotoxin and prostaglandins. *J Clin Invest* **50**, 1218-1230
29. Riordan, J. R., Rommens, J. M., Kerem, B., Alon, N., Rozmahel, R., Grzelczak, Z., Zielenski, J., Lok, S., Plavsic, N., Chou, J. L., and et al. (1989) Identification of the cystic fibrosis gene: cloning and characterization of complementary DNA. *Science* **245**, 1066-1073
30. O'Sullivan, B. P., and Freedman, S. D. (2009) Cystic fibrosis. *Lancet* **373**, 1891-1904
31. Donowitz, M., and Welsh, M. J. (1986) Ca<sup>2+</sup> and cyclic AMP in regulation of intestinal Na, K, and Cl transport. *Annu Rev Physiol* **48**, 135-150
32. Cassel, D., and Selinger, Z. (1977) Mechanism of adenylate cyclase activation by cholera toxin: inhibition of GTP hydrolysis at the regulatory site. *Proc Natl Acad Sci U S A* **74**, 3307-3311
33. Bolton, J. E., and Field, M. (1977) Ca ionophore-stimulated ion secretion in rabbit ileal mucosa: relation to actions of cyclic 3',5'-AMP and carbamylcholine. *The Journal of membrane biology* **35**, 159-173
34. Donowitz, M., Cohen, M. E., Gould, M., and Sharp, G. W. (1989) Elevated intracellular Ca<sup>2+</sup> acts through protein kinase C to regulate rabbit ileal NaCl absorption. Evidence for sequential control by Ca<sup>2+</sup>/calmodulin and protein kinase C. *J Clin Invest* **83**, 1953-1962
35. Guandalini, S., Rao, M. C., Smith, P. L., and Field, M. (1982) cGMP modulation of ileal ion transport: in vitro effects of *Escherichia coli* heat-stable enterotoxin. *Am J Physiol* **243**, G36-41

36. Donowitz, M., and Li, X. (2007) Regulatory binding partners and complexes of NHE3. *Physiological reviews* **87**, 825-872
37. Jakab, R. L., Collaco, A. M., and Ameen, N. A. (2011) Physiological relevance of cell-specific distribution patterns of CFTR, NKCC1, NBCe1, and NHE3 along the crypt-villus axis in the intestine. *Am J Physiol Gastrointest Liver Physiol* **300**, G82-98
38. Yun, C. C., Chen, Y., and Lang, F. (2002) Glucocorticoid activation of Na(+)/H(+) exchanger isoform 3 revisited. The roles of SGK1 and NHERF2. *J Biol Chem* **277**, 7676-7683
39. Dieter, M., Palmada, M., Rajamanickam, J., Aydin, A., Busjahn, A., Boehmer, C., Luft, F. C., and Lang, F. (2004) Regulation of glucose transporter SGLT1 by ubiquitin ligase Nedd4-2 and kinases SGK1, SGK3, and PKB. *Obesity research* **12**, 862-870
40. Sindic, A., and Schlatter, E. (2006) Cellular effects of guanylin and uroguanylin. *Journal of the American Society of Nephrology : JASN* **17**, 607-616
41. Schulz, S., Green, C. K., Yuen, P. S., and Garbers, D. L. (1990) Guanylyl cyclase is a heat-stable enterotoxin receptor. *Cell* **63**, 941-948
42. Currie, M. G., Fok, K. F., Kato, J., Moore, R. J., Hamra, F. K., Duffin, K. L., and Smith, C. E. (1992) Guanylin: an endogenous activator of intestinal guanylate cyclase. *Proc Natl Acad Sci U S A* **89**, 947-951
43. Fiskerstrand, T., Arshad, N., Haukanes, B. I., Tronstad, R. R., Pham, K. D., Johansson, S., Havik, B., Tonder, S. L., Levy, S. E., Brackman, D., Boman, H., Biswas, K. H., Apold, J., Hovdenak, N., Visweswariah, S. S., and Knappskog, P. M. (2012) Familial diarrhea syndrome caused by an activating GUCY2C mutation. *N Engl J Med* **366**, 1586-1595
44. Romi, H., Cohen, I., Landau, D., Alkrinawi, S., Yerushalmi, B., Hershkovitz, R., Newman-Heiman, N., Cutting, G. R., Ofir, R., Sivan, S., and Birk, O. S. (2012) Meconium ileus caused by mutations in GUCY2C, encoding the CFTR-activating guanylate cyclase 2C. *Am J Hum Genet* **90**, 893-899
45. Arshad, N., and Visweswariah, S. S. (2012) The multiple and enigmatic roles of guanylyl cyclase C in intestinal homeostasis. *FEBS Lett* **586**, 2835-2840
46. Brierley, S. M. (2012) Guanylate cyclase-C receptor activation: unexpected biology. *Current opinion in pharmacology* **12**, 632-640
47. Valentino, M. A., Lin, J. E., Snook, A. E., Li, P., Kim, G. W., Marszalowicz, G., Magee, M. S., Hyslop, T., Schulz, S., and Waldman, S. A. (2011) A uroguanylin-GUCY2C endocrine axis regulates feeding in mice. *J Clin Invest* **121**, 3578-3588
48. Preston, R. A., Afshartous, D., Forte, L. R., Rodco, R., Alonso, A. B., Garg, D., and Raij, L. (2012) Sodium challenge does not support an acute gastrointestinal-renal natriuretic signaling axis in humans. *Kidney Int* **82**, 1313-1320
49. Gong, R., Ding, C., Hu, J., Lu, Y., Liu, F., Mann, E., Xu, F., Cohen, M. B., and Luo, M. (2011) Role for the membrane receptor guanylyl cyclase-C in attention deficiency and hyperactive behavior. *Science* **333**, 1642-1646
50. Cooke, H. J. (2000) Neurotransmitters in neuronal reflexes regulating intestinal secretion. *Ann N Y Acad Sci* **915**, 77-80
51. Castro, G. A., Harari, Y., and Russell, D. (1987) Mediators of anaphylaxis-induced ion transport changes in small intestine. *Am J Physiol* **253**, G540-548
52. Rocha, F., Musch, M. W., Lishanskiy, L., Bookstein, C., Sugi, K., Xie, Y., and Chang, E. B. (2001) IFN-gamma downregulates expression of Na(+)/H(+) exchangers NHE2 and NHE3 in rat intestine and human Caco-2/bbe cells. *Am J Physiol Cell Physiol* **280**, C1224-1232

53. Clayburgh, D. R., Musch, M. W., Leitges, M., Fu, Y. X., and Turner, J. R. (2006) Coordinated epithelial NHE3 inhibition and barrier dysfunction are required for TNF-mediated diarrhea in vivo. *J Clin Invest* **116**, 2682-2694
54. Berni Canani, R., Terrin, G., Cardillo, G., Tomaiuolo, R., and Castaldo, G. (2010) Congenital diarrheal disorders: improved understanding of gene defects is leading to advances in intestinal physiology and clinical management. *J Pediatr Gastroenterol Nutr* **50**, 360-366
55. Canani, R. B., and Terrin, G. (2011) Recent progress in congenital diarrheal disorders. *Current gastroenterology reports* **13**, 257-264
56. Hoskova, A., Sabacky, J., Mrskos, A., and Pospisil, R. (1980) Severe lactose intolerance with lactosuria and vomiting. *Arch Dis Child* **55**, 304-305
57. Hadorn, B., Tarlow, M. J., Lloyd, J. K., and Wolff, O. H. (1969) Intestinal enterokinase deficiency. *Lancet* **1**, 812-813
58. Holzinger, A., Maier, E. M., Buck, C., Mayerhofer, P. U., Kappler, M., Haworth, J. C., Moroz, S. P., Hadorn, H. B., Sadler, J. E., and Roscher, A. A. (2002) Mutations in the proenteropeptidase gene are the molecular cause of congenital enteropeptidase deficiency. *Am J Hum Genet* **70**, 20-25
59. Jarvela, I., Torniainen, S., and Kolho, K. L. (2009) Molecular genetics of human lactase deficiencies. *Annals of medicine* **41**, 568-575
60. Muller, T., Wijmenga, C., Phillips, A. D., Janecke, A., Houwen, R. H., Fischer, H., Ellemunter, H., Fruhwirth, M., Offner, F., Hofer, S., Muller, W., Booth, I. W., and Heinz-Erian, P. (2000) Congenital sodium diarrhea is an autosomal recessive disorder of sodium/proton exchange but unrelated to known candidate genes. *Gastroenterology* **119**, 1506-1513
61. Heinz-Erian, P., Muller, T., Krabichler, B., Schranz, M., Becker, C., Ruschendorf, F., Nurnberg, P., Rossier, B., Vujic, M., Booth, I. W., Holmberg, C., Wijmenga, C., Grigelioniene, G., Kneepkens, C. M., Rosipal, S., Mistrik, M., Kappler, M., Michaud, L., Doczy, L. C., Siu, V. M., Krantz, M., Zoller, H., Utermann, G., and Janecke, A. R. (2009) Mutations in SPINT2 cause a syndromic form of congenital sodium diarrhea. *Am J Hum Genet* **84**, 188-196
62. Jones, B., Jones, E. L., Bonney, S. A., Patel, H. N., Mensenkamp, A. R., Eichenbaum-Voline, S., Rudling, M., Myrdal, U., Annesi, G., Naik, S., Meadows, N., Quattrone, A., Islam, S. A., Naoumova, R. P., Angelin, B., Infante, R., Levy, E., Roy, C. C., Freemont, P. S., Scott, J., and Shoulders, C. C. (2003) Mutations in a Sar1 GTPase of COPII vesicles are associated with lipid absorption disorders. *Nat Genet* **34**, 29-31
63. Muller, T., Hess, M. W., Schiefermeier, N., Pfaller, K., Ebner, H. L., Heinz-Erian, P., Ponstingl, H., Partsch, J., Rollinghoff, B., Kohler, H., Berger, T., Lenhartz, H., Schlenck, B., Houwen, R. J., Taylor, C. J., Zoller, H., Lechner, S., Goulet, O., Utermann, G., Ruemmele, F. M., Huber, L. A., and Janecke, A. R. (2008) MYO5B mutations cause microvillus inclusion disease and disrupt epithelial cell polarity. *Nat Genet* **40**, 1163-1165
64. Wang, J., Cortina, G., Wu, S. V., Tran, R., Cho, J. H., Tsai, M. J., Bailey, T. J., Jamrich, M., Ament, M. E., Treem, W. R., Hill, I. D., Vargas, J. H., Gershman, G., Farmer, D. G., Reyen, L., and Martin, M. G. (2006) Mutant neurogenin-3 in congenital malabsorptive diarrhea. *N Engl J Med* **355**, 270-280
65. Bennett, C. L., Christie, J., Ramsdell, F., Brunkow, M. E., Ferguson, P. J., Whitesell, L., Kelly, T. E., Saulsbury, F. T., Chance, P. F., and Ochs, H. D. (2001) The immune dysregulation, polyendocrinopathy, enteropathy, X-linked syndrome (IPEX) is caused by mutations of FOXP3. *Nat Genet* **27**, 20-21

66. Gamble, J. L., Fahey, K. R., Appleton, J., and Maclachlan, E. (1945) Congenital Alkalosis with Diarrhea. *Journal of Pediatrics* **26**, 509-518
67. Darrow, D. C. (1945) Congenital Alkalosis with Diarrhea. *Journal of Pediatrics* **26**, 519-532
68. Wedenoja, S., Ormala, T., Berg, U. B., Halling, S. F., Jalanko, H., Karikoski, R., Kere, J., Holmberg, C., and Hoglund, P. (2008) The impact of sodium chloride and volume depletion in the chronic kidney disease of congenital chloride diarrhea. *Kidney Int* **74**, 1085-1093
69. Hihnala, S., Hoglund, P., Lammi, L., Kokkonen, J., Ormala, T., and Holmberg, C. (2006) Long-term clinical outcome in patients with congenital chloride diarrhea. *J Pediatr Gastroenterol Nutr* **42**, 369-375
70. Hoglund, P., Hihnala, S., Kujala, M., Tiitinen, A., Dunkel, L., and Holmberg, C. (2006) Disruption of the SLC26A3-mediated anion transport is associated with male subfertility. *Fertility and sterility* **85**, 232-235
71. Dorwart, M. R., Shcheynikov, N., Yang, D., and Muallem, S. (2008) The solute carrier 26 family of proteins in epithelial ion transport. *Physiology (Bethesda)* **23**, 104-114
72. Wedenoja, S., Pekansaari, E., Hoglund, P., Makela, S., Holmberg, C., and Kere, J. (2011) Update on SLC26A3 mutations in congenital chloride diarrhea. *Hum Mutat* **32**, 715-722
73. Lindquist, B., and Meeuwisse, G. W. (1962) Chronic diarrhoea caused by monosaccharide malabsorption. *Acta Paediatr* **51**, 674-685
74. Hediger, M. A., Coady, M. J., Ikeda, T. S., and Wright, E. M. (1987) Expression cloning and cDNA sequencing of the Na<sup>+</sup>/glucose co-transporter. *Nature* **330**, 379-381
75. Hediger, M. A., Turk, E., and Wright, E. M. (1989) Homology of the human intestinal Na<sup>+</sup>/glucose and Escherichia coli Na<sup>+</sup>/proline cotransporters. *Proc Natl Acad Sci U S A* **86**, 5748-5752
76. Turk, E., Zabel, B., Mundlos, S., Dyer, J., and Wright, E. M. (1991) Glucose/galactose malabsorption caused by a defect in the Na<sup>+</sup>/glucose cotransporter. *Nature* **350**, 354-356
77. Lembo, A. J., Schneier, H. A., Shiff, S. J., Kurtz, C. B., MacDougall, J. E., Jia, X. D., Shao, J. Z., Lavins, B. J., Currie, M. G., Fitch, D. A., Jeglinski, B. I., Eng, P., Fox, S. M., and Johnston, J. M. (2011) Two randomized trials of linaclotide for chronic constipation. *N Engl J Med* **365**, 527-536
78. Kots, A. Y., Choi, B. K., Estrella-Jimenez, M. E., Warren, C. A., Gilbertson, S. R., Guerrant, R. L., and Murad, F. (2008) Pyridopyrimidine derivatives as inhibitors of cyclic nucleotide synthesis: Application for treatment of diarrhea. *Proc Natl Acad Sci U S A* **105**, 8440-8445
79. Holmberg, C., and Perheentupa, J. (1985) Congenital Na<sup>+</sup> diarrhea: a new type of secretory diarrhea. *J Pediatr* **106**, 56-61
80. Booth, I. W., Stange, G., Murer, H., Fenton, T. R., and Milla, P. J. (1985) Defective jejunal brush-border Na<sup>+</sup>/H<sup>+</sup> exchange: a cause of congenital secretory diarrhoea. *Lancet* **1**, 1066-1069
81. Keller, K. M., Wirth, S., Baumann, W., Sule, D., and Booth, I. W. (1990) Defective jejunal brush border membrane sodium/proton exchange in association with lethal familial protracted diarrhoea. *Gut* **31**, 1156-1158
82. Fell, J. M., Miller, M. P., Finkel, Y., and Booth, I. W. (1992) Congenital sodium diarrhea with a partial defect in jejunal brush border membrane sodium transport,

- normal rectal transport, and resolving diarrhea. *J Pediatr Gastroenterol Nutr* **15**, 112-116
83. Kidowaki, T., Funaki, H., Mizuta, R., Nishiki, T., and Takada, H. (1993) Treatment of an infant with congenital sodium diarrhea by oral rehydration. *Acta Paediatr Jpn* **35**, 49-52
  84. Koh, E. T., Chan, D. K., Ho, L. Y., and Yeo, C. L. (1998) Congenital sodium diarrhoea in an Indian girl. *Singapore Med J* **39**, 468-470
  85. Al Makadma, A. S., Al-Akash, S. I., Al Dalaan, I., Al Turaiki, M., and Shabib, S. M. (2004) Congenital sodium diarrhea in a neonate presenting as acute renal failure. *Pediatr Nephrol* **19**, 905-907
  86. Baum, M., Martin, M. G., Booth, I. W., Holmberg, C., Twombly, K., Zhang, Q., Gattineni, J., and Moe, O. (2011) Nucleotide sequence of the Na<sup>+</sup>/H<sup>+</sup> exchanger-8 in patients with congenital sodium diarrhea. *J Pediatr Gastroenterol Nutr* **53**, 474-477
  87. Kawaguchi, T., Qin, L., Shimomura, T., Kondo, J., Matsumoto, K., Denda, K., and Kitamura, N. (1997) Purification and cloning of hepatocyte growth factor activator inhibitor type 2, a Kunitz-type serine protease inhibitor. *J Biol Chem* **272**, 27558-27564
  88. Marlor, C. W., Delaria, K. A., Davis, G., Muller, D. K., Greve, J. M., and Tamburini, P. P. (1997) Identification and cloning of human placental bikunin, a novel serine protease inhibitor containing two Kunitz domains. *J Biol Chem* **272**, 12202-12208
  89. Muller-Pillasch, F., Wallrapp, C., Bartels, K., Varga, G., Friess, H., Buchler, M., Adler, G., and Gress, T. M. (1998) Cloning of a new Kunitz-type protease inhibitor with a putative transmembrane domain overexpressed in pancreatic cancer. *Biochim Biophys Acta* **1395**, 88-95
  90. Qin, L., Denda, K., Shimomura, T., Kawaguchi, T., and Kitamura, N. (1998) Functional characterization of Kunitz domains in hepatocyte growth factor activator inhibitor type 2. *FEBS Lett* **436**, 111-114
  91. Itoh, H., Kataoka, H., Hamasuna, R., Kitamura, N., and Koono, M. (1999) Hepatocyte growth factor activator inhibitor type 2 lacking the first Kunitz-type serine proteinase inhibitor domain is a predominant product in mouse but not in human. *Biochem Biophys Res Commun* **255**, 740-748
  92. Szabo, R., Hobson, J. P., List, K., Molinolo, A., Lin, C. Y., and Bugge, T. H. (2008) Potent inhibition and global co-localization implicate the transmembrane Kunitz-type serine protease inhibitor hepatocyte growth factor activator inhibitor-2 in the regulation of epithelial matriptase activity. *J Biol Chem* **283**, 29495-29504
  93. Larsen, B. R., Steffensen, S. D., Nielsen, N. V., Friis, S., Godiksen, S., Bornholdt, J., Soendergaard, C., Nonboe, A. W., Andersen, M. N., Poulsen, S. S., Szabo, R., Bugge, T. H., Lin, C. Y., Skovbjerg, H., Jensen, J. K., and Vogel, L. K. (2013) Hepatocyte growth factor activator inhibitor-2 prevents shedding of matriptase. *Exp Cell Res*
  94. Delaria, K. A., Muller, D. K., Marlor, C. W., Brown, J. E., Das, R. C., Rocznik, S. O., and Tamburini, P. P. (1997) Characterization of placental bikunin, a novel human serine protease inhibitor. *J Biol Chem* **272**, 12209-12214
  95. Kataoka, H., Itoh, H., Nuki, Y., Hamasuna, R., Naganuma, S., Kitamura, N., and Shimomura, T. (2002) Mouse hepatocyte growth factor (HGF) activator inhibitor type 2 lacking the first Kunitz domain potently inhibits the HGF activator. *Biochem Biophys Res Commun* **290**, 1096-1100
  96. Maurer, E., Gutschow, M., and Stirnberg, M. (2013) Hepatocyte growth factor activator inhibitor type 2 (HAI-2) modulates hepcidin expression by inhibiting cell surface protease matriptase-2. *Biochem J*



97. Kirchhofer, D., Peek, M., Lipari, M. T., Billeci, K., Fan, B., and Moran, P. (2005) Hepsin activates pro-hepatocyte growth factor and is inhibited by hepatocyte growth factor activator inhibitor-1B (HAI-1B) and HAI-2. *FEBS Lett* **579**, 1945-1950
98. Herter, S., Piper, D. E., Aaron, W., Gabriele, T., Cutler, G., Cao, P., Bhatt, A. S., Choe, Y., Craik, C. S., Walker, N., Meininger, D., Hoey, T., and Austin, R. J. (2005) Hepatocyte growth factor is a preferred in vitro substrate for human hepsin, a membrane-anchored serine protease implicated in prostate and ovarian cancers. *Biochem J* **390**, 125-136
99. Hashimoto, T., Kato, M., Shimomura, T., and Kitamura, N. (2010) TMPRSS13, a type II transmembrane serine protease, is inhibited by hepatocyte growth factor activator inhibitor type 1 and activates pro-hepatocyte growth factor. *FEBS J* **277**, 4888-4900
100. Kongkham, P. N., Northcott, P. A., Ra, Y. S., Nakahara, Y., Mainprize, T. G., Croul, S. E., Smith, C. A., Taylor, M. D., and Rutka, J. T. (2008) An epigenetic genome-wide screen identifies SPINT2 as a novel tumor suppressor gene in pediatric medulloblastoma. *Cancer Res* **68**, 9945-9953
101. Dong, W., Chen, X., Xie, J., Sun, P., and Wu, Y. (2010) Epigenetic inactivation and tumor suppressor activity of HAI-2/SPINT2 in gastric cancer. *Int J Cancer* **127**, 1526-1534
102. Nakamura, K., Abarzua, F., Hongo, A., Kodama, J., Nasu, Y., Kumon, H., and Hiramatsu, Y. (2010) Hepatocyte growth factor activator inhibitors (HAI-1 and HAI-2) are potential targets in uterine leiomyosarcoma. *Int J Oncol* **37**, 605-614
103. Bergum, C., and List, K. (2010) Loss of the matriptase inhibitor HAI-2 during prostate cancer progression. *The Prostate* **70**, 1422-1428
104. Nakamura, K., Hongo, A., Kodama, J., and Hiramatsu, Y. (2011) The role of hepatocyte growth factor activator inhibitor (HAI)-1 and HAI-2 in endometrial cancer. *Int J Cancer* **128**, 2613-2624
105. Hamasuna, R., Kataoka, H., Meng, J. Y., Itoh, H., Moriyama, T., Wakisaka, S., and Koono, M. (2001) Reduced expression of hepatocyte growth factor activator inhibitor type-2/placental bikunin (HAI-2/PB) in human glioblastomas: implication for anti-invasive role of HAI-2/PB in glioblastoma cells. *Int J Cancer* **93**, 339-345
106. Fukai, K., Yokosuka, O., Chiba, T., Hirasawa, Y., Tada, M., Imazeki, F., Kataoka, H., and Saisho, H. (2003) Hepatocyte growth factor activator inhibitor 2/placental bikunin (HAI-2/PB) gene is frequently hypermethylated in human hepatocellular carcinoma. *Cancer Res* **63**, 8674-8679
107. Yamauchi, M., Kataoka, H., Itoh, H., Seguchi, T., Hasui, Y., and Osada, Y. (2004) Hepatocyte growth factor activator inhibitor types 1 and 2 are expressed by tubular epithelium in kidney and down-regulated in renal cell carcinoma. *J Urol* **171**, 890-896
108. Morris, M. R., Gentle, D., Abdulrahman, M., Maina, E. N., Gupta, K., Banks, R. E., Wiesener, M. S., Kishida, T., Yao, M., Teh, B., Latif, F., and Maher, E. R. (2005) Tumor suppressor activity and epigenetic inactivation of hepatocyte growth factor activator inhibitor type 2/SPINT2 in papillary and clear cell renal cell carcinoma. *Cancer Res* **65**, 4598-4606
109. Betsunoh, H., Mukai, S., Akiyama, Y., Fukushima, T., Minamiguchi, N., Hasui, Y., Osada, Y., and Kataoka, H. (2007) Clinical relevance of hepsin and hepatocyte growth factor activator inhibitor type 2 expression in renal cell carcinoma. *Cancer Sci* **98**, 491-498
110. Parr, C., and Jiang, W. G. (2006) Hepatocyte growth factor activation inhibitors (HAI-1 and HAI-2) regulate HGF-induced invasion of human breast cancer cells. *Int J Cancer* **119**, 1176-1183

111. Parr, C., Watkins, G., Mansel, R. E., and Jiang, W. G. (2004) The hepatocyte growth factor regulatory factors in human breast cancer. *Clinical cancer research : an official journal of the American Association for Cancer Research* **10**, 202-211
112. Nakamura, K., Abarzua, F., Hongo, A., Kodama, J., Nasu, Y., Kumon, H., and Hiramatsu, Y. (2009) Hepatocyte growth factor activator inhibitor-2 (HAI-2) is a favorable prognosis marker and inhibits cell growth through the apoptotic pathway in cervical cancer. *Ann Oncol* **20**, 63-70
113. Nakamura, K., Abarzua, F., Kodama, J., Hongo, A., Nasu, Y., Kumon, H., and Hiramatsu, Y. (2009) Expression of hepatocyte growth factor activator inhibitors (HAI-1 and HAI-2) in ovarian cancer. *Int J Oncol* **34**, 345-353
114. Tung, E. K., Wong, C. M., Yau, T. O., Lee, J. M., Ching, Y. P., and Ng, I. O. (2009) HAI-2 is epigenetically downregulated in human hepatocellular carcinoma, and its Kunitz domain type 1 is critical for anti-invasive functions. *Int J Cancer* **124**, 1811-1819
115. Generali, D., Fox, S. B., Berruti, A., Moore, J. W., Brizzi, M. P., Patel, N., Allevi, G., Bonardi, S., Aguggini, S., Bersiga, A., Campo, L., Dogliotti, L., Bottini, A., and Harris, A. L. (2007) Regulation of hepatocyte growth factor activator inhibitor 2 by hypoxia in breast cancer. *Clinical cancer research : an official journal of the American Association for Cancer Research* **13**, 550-558
116. Mitchell, K. J., Pinson, K. I., Kelly, O. G., Brennan, J., Zupicich, J., Scherz, P., Leighton, P. A., Goodrich, L. V., Lu, X., Avery, B. J., Tate, P., Dill, K., Pangilinan, E., Wakenight, P., Tessier-Lavigne, M., and Skarnes, W. C. (2001) Functional analysis of secreted and transmembrane proteins critical to mouse development. *Nat Genet* **28**, 241-249
117. Szabo, R., Hobson, J. P., Christoph, K., Kosa, P., List, K., and Bugge, T. H. (2009) Regulation of cell surface protease matriptase by HAI2 is essential for placental development, neural tube closure and embryonic survival in mice. *Development* **136**, 2653-2663
118. Frateschi, S., Keppner, A., Malsure, S., Iwaszkiewicz, J., Sergi, C., Merillat, A. M., Fowler-Jaeger, N., Randrianarison, N., Planes, C., and Hummler, E. (2012) Mutations of the serine protease CAP1/Prss8 lead to reduced embryonic viability, skin defects, and decreased ENaC activity. *Am J Pathol* **181**, 605-615
119. Szabo, R., Uzzun Sales, K., Kosa, P., Shylo, N. A., Godiksen, S., Hansen, K. K., Friis, S., Gutkind, J. S., Vogel, L. K., Hummler, E., Camerer, E., and Bugge, T. H. (2012) Reduced prostatic (CAP1/PRSS8) activity eliminates HAI-1 and HAI-2 deficiency-associated developmental defects by preventing matriptase activation. *PLoS Genet* **8**, e1002937
120. Marchand-Adam, S., Fabre, A., Mailleux, A. A., Marchal, J., Quesnel, C., Kataoka, H., Aubier, M., Dehoux, M., Soler, P., and Crestani, B. (2006) Defect of pro-hepatocyte growth factor activation by fibroblasts in idiopathic pulmonary fibrosis. *American journal of respiratory and critical care medicine* **174**, 58-66
121. Bridges, R. J., Newton, B. B., Pilewski, J. M., Devor, D. C., Poll, C. T., and Hall, R. L. (2001) Na<sup>+</sup> transport in normal and CF human bronchial epithelial cells is inhibited by BAY 39-9437. *Am J Physiol Lung Cell Mol Physiol* **281**, L16-23
122. Coote, K. J., Atherton, H., Young, A., Sugar, R., Burrows, R., Smith, N. J., Schlaeppi, J. M., Groot-Kormelink, P. J., Gosling, M., and Danahay, H. (2008) The guinea-pig tracheal potential difference as an in vivo model for the study of epithelial sodium channel function in the airways. *British journal of pharmacology* **155**, 1025-1033
123. Coote, K., Atherton-Watson, H. C., Sugar, R., Young, A., MacKenzie-Beevor, A., Gosling, M., Bhalay, G., Bloomfield, G., Dunstan, A., Bridges, R. J., Sabater, J. R.,

- Abraham, W. M., Tully, D., Pacoma, R., Schumacher, A., Harris, J., and Danahay, H. (2009) Camostat attenuates airway epithelial sodium channel function in vivo through the inhibition of a channel-activating protease. *The Journal of pharmacology and experimental therapeutics* **329**, 764-774
124. Huang, H. P., Chang, M. H., Chen, Y. T., Hsu, H. Y., Chiang, C. L., Cheng, T. S., Wu, Y. M., Wu, M. Z., Hsu, Y. C., Shen, C. C., Lee, C. N., Chuang, Y. H., Hong, C. L., Jeng, Y. M., Chen, P. H., Chen, H. L., and Lee, M. S. (2012) Persistent elevation of hepatocyte growth factor activator inhibitors in cholangiopathies affects liver fibrosis and differentiation. *Hepatology* **55**, 161-172
125. Shimomura, T., Denda, K., Kitamura, A., Kawaguchi, T., Kito, M., Kondo, J., Kagaya, S., Qin, L., Takata, H., Miyazawa, K., and Kitamura, N. (1997) Hepatocyte growth factor activator inhibitor, a novel Kunitz-type serine protease inhibitor. *J Biol Chem* **272**, 6370-6376
126. Tsuzuki, S., Murai, N., Miyake, Y., Inouye, K., Hirayasu, H., Iwanaga, T., and Fushiki, T. (2005) Evidence for the occurrence of membrane-type serine protease 1/matriptase on the basolateral sides of enterocytes. *Biochem J* **388**, 679-687
127. Kataoka, H., Suganuma, T., Shimomura, T., Itoh, H., Kitamura, N., Nabeshima, K., and Koono, M. (1999) Distribution of hepatocyte growth factor activator inhibitor type 1 (HAI-1) in human tissues. Cellular surface localization of HAI-1 in simple columnar epithelium and its modulated expression in injured and regenerative tissues. *The journal of histochemistry and cytochemistry : official journal of the Histochemistry Society* **47**, 673-682
128. Denda, K., Shimomura, T., Kawaguchi, T., Miyazawa, K., and Kitamura, N. (2002) Functional characterization of Kunitz domains in hepatocyte growth factor activator inhibitor type 1. *J Biol Chem* **277**, 14053-14059
129. Kato, M., Hashimoto, T., Shimomura, T., Kataoka, H., Ohi, H., and Kitamura, N. (2012) Hepatocyte growth factor activator inhibitor type 1 inhibits protease activity and proteolytic activation of human airway trypsin-like protease. *J Biochem* **151**, 179-187
130. Fan, B., Wu, T. D., Li, W., and Kirchhofer, D. (2005) Identification of hepatocyte growth factor activator inhibitor-1B as a potential physiological inhibitor of prostasin. *J Biol Chem* **280**, 34513-34520
131. Lin, C. Y., Anders, J., Johnson, M., and Dickson, R. B. (1999) Purification and characterization of a complex containing matriptase and a Kunitz-type serine protease inhibitor from human milk. *J Biol Chem* **274**, 18237-18242
132. Kojima, K., Tsuzuki, S., Fushiki, T., and Inouye, K. (2008) Roles of functional and structural domains of hepatocyte growth factor activator inhibitor type 1 in the inhibition of matriptase. *J Biol Chem* **283**, 2478-2487
133. Oberst, M. D., Williams, C. A., Dickson, R. B., Johnson, M. D., and Lin, C. Y. (2003) The activation of matriptase requires its noncatalytic domains, serine protease domain, and its cognate inhibitor. *J Biol Chem* **278**, 26773-26779
134. Oberst, M. D., Chen, L. Y., Kiyomiya, K., Williams, C. A., Lee, M. S., Johnson, M. D., Dickson, R. B., and Lin, C. Y. (2005) HAI-1 regulates activation and expression of matriptase, a membrane-bound serine protease. *Am J Physiol Cell Physiol* **289**, C462-470
135. Lee, M. S., Kiyomiya, K., Benaud, C., Dickson, R. B., and Lin, C. Y. (2005) Simultaneous activation and hepatocyte growth factor activator inhibitor 1-mediated inhibition of matriptase induced at activation foci in human mammary epithelial cells. *Am J Physiol Cell Physiol* **288**, C932-941

136. Godiksen, S., Selzer-Plon, J., Pedersen, E. D., Abell, K., Rasmussen, H. B., Szabo, R., Bugge, T. H., and Vogel, L. K. (2008) Hepatocyte growth factor activator inhibitor-1 has a complex subcellular itinerary. *Biochem J* **413**, 251-259
137. Tanaka, H., Nagaike, K., Takeda, N., Itoh, H., Kohama, K., Fukushima, T., Miyata, S., Uchiyama, S., Uchinokura, S., Shimomura, T., Miyazawa, K., Kitamura, N., Yamada, G., and Kataoka, H. (2005) Hepatocyte growth factor activator inhibitor type 1 (HAI-1) is required for branching morphogenesis in the chorioallantoic placenta. *Mol Cell Biol* **25**, 5687-5698
138. Fan, B., Brennan, J., Grant, D., Peale, F., Rangell, L., and Kirchhofer, D. (2007) Hepatocyte growth factor activator inhibitor-1 (HAI-1) is essential for the integrity of basement membranes in the developing placental labyrinth. *Dev Biol* **303**, 222-230
139. Szabo, R., Molinolo, A., List, K., and Bugge, T. H. (2007) Matriptase inhibition by hepatocyte growth factor activator inhibitor-1 is essential for placental development. *Oncogene* **26**, 1546-1556
140. Nagaike, K., Kawaguchi, M., Takeda, N., Fukushima, T., Sawaguchi, A., Kohama, K., Setoyama, M., and Kataoka, H. (2008) Defect of hepatocyte growth factor activator inhibitor type 1/serine protease inhibitor, Kunitz type 1 (Hai-1/Spint1) leads to ichthyosis-like condition and abnormal hair development in mice. *Am J Pathol* **173**, 1464-1475
141. Szabo, R., Kosa, P., List, K., and Bugge, T. H. (2009) Loss of matriptase suppression underlies spint1 mutation-associated ichthyosis and postnatal lethality. *Am J Pathol* **174**, 2015-2022
142. Chen, Y. W., Wang, J. K., Chou, F. P., Chen, C. Y., Rorke, E. A., Chen, L. M., Chai, K. X., Eckert, R. L., Johnson, M. D., and Lin, C. Y. (2010) Regulation of the matriptase-prostasin cell surface proteolytic cascade by hepatocyte growth factor activator inhibitor-1 during epidermal differentiation. *J Biol Chem* **285**, 31755-31762
143. Friis, S., Godiksen, S., Bornholdt, J., Selzer-Plon, J., Rasmussen, H. B., Bugge, T. H., Lin, C. Y., and Vogel, L. K. (2011) Transport via the transcytotic pathway makes prostasin available as a substrate for matriptase. *J Biol Chem* **286**, 5793-5802
144. Kawaguchi, M., Takeda, N., Hoshiko, S., Yorita, K., Baba, T., Sawaguchi, A., Nezu, Y., Yoshikawa, T., Fukushima, T., and Kataoka, H. (2011) Membrane-bound serine protease inhibitor HAI-1 is required for maintenance of intestinal epithelial integrity. *Am J Pathol* **179**, 1815-1826
145. Itoh, H., Kataoka, H., Tomita, M., Hamasuna, R., Nawa, Y., Kitamura, N., and Kono, M. (2000) Upregulation of HGF activator inhibitor type 1 but not type 2 along with regeneration of intestinal mucosa. *Am J Physiol Gastrointest Liver Physiol* **278**, G635-643
146. Parr, C., Sanders, A. J., and Jiang, W. G. (2010) Hepatocyte growth factor activation inhibitors - therapeutic potential in cancer. *Anti-cancer agents in medicinal chemistry* **10**, 47-57
147. Phin, S., Marchand-Adam, S., Fabre, A., Marchal-Somme, J., Bantsimba-Malanda, C., Kataoka, H., Soler, P., and Crestani, B. (2010) Imbalance in the pro-hepatocyte growth factor activation system in bleomycin-induced lung fibrosis in mice. *Am J Respir Cell Mol Biol* **42**, 286-293
148. Laskowski, M., Jr., and Kato, I. (1980) Protein inhibitors of proteinases. *Annual review of biochemistry* **49**, 593-626
149. Turk, B. (2006) Targeting proteases: successes, failures and future prospects. *Nature reviews. Drug discovery* **5**, 785-799
150. Otlewski, J., Jelen, F., Zakrzewska, M., and Oleksy, A. (2005) The many faces of protease-protein inhibitor interaction. *EMBO J* **24**, 1303-1310

151. Krowarsch, D., Cierpicki, T., Jelen, F., and Otlewski, J. (2003) Canonical protein inhibitors of serine proteases. *Cell Mol Life Sci* **60**, 2427-2444
152. Page, M. J., and Di Cera, E. (2008) Serine peptidases: classification, structure and function. *Cell Mol Life Sci* **65**, 1220-1236
153. Hedstrom, L. (2002) Serine protease mechanism and specificity. *Chemical reviews* **102**, 4501-4524
154. Bode, W., and Huber, R. (1992) Natural protein proteinase inhibitors and their interaction with proteinases. *European journal of biochemistry / FEBS* **204**, 433-451
155. Abbenante, G., and Fairlie, D. P. (2005) Protease inhibitors in the clinic. *Med Chem* **1**, 71-104
156. Puente, X. S., Sanchez, L. M., Overall, C. M., and Lopez-Otin, C. (2003) Human and mouse proteases: a comparative genomic approach. *Nat Rev Genet* **4**, 544-558
157. Erez, E., Fass, D., and Bibi, E. (2009) How intramembrane proteases bury hydrolytic reactions in the membrane. *Nature* **459**, 371-378
158. Ciechanover, A. (2012) Intracellular protein degradation: from a vague idea thru the lysosome and the ubiquitin-proteasome system and onto human diseases and drug targeting. *Biochim Biophys Acta* **1824**, 3-13
159. Kaminsky, V., and Zhivotovsky, B. (2012) Proteases in autophagy. *Biochim Biophys Acta* **1824**, 44-50
160. Kunitz, M. (1945) Crystallization of a Trypsin Inhibitor from Soybean. *Science* **101**, 668-669
161. Rawlings, N. D., Barrett, A. J., and Bateman, A. (2012) MEROPS: the database of proteolytic enzymes, their substrates and inhibitors. *Nucleic Acids Res* **40**, D343-350
162. Cierpicki, T., and Otlewski, J. (2002) NMR structures of two variants of bovine pancreatic trypsin inhibitor (BPTI) reveal unexpected influence of mutations on protein structure and stability. *J Mol Biol* **321**, 647-658
163. Eigenbrot, C., Ganesan, R., and Kirchhofer, D. (2010) Hepatocyte growth factor activator (HGFA): molecular structure and interactions with HGFA inhibitor-1 (HAI-1). *FEBS J* **277**, 2215-2222
164. Shia, S., Stamos, J., Kirchhofer, D., Fan, B., Wu, J., Corpuz, R. T., Santell, L., Lazarus, R. A., and Eigenbrot, C. (2005) Conformational lability in serine protease active sites: structures of hepatocyte growth factor activator (HGFA) alone and with the inhibitory domain from HGFA inhibitor-1B. *J Mol Biol* **346**, 1335-1349
165. Friedrich, R., Fuentes-Prior, P., Ong, E., Coombs, G., Hunter, M., Oehler, R., Pierson, D., Gonzalez, R., Huber, R., Bode, W., and Madison, E. L. (2002) Catalytic domain structures of MT-SP1/matriptase, a matrix-degrading transmembrane serine proteinase. *J Biol Chem* **277**, 2160-2168
166. Coppens, M., Eikelboom, J. W., Gustafsson, D., Weitz, J. I., and Hirsh, J. (2012) Translational success stories: development of direct thrombin inhibitors. *Circ Res* **111**, 920-929
167. Grutter, M. G., Priestle, J. P., Rahuel, J., Grossenbacher, H., Bode, W., Hofsteenge, J., and Stone, S. R. (1990) Crystal structure of the thrombin-hirudin complex: a novel mode of serine protease inhibition. *EMBO J* **9**, 2361-2365
168. Rydel, T. J., Ravichandran, K. G., Tulinsky, A., Bode, W., Huber, R., Roitsch, C., and Fenton, J. W., 2nd. (1990) The structure of a complex of recombinant hirudin and human alpha-thrombin. *Science* **249**, 277-280
169. van de Locht, A., Stubbs, M. T., Bode, W., Friedrich, T., Bollschweiler, C., Hoffken, W., and Huber, R. (1996) The ornithodorin-thrombin crystal structure, a key to the TAP enigma? *EMBO J* **15**, 6011-6017

170. Huntington, J. A. (2011) Serpin structure, function and dysfunction. *Journal of thrombosis and haemostasis : JTH* **9 Suppl 1**, 26-34
171. Dubin, G. (2005) Proteinaceous cysteine protease inhibitors. *Cell Mol Life Sci* **62**, 653-669
172. Davies, M. J., and Lomas, D. A. (2008) The molecular aetiology of the serpinopathies. *The international journal of biochemistry & cell biology* **40**, 1273-1286
173. Huntington, J. A., Read, R. J., and Carrell, R. W. (2000) Structure of a serpin-protease complex shows inhibition by deformation. *Nature* **407**, 923-926
174. Szabo, R., and Bugge, T. H. (2011) Membrane-anchored serine proteases in vertebrate cell and developmental biology. *Annu Rev Cell Dev Biol* **27**, 213-235
175. Leyvraz, C., Charles, R. P., Rubera, I., Guitard, M., Rotman, S., Breiden, B., Sandhoff, K., and Hummler, E. (2005) The epidermal barrier function is dependent on the serine protease CAP1/Prss8. *J Cell Biol* **170**, 487-496
176. List, K., Haudenschild, C. C., Szabo, R., Chen, W., Wahl, S. M., Swaim, W., Engelholm, L. H., Behrendt, N., and Bugge, T. H. (2002) Matriptase/MT-SP1 is required for postnatal survival, epidermal barrier function, hair follicle development, and thymic homeostasis. *Oncogene* **21**, 3765-3779
177. Sales, K. U., Masedunskas, A., Bey, A. L., Rasmussen, A. L., Weigert, R., List, K., Szabo, R., Overbeek, P. A., and Bugge, T. H. (2010) Matriptase initiates activation of epidermal pro-kallikrein and disease onset in a mouse model of Netherton syndrome. *Nat Genet* **42**, 676-683
178. List, K., Kosa, P., Szabo, R., Bey, A. L., Wang, C. B., Molinolo, A., and Bugge, T. H. (2009) Epithelial integrity is maintained by a matriptase-dependent proteolytic pathway. *Am J Pathol* **175**, 1453-1463
179. Buzza, M. S., Netzel-Arnett, S., Shea-Donohue, T., Zhao, A., Lin, C. Y., List, K., Szabo, R., Fasano, A., Bugge, T. H., and Antalis, T. M. (2010) Membrane-anchored serine protease matriptase regulates epithelial barrier formation and permeability in the intestine. *Proc Natl Acad Sci U S A* **107**, 4200-4205
180. Vuagniaux, G., Vallet, V., Jaeger, N. F., Hummler, E., and Rossier, B. C. (2002) Synergistic activation of ENaC by three membrane-bound channel-activating serine proteases (mCAP1, mCAP2, and mCAP3) and serum- and glucocorticoid-regulated kinase (Sgk1) in *Xenopus* Oocytes. *J Gen Physiol* **120**, 191-201
181. Guipponi, M., Vuagniaux, G., Wattenhofer, M., Shibuya, K., Vazquez, M., Dougherty, L., Scamuffa, N., Guida, E., Okui, M., Rossier, C., Hancock, M., Buchet, K., Reymond, A., Hummler, E., Marzella, P. L., Kudoh, J., Shimizu, N., Scott, H. S., Antonarakis, S. E., and Rossier, B. C. (2002) The transmembrane serine protease (TMPRSS3) mutated in deafness DFNB8/10 activates the epithelial sodium channel (ENaC) in vitro. *Hum Mol Genet* **11**, 2829-2836
182. Planes, C., Randrianarison, N. H., Charles, R. P., Frateschi, S., Cluzeaud, F., Vuagniaux, G., Soler, P., Clerici, C., Rossier, B. C., and Hummler, E. (2010) ENaC-mediated alveolar fluid clearance and lung fluid balance depend on the channel-activating protease 1. *EMBO Mol Med* **2**, 26-37
183. Scott, H. S., Kudoh, J., Wattenhofer, M., Shibuya, K., Berry, A., Chrast, R., Guipponi, M., Wang, J., Kawasaki, K., Asakawa, S., Minoshima, S., Younus, F., Mehdi, S. Q., Radhakrishna, U., Papasavvas, M. P., Gehrig, C., Rossier, C., Korostishevsky, M., Gal, A., Shimizu, N., Bonne-Tamir, B., and Antonarakis, S. E. (2001) Insertion of beta-satellite repeats identifies a transmembrane protease causing both congenital and childhood onset autosomal recessive deafness. *Nat Genet* **27**, 59-63
184. Guipponi, M., Toh, M. Y., Tan, J., Park, D., Hanson, K., Ballana, E., Kwong, D., Cannon, P. Z., Wu, Q., Gout, A., Delorenzi, M., Speed, T. P., Smith, R. J., Dahl, H.

- H., Petersen, M., Teasdale, R. D., Estivill, X., Park, W. J., and Scott, H. S. (2008) An integrated genetic and functional analysis of the role of type II transmembrane serine proteases (TMPRSSs) in hearing loss. *Hum Mutat* **29**, 130-141
185. Guipponi, M., Tan, J., Cannon, P. Z., Donley, L., Crewther, P., Clarke, M., Wu, Q., Shepherd, R. K., and Scott, H. S. (2007) Mice deficient for the type II transmembrane serine protease, TMPRSS1/hepsin, exhibit profound hearing loss. *Am J Pathol* **171**, 608-616
186. Chan, J. C., Knudson, O., Wu, F., Morser, J., Dole, W. P., and Wu, Q. (2005) Hypertension in mice lacking the proatrial natriuretic peptide convertase corin. *Proc Natl Acad Sci U S A* **102**, 785-790
187. Cui, Y., Wang, W., Dong, N., Lou, J., Srinivasan, D. K., Cheng, W., Huang, X., Liu, M., Fang, C., Peng, J., Chen, S., Wu, S., Liu, Z., Dong, L., Zhou, Y., and Wu, Q. (2012) Role of corin in trophoblast invasion and uterine spiral artery remodelling in pregnancy. *Nature* **484**, 246-250
188. Finberg, K. E., Heeney, M. M., Campagna, D. R., Aydinok, Y., Pearson, H. A., Hartman, K. R., Mayo, M. M., Samuel, S. M., Strouse, J. J., Markianos, K., Andrews, N. C., and Fleming, M. D. (2008) Mutations in TMPRSS6 cause iron-refractory iron deficiency anemia (IRIDA). *Nat Genet* **40**, 569-571
189. Kawano, N., Kang, W., Yamashita, M., Koga, Y., Yamazaki, T., Hata, T., Miyado, K., and Baba, T. (2010) Mice lacking two sperm serine proteases, ACR and PRSS21, are subfertile, but the mutant sperm are infertile in vitro. *Biol Reprod* **83**, 359-369
190. Basel-Vanagaite, L., Attia, R., Ishida-Yamamoto, A., Rainshtein, L., Ben Amitai, D., Lurie, R., Pasmanik-Chor, M., Indelman, M., Zvulunov, A., Saban, S., Magal, N., Sprecher, E., and Shohat, M. (2007) Autosomal recessive ichthyosis with hypotrichosis caused by a mutation in ST14, encoding type II transmembrane serine protease matriptase. *Am J Hum Genet* **80**, 467-477
191. Sales, K. U., Hobson, J. P., Wagenaar-Miller, R., Szabo, R., Rasmussen, A. L., Bey, A., Shah, M. F., Molinolo, A. A., and Bugge, T. H. (2011) Expression and genetic loss of function analysis of the HAT/DESC cluster proteases TMPRSS11A and HAT. *PLoS One* **6**, e23261
192. Kim, T. S., Heinlein, C., Hackman, R. C., and Nelson, P. S. (2006) Phenotypic analysis of mice lacking the Tmprss2-encoded protease. *Mol Cell Biol* **26**, 965-975
193. Brett, C. L., Donowitz, M., and Rao, R. (2005) Evolutionary origins of eukaryotic sodium/proton exchangers. *Am J Physiol Cell Physiol* **288**, C223-239
194. D'Souza, S., Garcia-Cabado, A., Yu, F., Teter, K., Lukacs, G., Skorecki, K., Moore, H. P., Orłowski, J., and Grinstein, S. (1998) The epithelial sodium-hydrogen antiporter Na<sup>+</sup>/H<sup>+</sup> exchanger 3 accumulates and is functional in recycling endosomes. *J Biol Chem* **273**, 2035-2043
195. Bobulescu, I. A., and Moe, O. W. (2009) Luminal Na<sup>(+)</sup>/H<sup>(+)</sup> exchange in the proximal tubule. *Pflugers Arch* **458**, 5-21
196. Schultheis, P. J., Clarke, L. L., Meneton, P., Miller, M. L., Soleimani, M., Gawenis, L. R., Riddle, T. M., Duffy, J. J., Doetschman, T., Wang, T., Giebisch, G., Aronson, P. S., Lorenz, J. N., and Shull, G. E. (1998) Renal and intestinal absorptive defects in mice lacking the NHE3 Na<sup>+</sup>/H<sup>+</sup> exchanger. *Nat Genet* **19**, 282-285
197. Ledoussal, C., Woo, A. L., Miller, M. L., and Shull, G. E. (2001) Loss of the NHE2 Na<sup>(+)</sup>/H<sup>(+)</sup> exchanger has no apparent effect on diarrheal state of NHE3-deficient mice. *Am J Physiol Gastrointest Liver Physiol* **281**, G1385-1396
198. Ledoussal, C., Lorenz, J. N., Nieman, M. L., Soleimani, M., Schultheis, P. J., and Shull, G. E. (2001) Renal salt wasting in mice lacking NHE3 Na<sup>+</sup>/H<sup>+</sup> exchanger but not in mice lacking NHE2. *Am J Physiol Renal Physiol* **281**, F718-727

199. Laubitz, D., Larmonier, C. B., Bai, A., Midura-Kiela, M. T., Lipko, M. A., Thurston, R. D., Kiela, P. R., and Ghishan, F. K. (2008) Colonic gene expression profile in NHE3-deficient mice: evidence for spontaneous distal colitis. *Am J Physiol Gastrointest Liver Physiol* **295**, G63-G77
200. Bobulescu, I. A., and Moe, O. W. (2006) Na<sup>+</sup>/H<sup>+</sup> exchangers in renal regulation of acid-base balance. *Seminars in nephrology* **26**, 334-344
201. Gekle, M., Freudinger, R., and Mildenerger, S. (2001) Inhibition of Na<sup>+</sup>-H<sup>+</sup> exchanger-3 interferes with apical receptor-mediated endocytosis via vesicle fusion. *J Physiol* **531**, 619-629
202. Gekle, M., Drumm, K., Mildenerger, S., Freudinger, R., Gassner, B., and Silbernagl, S. (1999) Inhibition of Na<sup>+</sup>-H<sup>+</sup> exchange impairs receptor-mediated albumin endocytosis in renal proximal tubule-derived epithelial cells from opossum. *J Physiol* **520 Pt 3**, 709-721
203. Zizak, M., Cavet, M. E., Bayle, D., Tse, C. M., Hallen, S., Sachs, G., and Donowitz, M. (2000) Na<sup>(+)</sup>/H<sup>(+)</sup> exchanger NHE3 has 11 membrane spanning domains and a cleaved signal peptide: topology analysis using in vitro transcription/translation. *Biochemistry* **39**, 8102-8112
204. Donowitz, M., Mohan, S., Zhu, C. X., Chen, T. E., Lin, R., Cha, B., Zachos, N. C., Murtazina, R., Sarker, R., and Li, X. (2009) NHE3 regulatory complexes. *The Journal of experimental biology* **212**, 1638-1646
205. Girardi, A. C., Degray, B. C., Nagy, T., Biemesderfer, D., and Aronson, P. S. (2001) Association of Na<sup>(+)</sup>-H<sup>(+)</sup> exchanger isoform NHE3 and dipeptidyl peptidase IV in the renal proximal tubule. *J Biol Chem* **276**, 46671-46677
206. Yu, D. M., Yao, T. W., Chowdhury, S., Nadvi, N. A., Osborne, B., Church, W. B., McCaughan, G. W., and Gorrell, M. D. (2010) The dipeptidyl peptidase IV family in cancer and cell biology. *FEBS J* **277**, 1126-1144
207. Russell-Jones, D., and Gough, S. (2012) Recent advances in incretin-based therapies. *Clinical endocrinology* **77**, 489-499
208. Aroda, V. R., Henry, R. R., Han, J., Huang, W., DeYoung, M. B., Darsow, T., and Hoogwerf, B. J. (2012) Efficacy of GLP-1 receptor agonists and DPP-4 inhibitors: meta-analysis and systematic review. *Clinical therapeutics* **34**, 1247-1258 e1222
209. Girardi, A. C., Knauf, F., Demuth, H. U., and Aronson, P. S. (2004) Role of dipeptidyl peptidase IV in regulating activity of Na<sup>+</sup>/H<sup>+</sup> exchanger isoform NHE3 in proximal tubule cells. *Am J Physiol Cell Physiol* **287**, C1238-1245
210. Girardi, A. C., Fukuda, L. E., Rossoni, L. V., Malnic, G., and Reboucas, N. A. (2008) Dipeptidyl peptidase IV inhibition downregulates Na<sup>+</sup> - H<sup>+</sup> exchanger NHE3 in rat renal proximal tubule. *Am J Physiol Renal Physiol* **294**, F414-422
211. Pacheco, B. P., Crajoinas, R. O., Couto, G. K., Davel, A. P., Lessa, L. M., Rossoni, L. V., and Girardi, A. C. (2011) Dipeptidyl peptidase IV inhibition attenuates blood pressure rising in young spontaneously hypertensive rats. *Journal of hypertension* **29**, 520-528
212. Watten, R. H., Morgan, F. M., Yachai Na, S., Vanikiati, B., and Phillips, R. A. (1959) Water and electrolyte studies in cholera. *J Clin Invest* **38**, 1879-1889
213. Igarashi, T., Inatomi, J., Sekine, T., Cha, S. H., Kanai, Y., Kunimi, M., Tsukamoto, K., Satoh, H., Shimadzu, M., Tozawa, F., Mori, T., Shiobara, M., Seki, G., and Endou, H. (1999) Mutations in SLC4A4 cause permanent isolated proximal renal tubular acidosis with ocular abnormalities. *Nat Genet* **23**, 264-266
214. Romero, M. F., Fulton, C. M., and Boron, W. F. (2004) The SLC4 family of HCO<sub>3</sub><sup>-</sup> transporters. *Pflugers Arch* **447**, 495-509



215. Gawenis, L. R., Bradford, E. M., Prasad, V., Lorenz, J. N., Simpson, J. E., Clarke, L. L., Woo, A. L., Grisham, C., Sanford, L. P., Doetschman, T., Miller, M. L., and Shull, G. E. (2007) Colonic anion secretory defects and metabolic acidosis in mice lacking the NBC1 Na<sup>+</sup>/HCO<sub>3</sub><sup>-</sup> cotransporter. *J Biol Chem* **282**, 9042-9052
216. Snouwaert, J. N., Brigman, K. K., Latour, A. M., Malouf, N. N., Boucher, R. C., Smithies, O., and Koller, B. H. (1992) An animal model for cystic fibrosis made by gene targeting. *Science* **257**, 1083-1088
217. Konrad, M., Schaller, A., Seelow, D., Pandey, A. V., Waldegger, S., Lesslauer, A., Vitzthum, H., Suzuki, Y., Luk, J. M., Becker, C., Schlingmann, K. P., Schmid, M., Rodriguez-Soriano, J., Ariceta, G., Cano, F., Enriquez, R., Juppner, H., Bakkaloglu, S. A., Hediger, M. A., Gallati, S., Neuhaus, S. C., Nurnberg, P., and Weber, S. (2006) Mutations in the tight-junction gene claudin 19 (CLDN19) are associated with renal magnesium wasting, renal failure, and severe ocular involvement. *Am J Hum Genet* **79**, 949-957
218. Simon, D. B., Lu, Y., Choate, K. A., Velazquez, H., Al-Sabban, E., Praga, M., Casari, G., Bettinelli, A., Colussi, G., Rodriguez-Soriano, J., McCredie, D., Milford, D., Sanjad, S., and Lifton, R. P. (1999) Paracellin-1, a renal tight junction protein required for paracellular Mg<sup>2+</sup> resorption. *Science* **285**, 103-106
219. Breiderhoff, T., Himmerkus, N., Stuiver, M., Mutig, K., Will, C., Meij, I. C., Bachmann, S., Bleich, M., Willnow, T. E., and Muller, D. (2012) Deletion of claudin-10 (Cldn10) in the thick ascending limb impairs paracellular sodium permeability and leads to hypermagnesemia and nephrocalcinosis. *Proc Natl Acad Sci U S A* **109**, 14241-14246
220. Muto, S., Hata, M., Taniguchi, J., Tsuruoka, S., Moriwaki, K., Saitou, M., Furuse, K., Sasaki, H., Fujimura, A., Imai, M., Kusano, E., Tsukita, S., and Furuse, M. (2010) Claudin-2-deficient mice are defective in the leaky and cation-selective paracellular permeability properties of renal proximal tubules. *Proc Natl Acad Sci U S A* **107**, 8011-8016
221. Tamura, A., Hayashi, H., Imasato, M., Yamazaki, Y., Hagiwara, A., Wada, M., Noda, T., Watanabe, M., Suzuki, Y., and Tsukita, S. (2011) Loss of claudin-15, but not claudin-2, causes Na<sup>+</sup> deficiency and glucose malabsorption in mouse small intestine. *Gastroenterology* **140**, 913-923
222. Lin, C. Y., Tseng, I. C., Chou, F. P., Su, S. F., Chen, Y. W., Johnson, M. D., and Dickson, R. B. (2008) Zymogen activation, inhibition, and ectodomain shedding of matriptase. *Front Biosci* **13**, 621-635
223. Koller, B. H., and Smithies, O. (1992) Altering genes in animals by gene targeting. *Annual review of immunology* **10**, 705-730
224. Stanford, W. L., Cohn, J. B., and Cordes, S. P. (2001) Gene-trap mutagenesis: past, present and beyond. *Nat Rev Genet* **2**, 756-768
225. Nagy, A. (2000) Cre recombinase: the universal reagent for genome tailoring. *Genesis* **26**, 99-109
226. Schnutgen, F., De-Zolt, S., Van Sloun, P., Hollatz, M., Floss, T., Hansen, J., Altschmied, J., Seisenberger, C., Ghyselinck, N. B., Ruiz, P., Chambon, P., Wurst, W., and von Melchner, H. (2005) Genomewide production of multipurpose alleles for the functional analysis of the mouse genome. *Proc Natl Acad Sci U S A* **102**, 7221-7226
227. Farley, F. W., Soriano, P., Steffen, L. S., and Dymecki, S. M. (2000) Widespread recombinase expression using FLP<sub>er</sub> (flipper) mice. *Genesis* **28**, 106-110

228. el Marjou, F., Janssen, K. P., Chang, B. H., Li, M., Hindie, V., Chan, L., Louvard, D., Chambon, P., Metzger, D., and Robine, S. (2004) Tissue-specific and inducible Cre-mediated recombination in the gut epithelium. *Genesis* **39**, 186-193
229. Hayashi, S., and McMahon, A. P. (2002) Efficient recombination in diverse tissues by a tamoxifen-inducible form of Cre: a tool for temporally regulated gene activation/inactivation in the mouse. *Dev Biol* **244**, 305-318
230. Kohan, D. E. (2008) Progress in gene targeting: using mutant mice to study renal function and disease. *Kidney Int* **74**, 427-437
231. Pinto, M., Robineleon, S., Appay, M. D., Kedinger, M., Triadou, N., Dussaulx, E., Lacroix, B., Simonassmann, P., Haffen, K., Fogh, J., and Zweibaum, A. (1983) Enterocyte-Like Differentiation and Polarization of the Human-Colon Carcinoma Cell-Line Caco-2 in Culture. *Biol Cell* **47**, 323-330
232. Bibert, S., Aebischer, D., Desgranges, F., Roy, S., Schaer, D., Kharoubi-Hess, S., Horisberger, J. D., and Geering, K. (2009) A link between FXD3 (Mat-8)-mediated Na,K-ATPase regulation and differentiation of Caco-2 intestinal epithelial cells. *Mol Biol Cell* **20**, 1132-1140
233. Longet, S., Miled, S., Lotscher, M., Miescher, S. M., Zuercher, A. W., and Cortesy, B. (2013) Human Plasma-derived Polymeric IgA and IgM Antibodies Associate with Secretory Component to Yield Biologically Active Secretory-like Antibodies. *J Biol Chem* **288**, 4085-4094
234. Rossier, B. C., and Stutts, M. J. (2009) Activation of the epithelial sodium channel (ENaC) by serine proteases. *Annu Rev Physiol* **71**, 361-379
235. Moe, O. W., Amemiya, M., and Yamaji, Y. (1995) Activation of protein kinase A acutely inhibits and phosphorylates Na/H exchanger NHE-3. *J Clin Invest* **96**, 2187-2194
236. Amemiya, M., Yamaji, Y., Cano, A., Moe, O. W., and Alpern, R. J. (1995) Acid incubation increases NHE-3 mRNA abundance in OKP cells. *Am J Physiol* **269**, C126-133
237. Brant, S. R., Yun, C. H., Donowitz, M., and Tse, C. M. (1995) Cloning, tissue distribution, and functional analysis of the human Na<sup>+</sup>/H<sup>+</sup> exchanger isoform, NHE3. *Am J Physiol* **269**, C198-206
238. Busch, S., Roskopf, D., Lang, H. J., Weichert, A., and Siffert, W. (1998) Expression, functional characterization and tissue distribution of a Na<sup>+</sup>/H<sup>+</sup> exchanger cloned from *Xenopus laevis* oocytes (XL-NHE). *Pflugers Arch* **436**, 828-833
239. Kolb, A. F. (2001) Selection-marker-free modification of the murine beta-casein gene using a lox2272 [correction of lox2722] site. *Analytical biochemistry* **290**, 260-271
240. Lauth, M., Moerl, K., Barski, J. J., and Meyer, M. (2000) Characterization of Cre-mediated cassette exchange after plasmid microinjection in fertilized mouse oocytes. *Genesis* **27**, 153-158
241. Ni, T. T., Lu, J., Zhu, M., Maddison, L. A., Boyd, K. L., Huskey, L., Ju, B., Hesselson, D., Zhong, T. P., Page-McCaw, P. S., Stainier, D. Y., and Chen, W. (2012) Conditional control of gene function by an invertible gene trap in zebrafish. *Proc Natl Acad Sci U S A* **109**, 15389-15394
242. List, K., Currie, B., Scharschmidt, T. C., Szabo, R., Shireman, J., Molinolo, A., Cravatt, B. F., Segre, J., and Bugge, T. H. (2007) Autosomal ichthyosis with hypotrichosis syndrome displays low matriptase proteolytic activity and is phenocopied in ST14 hypomorphic mice. *J Biol Chem* **282**, 36714-36723
243. Ferretti, E., Villaescusa, J. C., Di Rosa, P., Fernandez-Diaz, L. C., Longobardi, E., Mazzieri, R., Miccio, A., Micali, N., Selleri, L., Ferrari, G., and Blasi, F. (2006) Hypomorphic mutation of the TALE gene Prep1 (pKnox1) causes a major reduction

- of Pbx and Meis proteins and a pleiotropic embryonic phenotype. *Mol Cell Biol* **26**, 5650-5662
244. Holst, C. R., Bou-Reslan, H., Gore, B. B., Wong, K., Grant, D., Chalasani, S., Carano, R. A., Frantz, G. D., Tessier-Lavigne, M., Bolon, B., French, D. M., and Ashkenazi, A. (2007) Secreted sulfatases Sulf1 and Sulf2 have overlapping yet essential roles in mouse neonatal survival. *PLoS One* **2**, e575
245. Malureanu, L., Jeganathan, K. B., Jin, F., Baker, D. J., van Ree, J. H., Gullon, O., Chen, Z., Henley, J. R., and van Deursen, J. M. (2010) Cdc20 hypomorphic mice fail to counteract de novo synthesis of cyclin B1 in mitosis. *J Cell Biol* **191**, 313-329
246. Wilson, M. P., Hugge, C., Bielinska, M., Nicholas, P., Majerus, P. W., and Wilson, D. B. (2009) Neural tube defects in mice with reduced levels of inositol 1,3,4-trisphosphate 5/6-kinase. *Proc Natl Acad Sci U S A* **106**, 9831-9835
247. Itoh, H., Kataoka, H., Meng, J. Y., Hamasuna, R., Kitamura, N., and Koono, M. (2001) Mouse hepatocyte growth factor activator inhibitor type 1 (HAI-1) and type 2 (HAI-2)/placental bikunin genes and their promoters. *Biochim Biophys Acta* **1519**, 92-95
248. Sambuy, Y., De Angelis, I., Ranaldi, G., Scarino, M. L., Stammati, A., and Zucco, F. (2005) The Caco-2 cell line as a model of the intestinal barrier: influence of cell and culture-related factors on Caco-2 cell functional characteristics. *Cell biology and toxicology* **21**, 1-26
249. Sun, H., Chow, E. C. Y., Liu, S., Du, Y., and Pang, K. S. (2008) The Caco-2 cell monolayer: usefulness and limitations. *Expert Opin Drug Met* **4**, 395-411
250. Kido, H., Okumura, Y., Takahashi, E., Pan, H. Y., Wang, S., Chida, J., Le, T. Q., and Yano, M. (2008) Host envelope glycoprotein processing proteases are indispensable for entry into human cells by seasonal and highly pathogenic avian influenza viruses. *J Mol Genet Med* **3**, 167-175
251. Janecki, A. J., Montrose, M. H., Tse, C. M., de Medina, F. S., Zweibaum, A., and Donowitz, M. (1999) Development of an endogenous epithelial Na<sup>(+)</sup>/H<sup>(+)</sup> exchanger (NHE3) in three clones of caco-2 cells. *Am J Physiol* **277**, G292-305
252. Cao, L., Owsianik, G., Jaspers, M., Janssens, A., Cuppens, H., Cassiman, J. J., and Nilius, B. (2003) Functional analysis of CFTR chloride channel activity in cells with elevated MDR1 expression. *Biochem Biophys Res Commun* **304**, 248-252
253. Raleigh, D. R., Boe, D. M., Yu, D., Weber, C. R., Marchiando, A. M., Bradford, E. M., Wang, Y., Wu, L., Schneeberger, E. E., Shen, L., and Turner, J. R. (2011) Occludin S408 phosphorylation regulates tight junction protein interactions and barrier function. *J Cell Biol* **193**, 565-582
254. Sarker, R., Valkhoff, V. E., Zachos, N. C., Lin, R., Cha, B., Chen, T. E., Guggino, S., Zizak, M., de Jonge, H., Hogema, B., and Donowitz, M. (2011) NHERF1 and NHERF2 are necessary for multiple but usually separate aspects of basal and acute regulation of NHE3 activity. *Am J Physiol Cell Physiol* **300**, C771-782
255. Frindt, G., Ergonul, Z., and Palmer, L. G. (2008) Surface expression of epithelial Na channel protein in rat kidney. *J Gen Physiol* **131**, 617-627
256. Frindt, G., and Palmer, L. G. (2009) Surface expression of sodium channels and transporters in rat kidney: effects of dietary sodium. *Am J Physiol Renal Physiol* **297**, F1249-1255
257. Pouyssegur, J., Sardet, C., Franchi, A., L'Allemain, G., and Paris, S. (1984) A specific mutation abolishing Na<sup>+</sup>/H<sup>+</sup> antiport activity in hamster fibroblasts precludes growth at neutral and acidic pH. *Proc Natl Acad Sci U S A* **81**, 4833-4837
258. Rotin, D., and Grinstein, S. (1989) Impaired cell volume regulation in Na<sup>(+)</sup>-H<sup>+</sup> exchange-deficient mutants. *Am J Physiol* **257**, C1158-1165

259. Janecki, A. J., Janecki, M., Akhter, S., and Donowitz, M. (2000) Quantitation of plasma membrane expression of a fusion protein of Na/H exchanger NHE3 and green fluorescence protein (GFP) in living PS120 fibroblasts. *The journal of histochemistry and cytochemistry : official journal of the Histochemistry Society* **48**, 1479-1492
260. Kurashima, K., Szabo, E. Z., Lukacs, G., Orłowski, J., and Grinstein, S. (1998) Endosomal recycling of the Na<sup>+</sup>/H<sup>+</sup> exchanger NHE3 isoform is regulated by the phosphatidylinositol 3-kinase pathway. *J Biol Chem* **273**, 20828-20836
261. Inouye, K., Tsuzuki, S., Yasumoto, M., Kojima, K., Mochida, S., and Fushiki, T. (2010) Identification of the matriptase second CUB domain as the secondary site for interaction with hepatocyte growth factor activator inhibitor type-1. *J Biol Chem* **285**, 33394-33403
262. Kojima, K., Tsuzuki, S., Fushiki, T., and Inouye, K. (2009) Role of the stem domain of matriptase in the interaction with its physiological inhibitor, hepatocyte growth factor activator inhibitor type I. *J Biochem* **145**, 783-790
263. Joung, J. K., and Sander, J. D. (2013) TALENs: a widely applicable technology for targeted genome editing. *Nature reviews. Molecular cell biology* **14**, 49-55
264. Tesson, L., Usal, C., Menoret, S., Leung, E., Niles, B. J., Remy, S., Santiago, Y., Vincent, A. I., Meng, X., Zhang, L., Gregory, P. D., Anegón, I., and Cost, G. J. (2011) Knockout rats generated by embryo microinjection of TALENs. *Nat Biotechnol* **29**, 695-696
265. Grubb, B. R., and Boucher, R. C. (1999) Pathophysiology of gene-targeted mouse models for cystic fibrosis. *Physiological reviews* **79**, S193-214

## RÉSUMÉ DESTINÉ À UN LARGE PUBLIC

La diarrhée est un problème de santé très fréquent dans le monde. Heureusement, la plupart des cas se résolvent spontanément. Cependant, une diarrhée peut parfois provoquer une déshydratation suffisamment importante pour mener à la mort ou persister pendant des semaines, mois ou années et diminuer considérablement la qualité de vie.

Il est donc impératif de mettre au point de nouveaux médicaments pour traiter ce problème et ceci implique notamment une bonne compréhension des mécanismes permettant l'absorption d'eau et de sels minéraux dans l'intestin. Dans ce but, les maladies génétiques, bien que rares, sont d'une grande aide dans la mesure où elles indiquent aux chercheurs un gène d'intérêt et donc une cible de potentiels nouveaux médicaments.

La diarrhée congénitale de sodium est l'une de ces maladies. Cette pathologie est caractérisée chez les enfants qui en sont atteints par une diarrhée très sévère et le plus souvent mortelle. Cette diarrhée entraîne la perte spécifique de sodium qui est un sel minéral particulièrement important de notre organisme. Des mutations dans le gène *Spint2* ont été identifiées chez des malades.

Le gène *Spint2* code pour un inhibiteur de protéase. Une protéase est une protéine capable de couper ou « digérer » en des points précis une autre protéine. *Spint2* empêche donc cette « digestion ». Le rôle de *Spint2* dans l'intestin, ainsi que la protéase bloquée par *Spint2* nous sont totalement inconnus.

Durant ce travail, des expériences effectuées dans un modèle cellulaire ont permis d'identifier deux nouvelles cibles potentielles de *Spint2*, à savoir les sérines protéases transmembranaires *CAP1* et *Tmprss13*. Un effet de la sérine protéase *Tmprss3* sur *NHE3*, une protéine responsable de l'absorption de sodium dans l'intestin, a pu être mis en évidence. Cependant, ces résultats n'ont malheureusement pas pu être vérifiés dans un organisme vivant.

Ces données représentent une première étape vers une meilleure compréhension de la diarrhée congénitale de sodium et permettent d'établir de nouvelles hypothèses quant au rôle de *Spint2*. Des expériences supplémentaires sont nécessaires en vue d'élucider les mécanismes causant la diarrhée congénitale de sodium.

# **ANNEXE**

Manuscript of the article submitted to the Journal of Biological Chemistry (currently under the reviewing process)

Functional analysis of a missense mutation in the serine protease inhibitor Spint2/HAI-2 associated with congenital sodium diarrhea\*

Nicolas Faller<sup>1</sup>, Ivan Gautschi, and Laurent Schild<sup>2</sup>

From the Department of Pharmacology and Toxicology, University of Lausanne, 1005 Lausanne, Switzerland

\*Running title: *Serine protease inhibition by Spint2 in Xenopus oocytes*

<sup>1</sup>This work was supported by a grant from the Swiss National Science Foundation (323530-128871, MD-PhD Program of the Swiss Academy of Medical Sciences) to NF.

<sup>2</sup>To whom correspondence should be addressed: Dept. of Pharmacology and Toxicology, University of Lausanne, Rue du Bugnon 27, 1005 Lausanne, Switzerland, Tel: 41-21-692-53-80, Fax: 41-21-692-53-55, E-mail: [Laurent.Schild@unil.ch](mailto:Laurent.Schild@unil.ch)

**Keywords:** serine protease inhibitor, Spint2/HAI-2, membrane-bound serine protease, congenital sodium diarrhea, ENaC

---

**Background:** Mutations in the serine protease inhibitor Spint2 are linked to congenital sodium diarrhea.

**Results:** The Spint2 Y163C mutant no longer inhibited the intestinal membrane-bound serine proteases CAP1 and Tmprss13 in *Xenopus* oocytes.

**Conclusion:** CAP1 and Tmprss13 are putative physiological partners of Spint2 in the intestine.

**Significance:** Our functional assay identifies targets of membrane-bound serine protease inhibitors and may help in deciphering the physiological role of Spint2.

## SUMMARY

**Membrane-bound serine proteases play important roles in different biological processes. Their regulation by endogenous inhibitors is poorly understood. A Y163C mutation in the Spint2 gene encoding a serine protease inhibitor has been associated with congenital sodium diarrhea, suggesting a role of serine proteases in water/electrolyte balance in intestinal tissues. However, physiological targets of Spint2 remain to be identified. We established a novel cellular assay in *Xenopus laevis* oocytes to study functional interactions between Spint2 and candidate membrane-bound serine proteases expressed in the gastro-intestinal tract. We found that the wild-type form of Spint2 was a potent inhibitor of nine gastro-intestinal serine proteases. The Y163C**

**mutation in the second Kunitz domain of Spint2 induced a complete loss of inhibitory activity on only two proteases, CAP1/prostasin and Tmprss13. Parallel analysis of the homologous mutation Y68C in the first Kunitz domain of Spint2 revealed differential involvement of the Kunitz domains in serine protease inhibition. Finally, the loss of function of the Y163C mutant was not due to an impaired binding interaction between Tmprss13 and Spint2. Based on these observations, we propose that CAP1/prostasin and Tmprss13 represent potential targets for Spint2 in controlling Na<sup>+</sup> absorption in the intestine.**

Membrane-bound or membrane-anchored serine proteases have lately emerged as a subfamily of 20 serine proteases that all share a conserved catalytic domain and a transmembrane domain (1). Diverse physiological and pathophysiological roles of some members of this family have been identified such as skin and intestinal barrier integrity (2-5), processing of atrial natriuretic peptide (6), iron homeostasis (7-9), trophoblastic development (10), hearing (11,12) and ion homeostasis (13,14). More elusive is the identity and the role of their potential physiological inhibitors such as Spint1 and Spint2 (also known as HAI-1 and HAI-2), two Kunitz-type serine protease inhibitors that have a transmembrane domain. Spint1, first purified from a stomach cancer cell line (15), has been shown to form a complex in human milk with the

membrane-bound serine protease CAP3/Matriptase (16). Furthermore, genetic evidence supports an interaction between Spint1 and CAP3 in mouse skin (17).

Spint2, with its two inhibitory domains of Kunitz-type and a transmembrane domain, is highly homologous to Spint1 except that it lacks the LDL-receptor class A domain. Spint2 was cloned from three different sources: placental tissue, a gastric and a pancreas cancer cell line (18-20). In cell-free *in vitro* systems, it is a potent inhibitor of the membrane-bound serine proteases Tmprss1/hepsin, CAP1/prostasin, CAP3 and Tmprss13 (21-24).

The physiological role of Spint2 is unknown. In mice, it contributes to the correct development of the embryo (25-27). In humans, mutations in the Spint2 gene have been linked to a syndromic form of congenital sodium diarrhea, indicating that Spint2 likely plays a role in intestinal ionic homeostasis (28). Among the mutations associated with the disease that predominantly involve intronic mutations, a unique missense mutation substitutes a conserved tyrosine in the second Kunitz domain for a cysteine (Spint2 Y163C). The functional consequence of this mutation has not yet been determined. Furthermore, the physiological partners of Spint2 remain unknown.

In this study, we investigated the inhibitory function of wild-type Spint2 and its mutant Y163C on different serine proteases that were chosen according to the following hypothesis. Since Spint2 has a putative transmembrane domain and given that Spint1 is considered as physiological inhibitor of CAP3, we selected members of the membrane-bound serine proteases family as potential targets for Spint2. Considering the role of Spint2 in intestinal ionic homeostasis, we focused our interest on membrane-bound serine proteases reported in the literature to be expressed in the gastro-intestinal (GI) tract. Functional interactions between serine proteases and protease inhibitors are frequently studied in cell-free *in vitro* systems. Here, we established a cellular assay using *Xenopus laevis* oocytes as a heterologous expression system to functionally assess the activity of the candidate serine proteases and their inhibition by Spint2 and Spint2 mutants. We took advantage of the high sensitivity of the epithelial sodium channel ENaC to

stimulation by a wide variety of serine proteases and used it as a reporter gene to quantify the inhibitory activity of Spint2 by electrophysiological methods (29).

We found that Spint2 is a powerful inhibitor of several membrane-bound serine proteases expressed in the GI tract. The Spint2 Y163C mutation associated with congenital sodium diarrhea induced a loss of inhibitory activity towards a limited number of serine proteases such as CAP1 and Tmprss13. Biochemical analysis shows that the Y163C mutation results in a loss of Spint2 activity despite a conserved ability to bind the serine protease.

## EXPERIMENTAL PROCEDURES

*Expression of human Spint2 and human membrane-bound serine proteases in Xenopus oocytes* - cDNA clones of human CAP1, CAP2, CAP3, Tmprss1, Tmprss2, Tmprss11a, Tmprss13, Tmprss15 and Spint2 were obtained from the Mammalian Gene Collection (MGC). Human Tmprss3 is a kind gift of Bernard Rossier (University of Lausanne). Membrane-bound serine proteases were selected based on their gastro-intestinal expression, as reported in the literature (see results). The other members of the membrane-bound serine proteases family were not tested because of a reported expression that appears to be restricted to specific tissues, even though we cannot rule out that they might display any gastro-intestinal expression. All cDNAs were subcloned into the pSD(BS)easy vector for expression in *Xenopus laevis* oocytes. A FLAG-tag sequence was added to Spint2 using a single BstEII restriction site located in the sequence encoding the region between both Kunitz domains of Spint2. PCR amplification was performed to add a tag of 8 histidines in the N-terminal part of Tmprss13. Point mutations in Spint2 cDNA were introduced by site-directed mutagenesis (Stratagene's QuickChange) to generate Spint2 mutants Y68C, Y163C, Y68S, Y163S and double mutant Y68C/Y163C.

Stage V and VI healthy oocytes were isolated from ovarian tissue of *Xenopus laevis* and pressure-injected with 100nl of cRNA solution. For the functional assay, oocytes were injected with  $\alpha$ ,  $\beta$  and  $\gamma$  subunits of rat ENaC cRNAs (0,11ng of each subunit per oocyte) and with cRNAs of membrane-bound serine proteases and



Spint2 wild-type or mutants as indicated in the results section. In this heterologous expression system, we found that the effects of the serine proteases on ENaC as well as the effects of Spint2 on the serine proteases were dose-dependent. To minimize artifacts due to overexpression, we determined for each serine protease the amount of cRNA to be injected for a robust proteolytic activation of ENaC similar to the activation by trypsin (Fig.2B). We also determined the minimal amount of Spint2 cRNA necessary to completely inhibit the effect of the protease (Fig.2C). For the biochemical assay, oocytes were injected with cRNAs of His-tagged hTmprss13 (1.7ng) and FLAG-tagged hSpint2 (8.3ng). This ratio Tmprss13/Spint2 is similar to the ratio used in the functional assay. Oocytes were kept at 19° C in a low Na<sup>+</sup> (for the functional experiments with ENaC) modified Barth solution (MBS) containing (in mM): 10 NaCl, 0.82 MgSO<sub>4</sub>, 0.41 CaCl<sub>2</sub>, 0.33 Ca(NO<sub>3</sub>)<sub>2</sub>, 80 N-methyl-D-glucamine (NMDG), 2 KCl and 5 HEPES or a normal Na<sup>+</sup> (for the biochemical experiments done without ENaC) modified Barth solution (MBS) containing (in mM): 85 NaCl, 1 KCl, 2.4 NaHCO<sub>3</sub>, 0.82 MgSO<sub>4</sub>, 0.41 CaCl<sub>2</sub>, 0.33 Ca(NO<sub>3</sub>)<sub>2</sub>, and 10 HEPES, 4.08 NaOH.

*Electrophysiology* - Electrophysiological measurements were made 12 hours after injection except for experiments with Tmprss3 and Tmprss15 which were performed 30 hours after injection. ENaC-mediated Na<sup>+</sup> currents were measured in oocytes using the standard two-electrodes voltage clamp technique using a Dagan TEV voltage clamp amplifier (Dagan, Minneapolis, MN), the Digidata 1322 digitizer, and the PClamp 9 data-acquisition and analysis package (Axon Instruments, Molecular Devices, Sunnyvale, CA). The two electrodes contained 1M KCl solution. All electrophysiological measurements were performed at room temperature (22 °C) in a perfusion solution containing (in mM) 120 NaCl, 2.5 KCl, 1.8 CaCl<sub>2</sub>-2H<sub>2</sub>O, and 10 HEPES-H<sup>+</sup>. The holding potential inside the oocytes was -100 mV.

*Data analysis* - The epithelial sodium channel (ENaC) is highly sensitive to amiloride with an IC<sub>50</sub> of 0.1 μM. ENaC activity was measured by the amiloride-sensitive Na<sup>+</sup> current (I<sub>Na</sub><sup>+</sup>), defined as the difference between Na<sup>+</sup> current obtained in the presence (10 μM) and in

the absence of amiloride. ENaC activity is increased by a variety of serine proteases as well as by trypsin (13,29,30), making ENaC an ideal tool for measuring serine protease activity. We used trypsin (Sigma-Aldrich Chemie) 5 μg/ml in the perfusion solution for 2-3 minutes to define a maximal proteolytic stimulation on ENaC activity as measured by the increase in I<sub>Na</sub><sup>+</sup>. In each condition, sensitivity of ENaC to trypsin (defined as the relative trypsin-mediated increase in I<sub>Na</sub><sup>+</sup>) can vary depending on whether proteases with or without Spint2 wt/mutants are co-expressed with ENaC and was quantified by dividing, for each oocyte, I<sub>Na</sub><sup>+</sup> after trypsin treatment by I<sub>Na</sub><sup>+</sup> before trypsin treatment. A relative trypsin-mediated increase in I<sub>Na</sub><sup>+</sup> close to one reflects resistance of ENaC to trypsin because of the presence of an activating co-expressed protease. When Spint2 fully inhibits the co-expressed protease, relative trypsin-mediated increase in I<sub>Na</sub><sup>+</sup> has a value (>1) similar to control oocytes injected with ENaC alone.

*Biochemistry* - The Spint2 - Tmprss13 complex was isolated by affinity purification on nickel-beads. 24 hours after injection, 60 oocytes/condition were lysed in lysis buffer (1 % triton X-100, 100 mM NaCl, 20 mM Tris-HCl pH 7.5, 10mM Imidazole, 1 mM PMSF and 10 μg/ml of each Leupeptin, Pepstatin and Aprotinin). Lysates were then vortexed and centrifuged for 10 minutes at 12'000rpm. The intermediate phase was withdrawn and a sample of each lysate was kept as a control of "total lysate fraction". The rest of the lysate was incubated overnight with 50μl of nickel-beads (Ni-NTA Agarose, Quiagen). Elution was performed with 50μl of 2x SDS-PAGE sample buffer (containing 25mM DTT and 50mM EDTA). All samples were heated at 95°C for 10 minutes before loading on the SDS-PAGE (5-15%). Blots were probed with the anti-FLAG mouse antibody (Sigma) at a 1:500 dilution and with the anti-His rabbit antibody (Rockland) at a 1:1000 dilution. The latter antibody is conjugated to an infrared dye IRdye800 (green color) that allows protein detection using the *Li-Cor*® technology. The anti-FLAG antibody was detected with an anti-mouse IRdye680 (red color) antibody. Co-purification of Spint2 with Tmprss13 was quantified by densitometric analysis normalized with Spint2 signal in total lysates and Tmprss13 signal in total lysates and nickel-beads fraction.

**Quantitative PCR analysis** – Tissues were removed from three C57/B6 8 week-old mice. Duodenal, jejunal, ileal, caecal and colonic (proximal and distal) tissues were longitudinally opened and mucosal side was scrapped with a razorblade to obtain a fraction enriched in mucosal cells. Total RNA was extracted from mouse tissues using the RNeasy kit from Qiagen according to the manufacturer's protocol. 500g RNA (RNA from the 3 mice was pooled together) was reverse transcribed into cDNA using the PrimeScript RTreagent kit (TaKaRa). RNA was treated with DNase I (Promega) to remove any possible traces of genomic DNA before the cDNA synthesis. The primers used in this study are reported in the supplementary table S1. qRT-PCR experiments were carried out on an ABI PRISM 7500 equipment (Applied Biosystems). PCR was performed in 96-well plates (Applied Biosystems) in 20- $\mu$ l reactions that contained 10  $\mu$ l of FastSYBR Green Master Mix (Applied Biosystems), 125 nM of each primer and 4  $\mu$ l of cDNA (diluted 30 times). For each gene, standard curves were obtained using tissues with the highest abundance and 1/1, 1/5, 1/25, 1/625 and 1/3125 dilutions. The analysis of the slope of the standard curves showed a PCR efficiency between 1.70 and 2. These values were used for absolute quantification. Relative quantification using reference genes such as actin or GAPDH was not used because detection levels of those genes varied up to a difference of 4 cycles between different mouse tissues. Each gene was assessed in duplicates in two independent experiments.

**Statistical analysis** – All data are represented as means  $\pm$  SEM. Statistical significance was determined with one-way/two way ANOVA followed by Dunnett or Tukey's multiple comparison test and indicated in the legend of the figures.

## RESULTS

**mRNA expression of Spint2 and candidate membrane-bound serine protease in gastro-intestinal tissues** – We selected, as putative partners of Spint2, 9 membrane-bound serine proteases reported in the literature to be expressed in gastro-intestinal tissues namely CAP1, CAP2/Tmprss4, CAP3, Tmprss1/hepsin, Tmprss2, Tmprss3, Tmprss11a/ECRG1, Tmprss13 and Tmprss15/enterokinase (11,21,31-43). Detailed

mRNA expression levels of Spint2 and these candidate proteases were assessed in mouse GI tissues, and compared to heart, lung and kidney. Since Spint2 is known to be mainly expressed in epithelial cells (21), we took intestinal tissue fractions enriched in mucosal cells. Fig.1 shows that Spint2 mRNA was found along the entire GI tract, but its expression increased in the distal part. As already reported, the short isoform of Spint2 that lacks the first Kunitz domain appeared more abundant than the long (full-length) isoform in mouse (opposite findings are known in human) (44). CAP3 had an expression pattern similar to Spint2. CAP1, CAP2 and Tmprss2 could be easily detected in the small and large intestines with a higher abundance in the distal part. The other candidates showed a more restricted expression along the GI tract (in oesophagus for Tmprss11a, in oesophagus and colon for Tmprss13, in duodenum and jejunum for Tmprss15). Although Tmprss1 was very abundant in the kidney, low expression levels could be observed in the colon. Finally, Tmprss3 mRNA was detected at very low levels in all tissues, with a higher expression in stomach and jejunum.

**Functional assay in *Xenopus laevis* oocytes** – In order to test whether Spint2 can inhibit these candidate serine proteases in a cellular assay, we injected *Xenopus laevis* oocytes with Spint2 and protease cRNAs. The activity of the co-injected protease was monitored using the epithelial sodium channel ENaC because of its sensitivity to stimulation by serine proteases (29). ENaC is a Na<sup>+</sup> selective ion channel that is constitutively open at the cell surface, and can be selectively inhibited with submicromolar concentrations of amiloride. Proteolytic activation of ENaC was used as the readout for the activity of the expressed serine protease; the ENaC activation by the serine protease was compared with maximal ENaC activity obtained in the presence of trypsin. Typical tracings of ENaC-mediated currents ( $I_{Na^+}$ ) in the presence or absence of trypsin are shown in Fig.2A. In an oocyte injected with ENaC alone, the amiloride-sensitive current dramatically increased in the presence of trypsin (left tracing); co-injection of ENaC with Tmprss13 increased  $I_{Na^+}$  to the level of  $I_{Na^+}$  recorded in the presence of trypsin (middle tracing); finally, co-injection of ENaC, Tmprss13 and Spint2 completely abolished the effect of Tmprss13 on  $I_{Na^+}$  (right tracing). In

other words, an active serine protease such as Tmprss13 nearly abolishes the trypsin effect on ENaC-mediated current, and Spint2, as inhibitor of Tmprss13, allows the recovery of the trypsin effect on ENaC.

We noticed an additional effect when Tmprss13 is overexpressed by injecting increasing amounts of cRNA; under these conditions ENaC-mediated  $I_{Na^+}$  decreased together with the suppression of the trypsin effect on ENaC (Fig.2B, left panel). This effect was interpreted as a non specific proteolytic effect (toxic effect) of the protease that kills the channel activity. In the case of Tmprss15, a robust activation of ENaC was obtained at higher doses of cRNA encoding the protease (Fig.2B, right panel). Due to the complexity of the dose-related effect of the serine proteases on ENaC activity, we systematically determined for each serine protease the appropriate amount of protease cRNA needed for a stimulation comparable to that of trypsin, as shown in Fig.2B for Tmprss13 (left) and Tmprss15 (right): co-injection of ENaC with 0.5ng of Tmprss13 cRNA increased  $I_{Na^+}$  to the level obtained with trypsin but higher amounts paradoxically decreased  $I_{Na^+}$ , whereas robust activation of ENaC could be obtained only with 6ng of Tmprss15. All candidate serine proteases tested were functional on ENaC as shown by the robust increase in  $I_{Na^+}$  (Table 1 and Fig.3). This effect varied from a 2 to 5 fold increase in ENaC activity depending on the protease and on the batch of oocytes used for the experiment.

*Inhibition of serine proteases by Spint2* - We then evaluated the ability of Spint2 to inhibit the different serine proteases by determining the minimal amount of Spint2 cRNA needed to completely reverse the effect of each protease tested on the magnitude of ENaC current and the effect of trypsin. The inhibition of Tmprss13 and 15 by Spint2 is given as examples. Experiments in Fig.2C show that 1ng and 1.5ng of Spint2 cRNA were sufficient to obtain a full inhibition of Tmprss13 and Tmprss15 respectively as seen by a return of  $I_{Na^+}$  to baseline and the recovery of the effect of trypsin. Similar preliminary experiments were performed with each protease. We also verified that Spint2 *per se* did not directly alter  $I_{Na^+}$ , neither the effect of trypsin on ENaC (Fig.2D). For all proteases tested in figure 3, the co-expression of Spint2 with the serine protease

reversed the stimulating effect of the protease on  $I_{Na^+}$  and restored the trypsin effect, indicating that Spint2 is a powerful inhibitor of membrane-bound serine proteases (Fig.3).

*Effect of the congenital sodium diarrhea-associated mutation of Spint2* - We tested the effect of the Spint2 Y163C mutation in the 2<sup>nd</sup> Kunitz domain associated with the congenital sodium diarrhea, together with its homologous Y68C mutation in the 1<sup>st</sup> Kunitz domain (this mutation has not been linked to the disease). These mutations were tested on the capacity of Spint2 to inhibit membrane-bound serine proteases. Although the wild type form of Spint2 efficiently inhibited all membrane-bound serine proteases tested in this study, differential effects of the Spint2 Y68C and Y163C mutants were observed on serine protease activity. For instance, the Y68C or Y163C did not change the ability Spint2 to inhibit Tmprss15, whereas these same mutations resulted in a loss of function Spint2 on Tmprss13. In figure 3B, in order to compensate for oocyte variability in ENaC expression and protease activation, we inferred the inhibitory effect of Spint2 on the serine protease by calculating for each oocyte the relative trypsin-mediated increase in  $I_{Na^+}$  (ratio  $I_{Na^+}$  after trypsin treatment/ $I_{Na^+}$  before trypsin treatment). When equal to one, this ratio indicates resistance of ENaC to trypsin due to the full effect of the serine protease, whereas a ratio  $\geq 3$  (value similar to that obtained for oocytes injected with ENaC alone) indicates a sensitivity of ENaC to trypsin and a lack of effect of the serine protease due to inhibition by Spint2. Fig.3B shows that both Spint2 mutants were still able to inhibit Tmprss15, but showed a strong reduction in inhibitory activity on CAP1 and Tmprss13 proteases. Spint2 Y163C inhibited Tmprss2, Tmprss11a and Tmprss1, whereas Spint2 Y68C lost its inhibitory activity on these specific proteases. The opposite pattern was seen with Tmprss3 and CAP3, namely Spint2 Y68C being fully functional and Spint2 Y163C showing a partial loss of its inhibitory activity (although not statistically significant). Finally a partial loss of function was seen in both mutants when co-injected with CAP2. Briefly, a strong loss of function of the congenital sodium diarrhea mutant Spint2 Y163C was seen only with CAP1 and Tmprss13 proteases. These latter proteases appear thus as interesting potential

partners of Spint2 in the regulation of Na<sup>+</sup> transport in the intestine.

*Effect of the double mutant Spint2 Y68C/Y163C* – Four candidate proteases (Tmprss15, Tmprss3, CAP2 and CAP3) were still, at least partially, blocked by either Spint2 Y68C or Y163C. Therefore, we assessed the effect of the double mutation Spint2 Y68C/Y163C on these proteases. As shown in Fig.4, the double mutation in both Kunitz domains of Spint2 decreased its inhibitory activity on Tmprss15, Tmprss3, CAP2 and CAP3. Values of relative-trypsin-mediated increase in I<sub>Na</sub><sup>+</sup> shown in Fig.4B indicate that the Y68C/Y163C double mutation results in an almost complete loss of function of Spint2 consistent with an additive effect of these two homologous mutations in either Kunitz domains.

*Effect of the serine mutants Spint2 Y68S and Spint2 Y163S* – To further understand the molecular basis of Spint2 Y163C loss of function mutation for Tmprss13 inhibition, we asked whether it was due to the loss of the tyrosine, which is highly conserved among Spint2 orthologs from different species, or to the addition of a sulfhydryl group (via the substitution of the tyrosine by a cysteine residue). We mutated this tyrosine into a serine and assessed the inhibitory effect of Spint2 Y68S and Spint2 Y163S on Tmprss13. In contrast to the cysteine mutants, the serine mutants Spint2 Y68S and Spint2 Y163S retained their activity and were able to fully inhibit the effect of Tmprss13 on ENaC (Fig.5), suggesting that the presence of a new cysteine rather than the loss of the conserved tyrosine abolishes the inhibitory activity of Spint2 on Tmprss13.

*Biochemical interaction between Spint2 and Tmprss13* – To ascertain that Spint2 WT and mutants are equally expressed in the oocytes and to investigate the binding interaction between Tmprss13 and the Y68C and Y163C Spint2 mutants, we affinity purified Tmprss13 onto nickel beads using a Histidine-tag on the N-terminal part of Tmprss13 and assessed the co-purification of a FLAG-tagged construct of Spint2. The presence of a His-tag in Tmprss13 and a FLAG-tag in Spint2 did not alter their function (Fig.6A). When oocytes were injected with Tmprss13 alone (Fig.6B, lane 2), we detected a specific signal with a very low molecular weight that probably represents a fully processed cleaved

form of Tmprss13. Fig.6B shows that Spint2WT could be co-purified with Tmprss13 as shown by a specific 35kDa band corresponding to Spint2 (lane 3). The absence of a non-specific binding of Spint2 to the nickel-beads was verified (Fig.6C). Surprisingly, all mutants, including the non-functional mutants Y68C and Y163C, are still able to interact with Tmprss13, (lanes 3 to 7). The intensity of the specific 35kDa band corresponding to Spint2 WT and mutants was quantified and showed even an increase for Spint2 Y163C and Y163S (lanes 5 and 7) (Fig.6B right panel). Furthermore, when Spint2 WT or mutants were co-injected with Tmprss13 (lanes 3 to 7), a specific 70kDa band was detected corresponding to the full-length form of Tmprss13. An intermediary cleaved form of around 45kDa was also present in oocytes co-injected with non-functional mutants of Spint2 (Y68C and Y163C in lanes 4 and 5). These experiments suggest that the Tmprss13 injected alone is rapidly processed, and that co-injection with Spint2 WT or mutants stabilizes its full-length form. The Y68C and Y163C mutations do not disrupt the formation of a Spint2-Tmprss13 complex indicating that the loss of function of Spint2 mutants is not due to changes in their ability to bind the protease. These inactive Spint2 mutants seem to increase the abundance of Tmprss13 forms of intermediate molecular weight that might include the active form of Tmprss13 (24).

## DISCUSSION

In this study, we used a cellular assay in *Xenopus laevis* oocytes to assess the functional interactions between Spint2 wild type or mutants and different membrane-bound serine proteases expressed in the gastro-intestinal tract.

*ENaC and serine-proteases* – ENaC, a Na<sup>+</sup> selective ion channel that mediates transepithelial Na<sup>+</sup> transport in renal distal tubules, distal colon and lung, was used in this assay as a reporter gene to monitor serine protease activity (45,46). ENaC has already been shown to be activated by CAP1, CAP2, CAP3 and Tmprss3 by cleavage of the  $\alpha$  and the  $\gamma$  subunits of the channel complex (13,33,39). Here, we report the activation of ENaC by Tmprss1, Tmprss11a, Tmprss13 and Tmprss15. All proteases tested activate ENaC by two- to fivefold; this range is similar to the four- to sevenfold effect of CAP1, CAP2 and CAP3

reported in the literature (29). The proteases presented in this study increase the list of serine proteases that activate ENaC and provide further evidence that ENaC is a relatively unspecific target for a large number of membrane-bound serine-proteases. We also observed an activating effect of Tmprss2 in contrary to a previous study showing a decrease in ENaC activity and protein levels when co-expressed with Tmprss2 (47). We observed that the effects of serine proteases on ENaC are dose-dependent, and as for Tmprss13 (see Fig.2) we noticed that an overexpression or activity of the protease can decrease ENaC-mediated currents. The decrease in ENaC-mediated currents might reflect an extensive proteolytic effect of the protease on ENaC channel complex leading to a loss of function.

The specificity and the physiological relevance of the modulation of ENaC activity by serine proteases is not yet firmly established, but *in vivo* ENaC activity at the cell surface can be correlated with the proteolytic cleavage of its subunits (48). Considering the ENaC sensitivity to a large number of serine proteases, it is likely that the protease-dependent regulation of ENaC is tissue-specific. The expression of Tmprss15 (also called enterokinase/enteropeptidase) is restricted to the small intestine where ENaC is not present. An interaction ENaC-Tmprss15 is therefore of little physiological relevance. Independently of the relevance of this regulation, we would like to emphasize that ENaC was used in this study essentially as a reporter gene for serine protease activity, without any consideration of its implication in the pathogenesis of the congenital sodium diarrhea.

*Spint2 and congenital sodium diarrhea* - Spint2 efficiently inhibits all candidate proteases tested in our assay. The inhibition of Tmprss1, CAP1, CAP3 and Tmprss13 has already been described (21-24) but experiments were performed in cell-free assays. Here we confirmed this inhibition in a cellular assay. In addition, we also showed that Spint2 inhibits CAP2, Tmprss2, Tmprss3, Tmprss11a and Tmprss15.

In spite of the broad inhibitory capacity of Spint2, the congenital sodium diarrhea mutant Y163C (2<sup>nd</sup> Kunitz domain) and its homologous mutant Y68C (1<sup>st</sup> Kunitz domain) have different effects depending on the target protease. However, both mutations strongly reduced the inhibitory

activity of Spint2 only towards CAP1 and Tmprss13. Thus, these two proteases appear as interesting targets of Spint2 in regulating Na<sup>+</sup> transport in the intestine. Na-H-exchange has been shown to be defective in jejunal biopsies of patients affected by congenital sodium diarrhea and mice deficient for the Na-H-exchanger NHE3 display a phenotype resembling to the disease, suggesting that NHE3 plays an important role in the pathogenesis of congenital sodium diarrhea (49-51). CAP1 shows significant mRNA levels in small intestine and colon like Spint2 and NHE3, and recent genetic evidence shows that disruption of the CAP1 gene rescues the embryonic lethality of Spint2 deficient mice (27). Regulation of NHE3 by membrane-bound serine proteases such as CAP1 has never been tested. Only the serine protease dipeptidyl peptidase IV (DPPIV, a membrane-bound serine protease unrelated to the family tested in this study) has been proposed so far as regulator of NHE3 in rat renal proximal tubule (52). However, DPPIV inhibition has been shown to downregulate NHE3 activity and loss of function mutations in Spint2 would thus be expected to result in an increase in Na<sup>+</sup>-absorption mediated by NHE3. CAP1 could also be a target of Spint2 during embryonic development since children with the syndromic form of congenital sodium diarrhea also have dysmorphic features (28). It should be mentioned that CAP1 has been proposed to be an activator of ENaC *in vivo* (14) and notably in colon (53). However, it is unlikely that ENaC, used in this study as a reporter gene, is the target of CAP1 in the pathogenesis of congenital sodium diarrhea. If we assume a loss of function of Spint2 in congenital sodium diarrhea, unopposed CAP1 would lead to an activation of ENaC and thus an increase in sodium (re)absorption in colon. On the other hand, too strong expression or activity of the serine protease as seen with Tmprss13 for instance (See Fig.2B) might lead to a toxic effect on ENaC or other transporter resulting in decrease in Na<sup>+</sup> transport. Thus, unopposed CAP1 activity in the distal colon would result in decreased ENaC expression and Na<sup>+</sup> absorption.

Tmprss13, whose physiological role is totally unknown, is also an interesting candidate since it is no longer inhibited by Spint2 mutants Y68C and Y163C. Furthermore, Tmprss13 is significantly expressed at the mRNA level in the

distal colon. Although, congenital sodium diarrhea is likely due to Na-H-exchange defect in the small intestine and/or proximal colon, involvement of ENaC in the distal colon via toxic proteolysis, as described above, is not excluded.

Other proteases were only partially inhibited by Spint2 Y163C mutant. They cannot be totally excluded as targets of Spint2 in the congenital sodium diarrhea and remain potential targets of Spint2 in other tissues since Spint2 has a very broad tissue distribution. The Spint2 expression pattern is for instance particularly similar to CAP3 (as shown in this study and in (21).

The functional target(s) of Spint2 and the pathophysiological basis for the intestinal loss of Na<sup>+</sup> ions in congenital sodium diarrhea remain to be identified. Work done in Spint2 knockout mouse models would be of great interest in order to decipher the physiological and pathophysiological role of Spint2.

*Interactions of Spint2 with Tmprss13* - Spint2 mutants Y68C and Y163C, which lose their inhibitory capacity on Tmprss13, provide an opportunity to study the role of the tyrosines at position 68 and 163 that are well conserved in Spint2 protein among several species and also in Kunitz domains of Spint1 and other Kunitz inhibitors (28). Our biochemical data support that substitutions of the tyrosine in the first and second Kunitz domains by cysteine or serine residues do not disrupt the binding interaction between Spint2 and Tmprss13; it seems rather that substitution of tyrosine 163, but not tyrosine 68, stabilizes the Spint2-Tmprss13 complex as shown by a higher abundance of Spint2 co-purified with Tmprss13 (Fig.6B). The loss of Spint2 activity observed for the Y68C and Y163C mutants, but not for the corresponding serine substitutions, supports the notion that the presence of a sulfhydryl side chain at position 68 and 163 is responsible for this effect. Kunitz domains contain 60 amino acids including 6 conserved cysteines involved in the formation of specific disulfide bonds (54). The cysteine at positions Y163 and Y68 may disrupt the canonical structure of the Kunitz domains by changing the pattern of the three disulfide bonds resulting in a Spint2 loss of function.

Kunitz inhibitors belong to the so-called canonical inhibitors, which block serine proteases via an interaction where the Kunitz domain binds

to the catalytic site of the protease in a substrate-like manner (55). Our results indicate that the loss of a serine protease inhibition by Spint2 mutations can occur despite a conserved binding interaction between inhibitor and its substrate. This suggests two separate functional regions in Spint2: one involved in the binding to the target protease, the other responsible for the inhibition of the catalytic side of the protease. According to this view, the loss of the conserved tyrosines 68 and 163 of Spint2 may alter the binding interaction with the substrate (see the functional serine mutant Y163S in the case of Tmprss13). In addition to this effect, the substitution of these tyrosines into cysteines specifically alters the inhibitory function of Spint2 depending on the target protease. Interestingly, the tyrosines 68 and 163 in each Kunitz domains are very close to the putative secondary binding segment of the Kunitz domain, which is distinct from the reactive site that binds to the catalytic site of the protease (21,56).

*In vivo* substrates of serine proteases and targets of serine protease inhibitors are known only in a few cases. Thus, our understanding on the detailed mechanisms of serine protease inhibition is scarce, and is based on experiments done with less or even non-specific proteases or substrates. Here, we used ENaC to monitor protease activity. CAP2 and CAP3, but not CAP1, require an active catalytic site to activate ENaC (57). Therefore, we cannot exclude that Tmprss13 activates ENaC via interaction with another protease or through its catalytic site. Similarly, we cannot be sure whether Spint2 prevents the effect of Tmprss13 on ENaC by inhibiting the catalytic site of Tmprss13 or not. In spite of this issue, the differential functional effects of the cysteine and the serine mutations, which show a similar binding pattern to Tmprss13, strongly suggest a loss of the inhibitory function of Spint2 on the catalytic activity of Tmprss13; this of Spint2 function is likely due to the introduction of the sulfhydryl group and alterations in binding due to loss of the conserved tyrosine. It should also be noted that membrane-bound serine proteases have accessory domains potentially involved in protein-protein interaction that makes the mechanism of interaction with their inhibitor difficult to interpret (58,59).

The molecular basis of the inhibitory activity of Spint2 on serine proteases appears even

more complex when we take into account that Spint2 has two inhibitory domains that may work synergistically. Our data suggest that the 2 Kunitz domains are differentially involved in the inhibition of specific serine proteases. For instance, the Y68C mutation specifically disrupts the inhibitory activity of Spint2 on Tmprss1, Tmprss2 and Tmprss11a in contrast to the Y163C mutation that abolishes the function of Spint2 on CAP1 and Tmprss13. In other cases, the contribution of each Kunitz domain appears synergistic. How each domain contributes to the binding and to the inhibition respectively remains poorly known.

Proteomics approaches are of great interest for the identification of physiological partners of serine protease inhibitors, that could then be studied in a functional assay as ours. In addition, crystallographic studies performed with intact

proteins might provide new insights into the mechanisms that regulate interactions between membrane-bound serine proteases and their inhibitors

In summary, we developed a cellular assay in *Xenopus* oocytes to study functional and biochemical interactions between membrane-bound serine proteases and inhibitors using ENaC as a reporter gene. Spint2, whose mutations have been linked to congenital sodium diarrhea, appears to be a potent inhibitor. Being no longer blocked by the Y68C and Y163C Spint2 mutants, CAP1 and Tmprss13 are interesting candidate partners of Spint2 for maintaining Na<sup>+</sup> homeostasis in the intestine. Moreover, our assay provides the possibility to study in further details the complex interaction between membrane-bound serine proteases and inhibitors in a cellular context and with native proteins.

## REFERENCES

1. Szabo, R., and Bugge, T. H. (2011) Membrane-anchored serine proteases in vertebrate cell and developmental biology. *Annu Rev Cell Dev Biol* **27**, 213-235
2. Leyvraz, C., Charles, R. P., Rubera, I., Guitard, M., Rotman, S., Breiden, B., Sandhoff, K., and Hummler, E. (2005) The epidermal barrier function is dependent on the serine protease CAP1/Prss8. *J Cell Biol* **170**, 487-496
3. List, K., Szabo, R., Wertz, P. W., Segre, J., Haudenschild, C. C., Kim, S. Y., and Bugge, T. H. (2003) Loss of proteolytically processed filaggrin caused by epidermal deletion of Matriptase/MT-SP1. *J Cell Biol* **163**, 901-910
4. Buzza, M. S., Netzel-Arnett, S., Shea-Donohue, T., Zhao, A., Lin, C. Y., List, K., Szabo, R., Fasano, A., Bugge, T. H., and Antalis, T. M. (2010) Membrane-anchored serine protease matriptase regulates epithelial barrier formation and permeability in the intestine. *Proc Natl Acad Sci U S A* **107**, 4200-4205
5. List, K., Kosa, P., Szabo, R., Bey, A. L., Wang, C. B., Molinolo, A., and Bugge, T. H. (2009) Epithelial integrity is maintained by a matriptase-dependent proteolytic pathway. *Am J Pathol* **175**, 1453-1463
6. Chan, J. C., Knudson, O., Wu, F., Morser, J., Dole, W. P., and Wu, Q. (2005) Hypertension in mice lacking the proatrial natriuretic peptide convertase corin. *Proc Natl Acad Sci U S A* **102**, 785-790
7. Finberg, K. E., Heeney, M. M., Campagna, D. R., Aydinok, Y., Pearson, H. A., Hartman, K. R., Mayo, M. M., Samuel, S. M., Strouse, J. J., Markianos, K., Andrews, N. C., and Fleming, M. D. (2008) Mutations in TMPRSS6 cause iron-refractory iron deficiency anemia (IRIDA). *Nat Genet* **40**, 569-571
8. Folgueras, A. R., de Lara, F. M., Pendas, A. M., Garabaya, C., Rodriguez, F., Astudillo, A., Bernal, T., Cabanillas, R., Lopez-Otin, C., and Velasco, G. (2008) Membrane-bound serine protease matriptase-2 (Tmprss6) is an essential regulator of iron homeostasis. *Blood* **112**, 2539-2545
9. Du, X., She, E., Gelbart, T., Truksa, J., Lee, P., Xia, Y., Khovananth, K., Mudd, S., Mann, N., Moresco, E. M., Beutler, E., and Beutler, B. (2008) The serine protease TMPRSS6 is required to sense iron deficiency. *Science* **320**, 1088-1092
10. Cui, Y., Wang, W., Dong, N., Lou, J., Srinivasan, D. K., Cheng, W., Huang, X., Liu, M., Fang, C., Peng, J., Chen, S., Wu, S., Liu, Z., Dong, L., Zhou, Y., and Wu, Q. (2012) Role of corin in trophoblast invasion and uterine spiral artery remodelling in pregnancy. *Nature* **484**, 246-250
11. Scott, H. S., Kudoh, J., Wattenhofer, M., Shibuya, K., Berry, A., Chrast, R., Guipponi, M., Wang, J., Kawasaki, K., Asakawa, S., Minoshima, S., Younus, F., Mehdi, S. Q., Radhakrishna, U., Papasavvas, M. P., Gehrig, C., Rossier, C., Korostishevsky, M., Gal, A., Shimizu, N., Bonne-Tamir, B., and Antonarakis, S. E. (2001) Insertion of beta-satellite repeats identifies a transmembrane protease causing both congenital and childhood onset autosomal recessive deafness. *Nat Genet* **27**, 59-63
12. Guipponi, M., Tan, J., Cannon, P. Z., Donley, L., Crewther, P., Clarke, M., Wu, Q., Shepherd, R. K., and Scott, H. S. (2007) Mice deficient for the type II transmembrane serine protease, TMPRSS1/hepsin, exhibit profound hearing loss. *Am J Pathol* **171**, 608-616
13. Vallet, V., Chraïbi, A., Gaeggeler, H. P., Horisberger, J. D., and Rossier, B. C. (1997) An epithelial serine protease activates the amiloride-sensitive sodium channel. *Nature* **389**, 607-610
14. Planes, C., Randrianarison, N. H., Charles, R. P., Frateschi, S., Cluzeaud, F., Vuagniaux, G., Soler, P., Clerici, C., Rossier, B. C., and Hummler, E. (2010) ENaC-mediated alveolar fluid clearance and lung fluid balance depend on the channel-activating protease 1. *EMBO Mol Med* **2**, 26-37
15. Shimomura, T., Denda, K., Kitamura, A., Kawaguchi, T., Kito, M., Kondo, J., Kagaya, S., Qin, L., Takata, H., Miyazawa, K., and Kitamura, N. (1997) Hepatocyte growth factor activator inhibitor, a novel Kunitz-type serine protease inhibitor. *J Biol Chem* **272**, 6370-6376



16. Lin, C. Y., Anders, J., Johnson, M., and Dickson, R. B. (1999) Purification and characterization of a complex containing matriptase and a Kunitz-type serine protease inhibitor from human milk. *J Biol Chem* **274**, 18237-18242
17. Szabo, R., Kosa, P., List, K., and Bugge, T. H. (2009) Loss of matriptase suppression underlies spint1 mutation-associated ichthyosis and postnatal lethality. *Am J Pathol* **174**, 2015-2022
18. Marlor, C. W., Delaria, K. A., Davis, G., Muller, D. K., Greve, J. M., and Tamburini, P. P. (1997) Identification and cloning of human placental bikunin, a novel serine protease inhibitor containing two Kunitz domains. *J Biol Chem* **272**, 12202-12208
19. Kawaguchi, T., Qin, L., Shimomura, T., Kondo, J., Matsumoto, K., Denda, K., and Kitamura, N. (1997) Purification and cloning of hepatocyte growth factor activator inhibitor type 2, a Kunitz-type serine protease inhibitor. *J Biol Chem* **272**, 27558-27564
20. Muller-Pillasch, F., Wallrapp, C., Bartels, K., Varga, G., Friess, H., Buchler, M., Adler, G., and Gress, T. M. (1998) Cloning of a new Kunitz-type protease inhibitor with a putative transmembrane domain overexpressed in pancreatic cancer. *Biochim Biophys Acta* **1395**, 88-95
21. Szabo, R., Hobson, J. P., List, K., Molinolo, A., Lin, C. Y., and Bugge, T. H. (2008) Potent inhibition and global co-localization implicate the transmembrane Kunitz-type serine protease inhibitor hepatocyte growth factor activator inhibitor-2 in the regulation of epithelial matriptase activity. *J Biol Chem* **283**, 29495-29504
22. Shipway, A., Danahay, H., Williams, J. A., Tully, D. C., Backes, B. J., and Harris, J. L. (2004) Biochemical characterization of prostasin, a channel activating protease. *Biochem Biophys Res Commun* **324**, 953-963
23. Herter, S., Piper, D. E., Aaron, W., Gabriele, T., Cutler, G., Cao, P., Bhatt, A. S., Choe, Y., Craik, C. S., Walker, N., Meininger, D., Hoey, T., and Austin, R. J. (2005) Hepatocyte growth factor is a preferred in vitro substrate for human hepsin, a membrane-anchored serine protease implicated in prostate and ovarian cancers. *Biochem J* **390**, 125-136
24. Hashimoto, T., Kato, M., Shimomura, T., and Kitamura, N. (2010) TMPRSS13, a type II transmembrane serine protease, is inhibited by hepatocyte growth factor activator inhibitor type 1 and activates pro-hepatocyte growth factor. *FEBS J* **277**, 4888-4900
25. Mitchell, K. J., Pinson, K. I., Kelly, O. G., Brennan, J., Zupicich, J., Scherz, P., Leighton, P. A., Goodrich, L. V., Lu, X., Avery, B. J., Tate, P., Dill, K., Pangilinan, E., Wakenight, P., Tessier-Lavigne, M., and Skarnes, W. C. (2001) Functional analysis of secreted and transmembrane proteins critical to mouse development. *Nat Genet* **28**, 241-249
26. Szabo, R., Hobson, J. P., Christoph, K., Kosa, P., List, K., and Bugge, T. H. (2009) Regulation of cell surface protease matriptase by HAI2 is essential for placental development, neural tube closure and embryonic survival in mice. *Development* **136**, 2653-2663
27. Szabo, R., Uzzun Sales, K., Kosa, P., Shylo, N. A., Godiksen, S., Hansen, K. K., Friis, S., Gutkind, J. S., Vogel, L. K., Hummler, E., Camerer, E., and Bugge, T. H. (2012) Reduced Proastasin (CAP1/PRSS8) Activity Eliminates HAI-1 and HAI-2 Deficiency-Associated Developmental Defects by Preventing Matriptase Activation. *PLoS Genet* **8**, e1002937
28. Heinz-Erian, P., Muller, T., Krabichler, B., Schranz, M., Becker, C., Ruschendorf, F., Nurnberg, P., Rossier, B., Vujic, M., Booth, I. W., Holmberg, C., Wijmenga, C., Grigelioniene, G., Kneepkens, C. M., Rosipal, S., Mistrik, M., Kappler, M., Michaud, L., Doczy, L. C., Siu, V. M., Krantz, M., Zoller, H., Utermann, G., and Janecke, A. R. (2009) Mutations in SPINT2 cause a syndromic form of congenital sodium diarrhea. *Am J Hum Genet* **84**, 188-196
29. Rossier, B. C., and Stutts, M. J. (2009) Activation of the epithelial sodium channel (ENaC) by serine proteases. *Annu Rev Physiol* **71**, 361-379

30. Chraïbi, A., Vallet, V., Firsov, D., Hess, S. K., and Horisberger, J. D. (1998) Protease modulation of the activity of the epithelial sodium channel expressed in *Xenopus* oocytes. *J Gen Physiol* **111**, 127-138
31. Vuagniaux, G., Vallet, V., Jaeger, N. F., Pfister, C., Bens, M., Farman, N., Courtois-Coutry, N., Vandewalle, A., Rossier, B. C., and Hummler, E. (2000) Activation of the amiloride-sensitive epithelial sodium channel by the serine protease mCAP1 expressed in a mouse cortical collecting duct cell line. *Journal of the American Society of Nephrology : JASN* **11**, 828-834
32. Adachi, M., Kitamura, K., Miyoshi, T., Narikiyo, T., Iwashita, K., Shiraishi, N., Nonoguchi, H., and Tomita, K. (2001) Activation of epithelial sodium channels by prostasin in *Xenopus* oocytes. *Journal of the American Society of Nephrology : JASN* **12**, 1114-1121
33. Vuagniaux, G., Vallet, V., Jaeger, N. F., Hummler, E., and Rossier, B. C. (2002) Synergistic activation of ENaC by three membrane-bound channel-activating serine proteases (mCAP1, mCAP2, and mCAP3) and serum- and glucocorticoid-regulated kinase (Sgk1) in *Xenopus* Oocytes. *J Gen Physiol* **120**, 191-201
34. List, K., Hobson, J. P., Molinolo, A., and Bugge, T. H. (2007) Co-localization of the channel activating protease prostasin/(CAP1/PRSS8) with its candidate activator, matriptase. *Journal of cellular physiology* **213**, 237-245
35. Oberst, M. D., Singh, B., Ozdemirli, M., Dickson, R. B., Johnson, M. D., and Lin, C. Y. (2003) Characterization of matriptase expression in normal human tissues. *The journal of histochemistry and cytochemistry : official journal of the Histochemistry Society* **51**, 1017-1025
36. Tsuji, A., Torres-Rosado, A., Arai, T., Le Beau, M. M., Lemons, R. S., Chou, S. H., and Kurachi, K. (1991) Hepsin, a cell membrane-associated protease. Characterization, tissue distribution, and gene localization. *J Biol Chem* **266**, 16948-16953
37. Ganesan, R., Kolumam, G. A., Lin, S. J., Xie, M. H., Santell, L., Wu, T. D., Lazarus, R. A., Chaudhuri, A., and Kirchhofer, D. (2011) Proteolytic activation of pro-macrophage-stimulating protein by hepsin. *Mol Cancer Res* **9**, 1175-1186
38. Vaarala, M. H., Porvari, K. S., Kellokumpu, S., Kyllonen, A. P., and Vihko, P. T. (2001) Expression of transmembrane serine protease TMPRSS2 in mouse and human tissues. *The Journal of pathology* **193**, 134-140
39. Guipponi, M., Vuagniaux, G., Wattenhofer, M., Shibuya, K., Vazquez, M., Dougherty, L., Scamuffa, N., Guida, E., Okui, M., Rossier, C., Hancock, M., Buchet, K., Reymond, A., Hummler, E., Marzella, P. L., Kudoh, J., Shimizu, N., Scott, H. S., Antonarakis, S. E., and Rossier, B. C. (2002) The transmembrane serine protease (TMPRSS3) mutated in deafness DFNB8/10 activates the epithelial sodium channel (ENaC) in vitro. *Hum Mol Genet* **11**, 2829-2836
40. Sales, K. U., Hobson, J. P., Wagenaar-Miller, R., Szabo, R., Rasmussen, A. L., Bey, A., Shah, M. F., Molinolo, A. A., and Bugge, T. H. (2011) Expression and genetic loss of function analysis of the HAT/DESC cluster proteases TMPRSS11A and HAT. *PLoS One* **6**, e23261
41. Kim, D. R., Sharmin, S., Inoue, M., and Kido, H. (2001) Cloning and expression of novel mosaic serine proteases with and without a transmembrane domain from human lung. *Biochim Biophys Acta* **1518**, 204-209
42. Kido, H., Okumura, Y., Takahashi, E., Pan, H. Y., Wang, S., Chida, J., Le, T. Q., and Yano, M. (2008) Host envelope glycoprotein processing proteases are indispensable for entry into human cells by seasonal and highly pathogenic avian influenza viruses. *J Mol Genet Med* **3**, 167-175
43. Yuan, X., Zheng, X., Lu, D., Rubin, D. C., Pung, C. Y., and Sadler, J. E. (1998) Structure of murine enterokinase (enteropeptidase) and expression in small intestine during development. *Am J Physiol* **274**, G342-349

44. Itoh, H., Kataoka, H., Hamasuna, R., Kitamura, N., and Koono, M. (1999) Hepatocyte growth factor activator inhibitor type 2 lacking the first Kunitz-type serine proteinase inhibitor domain is a predominant product in mouse but not in human. *Biochem Biophys Res Commun* **255**, 740-748
45. Rossier, B. C., Pradervand, S., Schild, L., and Hummler, E. (2002) Epithelial sodium channel and the control of sodium balance: interaction between genetic and environmental factors. *Annu Rev Physiol* **64**, 877-897
46. Schild, L. (2010) The epithelial sodium channel and the control of sodium balance. *Biochim Biophys Acta* **1802**, 1159-1165
47. Donaldson, S. H., Hirsh, A., Li, D. C., Holloway, G., Chao, J., Boucher, R. C., and Gabriel, S. E. (2002) Regulation of the epithelial sodium channel by serine proteases in human airways. *J Biol Chem* **277**, 8338-8345
48. Frindt, G., and Palmer, L. G. (2009) Surface expression of sodium channels and transporters in rat kidney: effects of dietary sodium. *Am J Physiol Renal Physiol* **297**, F1249-1255
49. Keller, K. M., Wirth, S., Baumann, W., Sule, D., and Booth, I. W. (1990) Defective jejunal brush border membrane sodium/proton exchange in association with lethal familial protracted diarrhoea. *Gut* **31**, 1156-1158
50. Booth, I. W., Stange, G., Murer, H., Fenton, T. R., and Milla, P. J. (1985) Defective jejunal brush-border Na<sup>+</sup>/H<sup>+</sup> exchange: a cause of congenital secretory diarrhoea. *Lancet* **1**, 1066-1069
51. Schultheis, P. J., Clarke, L. L., Meneton, P., Miller, M. L., Soleimani, M., Gawenis, L. R., Riddle, T. M., Duffy, J. J., Doetschman, T., Wang, T., Giebisch, G., Aronson, P. S., Lorenz, J. N., and Shull, G. E. (1998) Renal and intestinal absorptive defects in mice lacking the NHE3 Na<sup>+</sup>/H<sup>+</sup> exchanger. *Nat Genet* **19**, 282-285
52. Girardi, A. C., Fukuda, L. E., Rossoni, L. V., Malnic, G., and Reboucas, N. A. (2008) Dipeptidyl peptidase IV inhibition downregulates Na<sup>+</sup> - H<sup>+</sup> exchanger NHE3 in rat renal proximal tubule. *Am J Physiol Renal Physiol* **294**, F414-422
53. Frateschi, S., Keppner, A., Malsure, S., Iwaszkiewicz, J., Sergi, C., Merillat, A. M., Fowler-Jaeger, N., Randrianarison, N., Planes, C., and Hummler, E. (2012) Mutations of the serine protease CAP1/Prss8 lead to reduced embryonic viability, skin defects, and decreased ENaC activity. *Am J Pathol* **181**, 605-615
54. Laskowski, M., Jr., and Kato, I. (1980) Protein inhibitors of proteinases. *Annual review of biochemistry* **49**, 593-626
55. Bode, W., and Huber, R. (2000) Structural basis of the endoproteinase-protein inhibitor interaction. *Biochim Biophys Acta* **1477**, 241-252
56. Friedrich, R., Fuentes-Prior, P., Ong, E., Coombs, G., Hunter, M., Oehler, R., Pierson, D., Gonzalez, R., Huber, R., Bode, W., and Madison, E. L. (2002) Catalytic domain structures of MT-SP1/matriptase, a matrix-degrading transmembrane serine proteinase. *J Biol Chem* **277**, 2160-2168
57. Andreasen, D., Vuagniaux, G., Fowler-Jaeger, N., Hummler, E., and Rossier, B. C. (2006) Activation of epithelial sodium channels by mouse channel activating proteases (mCAP) expressed in *Xenopus* oocytes requires catalytic activity of mCAP3 and mCAP2 but not mCAP1. *Journal of the American Society of Nephrology : JASN* **17**, 968-976
58. Inouye, K., Tsuzuki, S., Yasumoto, M., Kojima, K., Mochida, S., and Fushiki, T. (2010) Identification of the matriptase second CUB domain as the secondary site for interaction with hepatocyte growth factor activator inhibitor type-1. *J Biol Chem* **285**, 33394-33403
59. Kojima, K., Tsuzuki, S., Fushiki, T., and Inouye, K. (2009) Role of the stem domain of matriptase in the interaction with its physiological inhibitor, hepatocyte growth factor activator inhibitor type I. *J Biochem* **145**, 783-790

## ACKNOWLEDGMENTS

We thank Stephan Kellenberger and Delphine Huser for critical reading of the manuscript.

## FOOTNOTES

<sup>1</sup>This work was supported by a grant from the Swiss National Science Foundation (323530-128871, MD-PhD Program of the Swiss Academy of Medical Sciences) to NF.

<sup>2</sup>To whom correspondence should be addressed: Dept. of Pharmacology and Toxicology, University of Lausanne, Rue du Bugnon 27, 1005 Lausanne, Switzerland, Tel: 41-21-692-53-80, Fax: 41-21-692-53-55, E-mail: [Laurent.Schild@unil.ch](mailto:Laurent.Schild@unil.ch)

The abbreviations used are: HAI-2, hepatocyte growth factor activator inhibitor type 2, ENaC, epithelial sodium channel, CAP, channel activating protease, Tmprss, transmembrane protease, serine, GI, gastrointestinal, WT, wild-type.

## FIGURE LEGENDS

**FIGURE 1. Tissue distribution of mRNA expression of Spint2 and membrane-bound serine proteases.** Quantitative RT-PCRs were performed on selected organs from three wild-type adult mice. From stomach to distal colon, tissues were scrapped to get fractions enriched in mucosal cells. Each gene was assessed in duplicates in two independent experiments. Results are expressed as arbitrary units (A.U.) based on standard dilution curves (see Experimental Procedures).

**FIGURE 2: Validation of the functional assay using ENaC as a reporter gene.** **A**, Representative recordings of amiloride-sensitive current ( $I_{Na^+}$ ) in the presence (filled bars) or absence of trypsin (5 $\mu$ g/ml), in *Xenopus* oocytes injected with 0.11ng/subunit rENaC alone (left panel), with rENaC and 0.25ng hTmprss13 (middle panel) and with rENaC, hTmprss13 and 1.5ng hSpint2 cRNA (right panel). 10  $\mu$ M amiloride was used to block the ENaC-mediated current. **B**, Effects of increasing the amounts of injected Tmprss13 and Tmprss15 cRNAs on  $I_{Na^+}$ .  $I_{Na^+}$  was measured in oocytes injected with rat ENaC with/without of Tmprss13 or Tmprss15 as indicated.  $I_{Na^+}$  was measured without (black bars) or with trypsin (5 $\mu$ g/ml) perfused extracellularly (white bars) as a positive control for ENaC activation. **C**, Effects of increasing the amounts of injected Spint2 cRNA to prevent the Tmprss13- or Tmprss15-mediated increase in  $I_{Na^+}$  (left and right panels, respectively). **D**, Effect of Spint2 on  $I_{Na^+}$ .  $I_{Na^+}$  was measured 12, 24 and 30 hours after injection (left, middle and right panels, respectively) performed in three independent experiments. n= 6 -9 measured oocytes per condition from 2 different batches for each experiment. Data are means  $\pm$  SEM; \*, p<0.05 / \*\*, p<0.01 compared to rENaC alone or rENaC + protease (as indicated) after two-way repeated measure ANOVA followed by Dunnett's multiple comparisons test.

**FIGURE 3. Functional analysis of interactions between Spint2 (wt and mutants) and membrane-bound serine proteases.** **A**, ENaC-mediated sodium currents ( $I_{Na^+}$ ) were measured in *Xenopus* oocytes injected with rat ENaC with/without candidate serine protease and Spint2 (wild-type or mutants Y68C and Y163C) as indicated.  $I_{Na^+}$  was measured without (black bars) or with trypsin (5 $\mu$ g/ml) perfused extracellularly (white bars) as a positive control for ENaC activation. n $\geq$ 15 measured oocytes per condition from at least 2 different animals. Each protease was tested in at least two independent experiments. Data are means  $\pm$  SEM. **B**, Relative trypsin-mediated increase in  $I_{Na^+}$  was calculated by dividing, for each oocyte from experiments of panel A,  $I_{Na^+}$  after treatment with trypsin by  $I_{Na^+}$  before treatment with trypsin. Data are means  $\pm$  SEM. \*/#/ $^{\circ}$ , p<0.05, \*\*/##/ $^{\circ\circ}$ , p<0.01, \*\*\*/###/ $^{\circ\circ\circ}$ , p<0.001, compared to ENaC alone, {ENaC + protease} or {ENaC + protease + Spint2 WT} respectively after One-way ANOVA followed by Tukey's multiple comparisons test.

**FIGURE 4. Effect of the double mutant Spint2 Y68C/Y163C on Tmprss15, Tmprss2, CAP2 and CAP3 proteases.** **A**, ENaC-mediated sodium currents ( $I_{Na^+}$ ), were measured in *Xenopus* oocytes injected with rat ENaC with or without serine protease and Spint2 (wild-type or double mutant Y68C/Y163C) as indicated.  $I_{Na^+}$  was measured without (black bars) and with trypsin (5 $\mu$ g/ml) perfused extracellularly (white bars) as a positive control for ENaC activation.  $n \geq 11$  measured oocytes from 4 different animals. Each protease was tested in two independent experiments. Data are means  $\pm$  SEM. **B**, Relative trypsin-mediated increase in  $I_{Na^+}$  was calculated by dividing, for each oocyte from experiments of panel A,  $I_{Na^+}$  after treatment with trypsin by  $I_{Na^+}$  before treatment with trypsin. Data are means  $\pm$  SEM. \*\*/###/°°,  $p < 0.01$ , \*\*\*/###/°°°,  $p < 0.001$ , compared to ENaC alone, {ENaC + protease} or {ENaC + protease + Spint2 WT} respectively after One-way ANOVA followed by Tukey's multiple comparisons test.

**FIGURE 5. Effect of Spint2 Y68S and Y163S mutation on Tmprss13 activity.** **A**, ENaC-mediated sodium currents ( $I_{Na^+}$ ), were measured in *Xenopus* oocytes injected with rat ENaC, Tmprss13 and Spint2 (wild-type or mutant).  $I_{Na^+}$  was measured without (black bars) and with trypsin (5 $\mu$ g/ml) perfused extracellularly (white bars) as a positive control for ENaC activation.  $n \geq 14$  measured oocytes from 4 different batches performed in two independent experiments. Data are means  $\pm$  SEM. **B**, Relative trypsin-mediated increase in  $I_{Na^+}$  was calculated by dividing, for each oocyte from experiments of panel A,  $I_{Na^+}$  after treatment with trypsin by  $I_{Na^+}$  before treatment with trypsin. Data are means  $\pm$  SEM. \*\*\*,  $p < 0.001$ , compared to ENaC alone, after One-way ANOVA followed by Tukey's multiple comparisons test.

**FIGURE 6. Biochemical interaction between Spint2 and Tmprss13.** **A**, Left panel: typical western blot performed using *Xenopus* oocytes coexpressing tagged His-Tmprss13 and FLAG-Spint2 as indicated. Cell lysates are shown in the lower part and the elution fraction from the Nickel beads in the upper part. Membranes were blotted with anti-FLAG (red) and anti-His (green) antibodies. Right panel: quantification of the 35kDa band of Spint2 wild-type and mutants co-purified with Tmprss3.  $n = 4$  experiments, \*,  $p < 0.05$ ; \*\*,  $p < 0.01$  compared to Spint2 WT after One-way ANOVA, followed by Dunnett's multiple comparison test. **B**, Control western blot. *Xenopus* oocytes were injected with FLAG-Spint2 WT with or without Tmprss13 (without His-Tag). Cell lysate were loaded onto nickel-beads for purification. Membranes were blotted with Anti-FLAG (red) and anti-His (green) antibodies. **C**, Effect of a His-tag and a FLAG-tag on the function of Tmprss13 and Spint2 in *Xenopus* oocytes. ENaC-mediated sodium currents ( $I_{Na^+}$ ), were measured in *Xenopus* oocytes injected with rat ENaC, Tmprss13 (+/- HIS-tag=H8) and Spint2 (+/- FLAG-tag=FLAG).  $I_{Na^+}$  was measured without (black bars) and with trypsin (5 $\mu$ g/ml) perfused extracellularly (white bars) as a positive control for ENaC activation.  $n = 8$  measured oocytes from 2 different batches. Data are means  $\pm$  SEM.

Table 1

<b>protease (ng of cRNA)</b>	<b>Fold increase in ENaC-mediated current</b>
hTmprss2 (5ng)	2.6 ± 0.2 (trypsin: 3.5 ± 0.3)
hTmprss11a (0.25ng)	2.1 ± 0.2 (trypsin: 3.7 ± 0.3)
hTmprss15 (6ng)	2.6 ± 0.3 (trypsin: 3.7 ± 0.3)
hTmprss1 (0.05ng)	2.5 ± 0.3 (trypsin: 3.7 ± 0.4)
hTmprss3 (2.5ng)	2.6 ± 0.3 (trypsin: 3.9 ± 0.3)
hCAP3 (1.5ng)	2.6 ± 0.3 (trypsin: 3.1 ± 0.3)
hCAP2 (2ng)	2.4 ± 0.4 (trypsin: 3 ± 0.2)
hCAP1 (1ng)	3.6 ± 0.4 (trypsin: 3.8 ± 0.5)
hTmprss13 (0.25ng)	5.2 ± 0.8 (trypsin: 4.4 ± 0.3)

Table 1. **Increase in ENaC activity by membrane-bound serine proteases.** Values were obtained from experiments in figure 3. Effect of trypsin is indicated in parentheses. Data are means ± SEM.

Figure 1

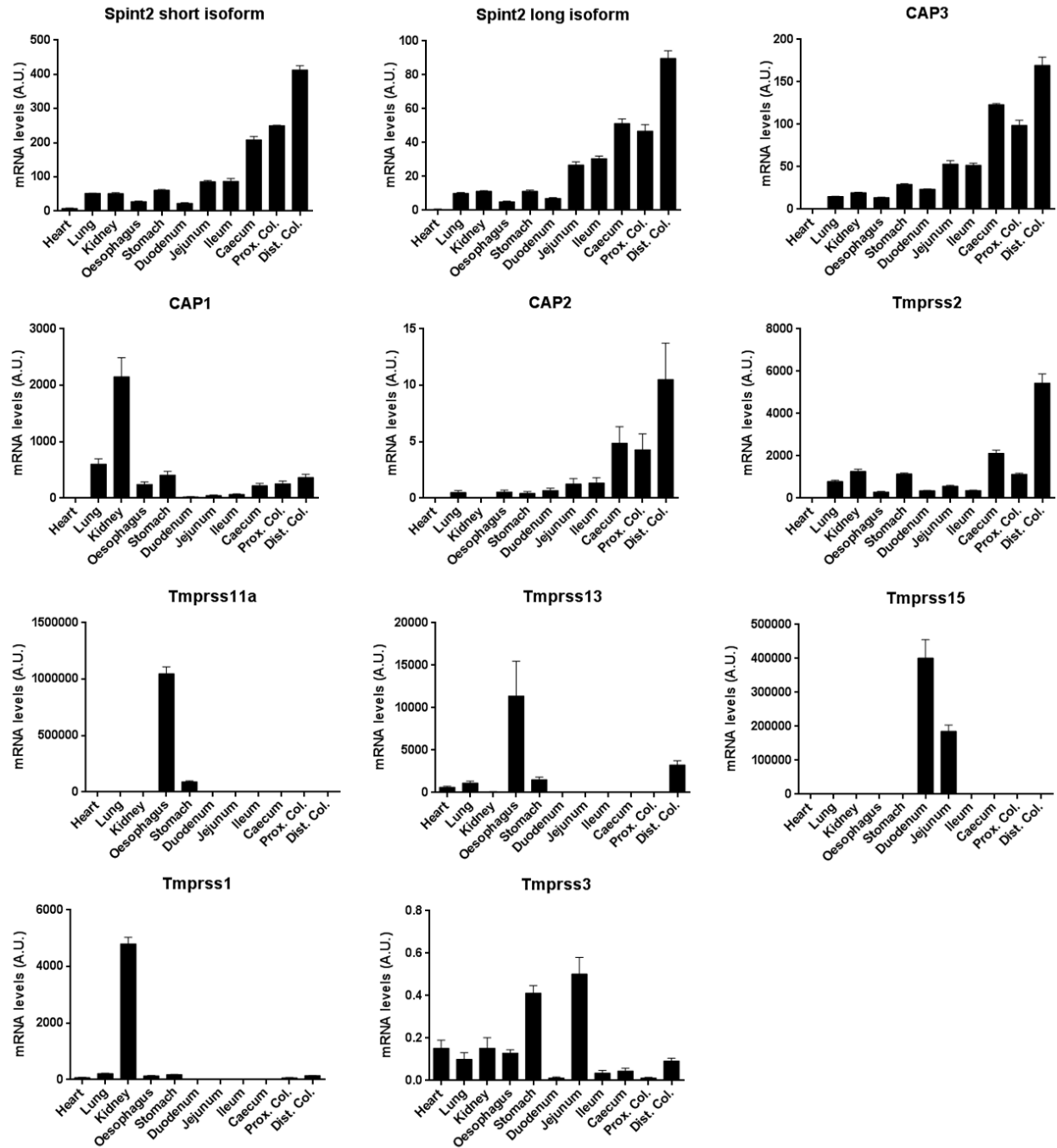


Figure 2

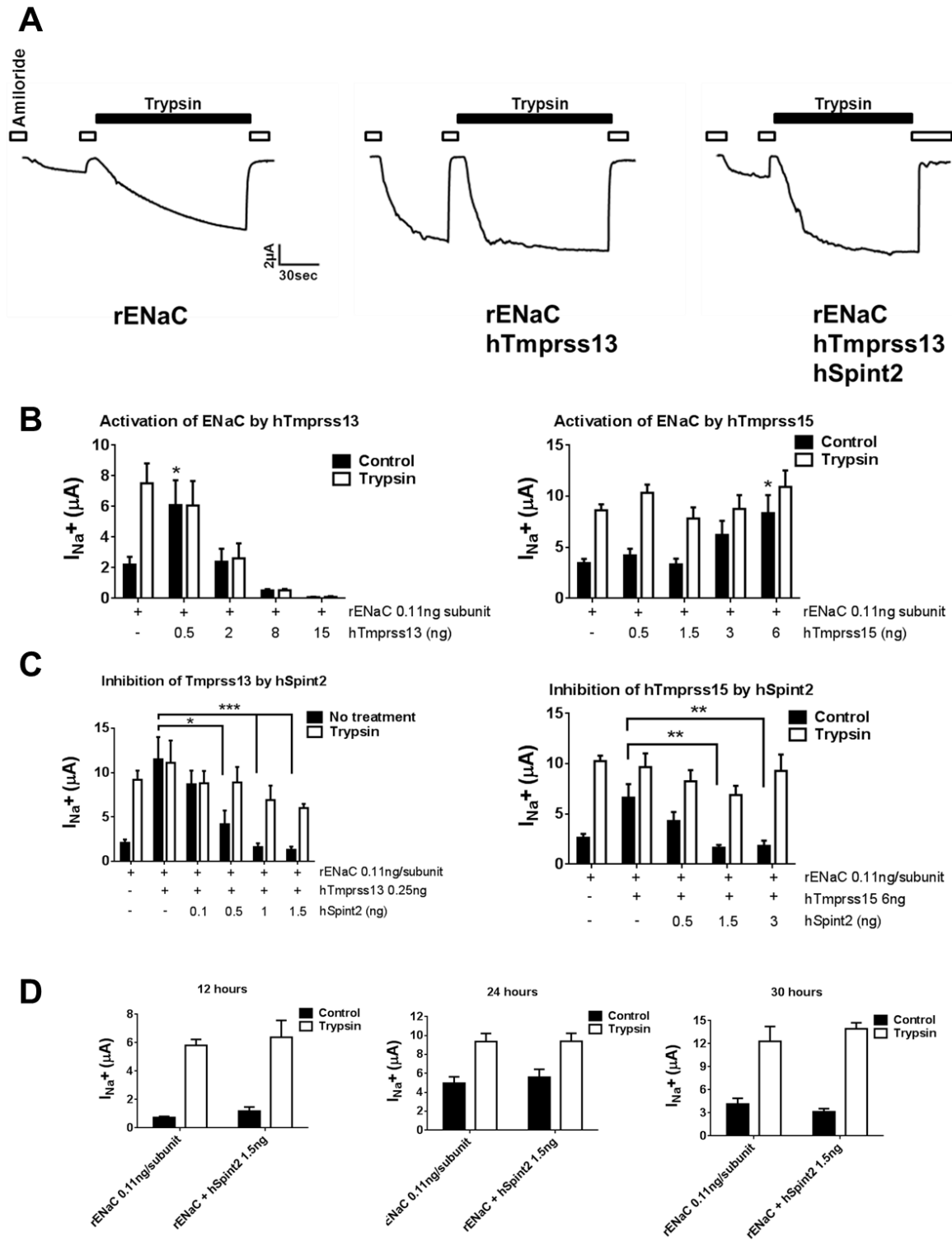
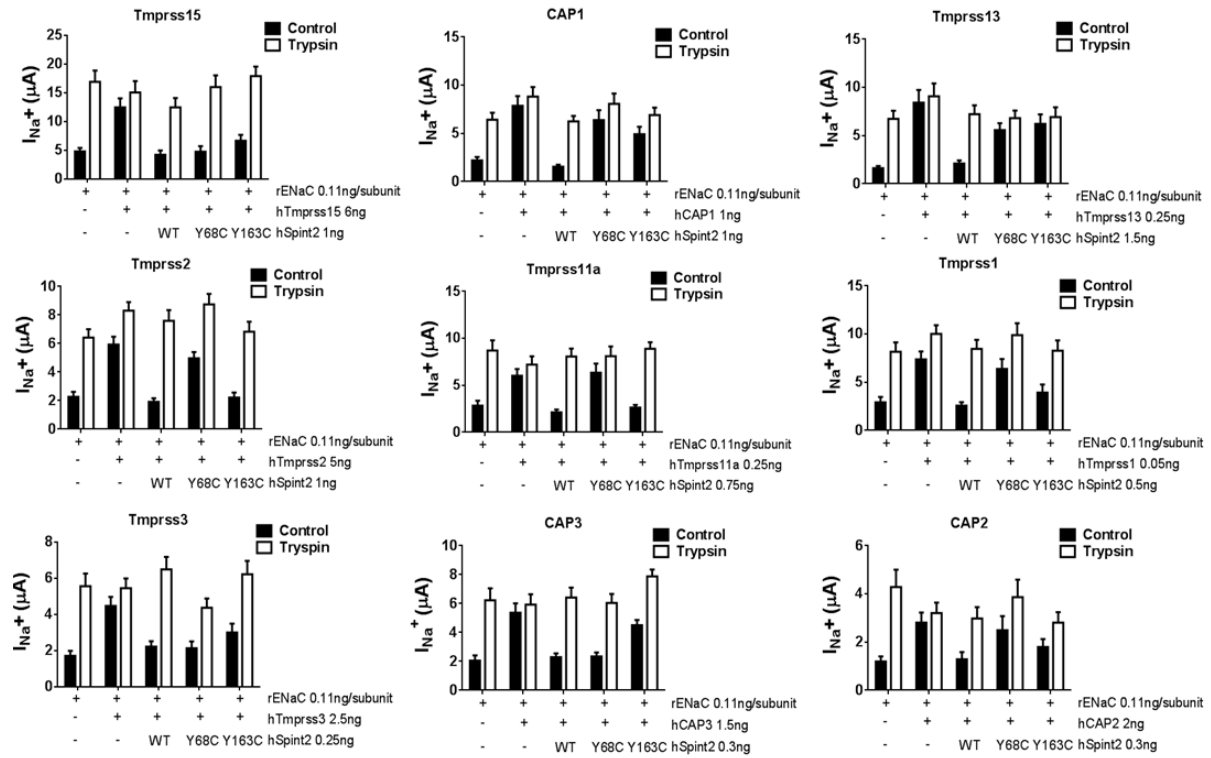




Figure 3

**A**



**B**

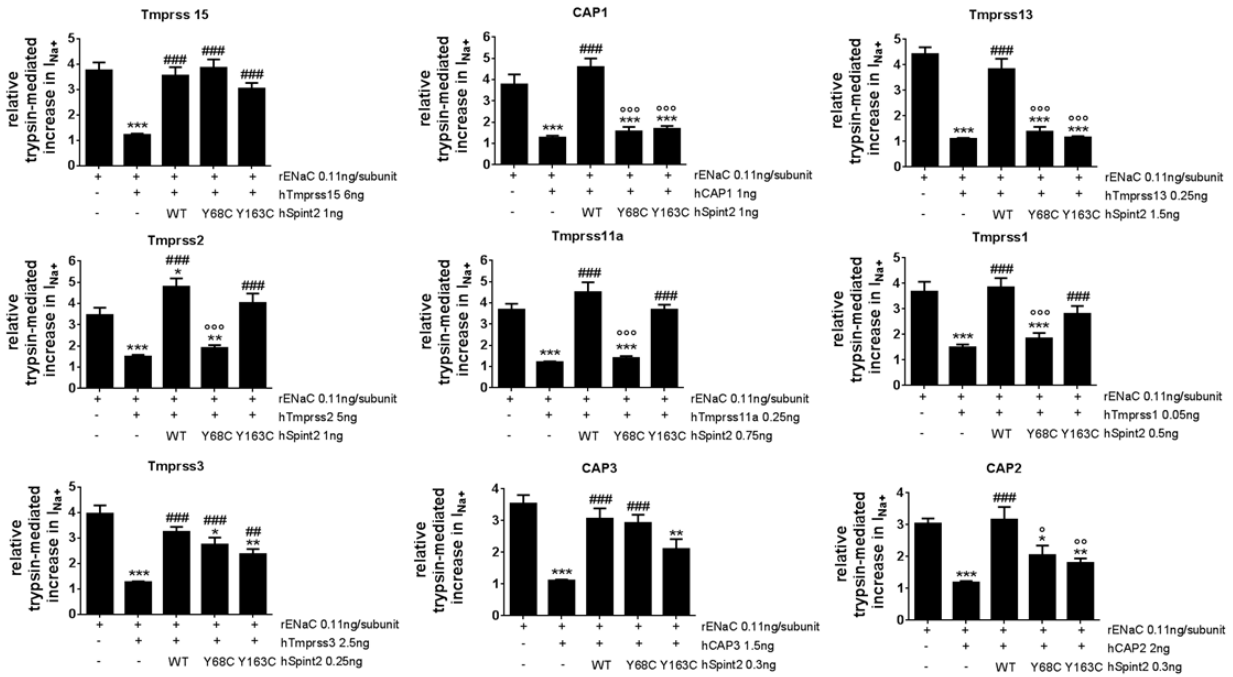


Figure 4

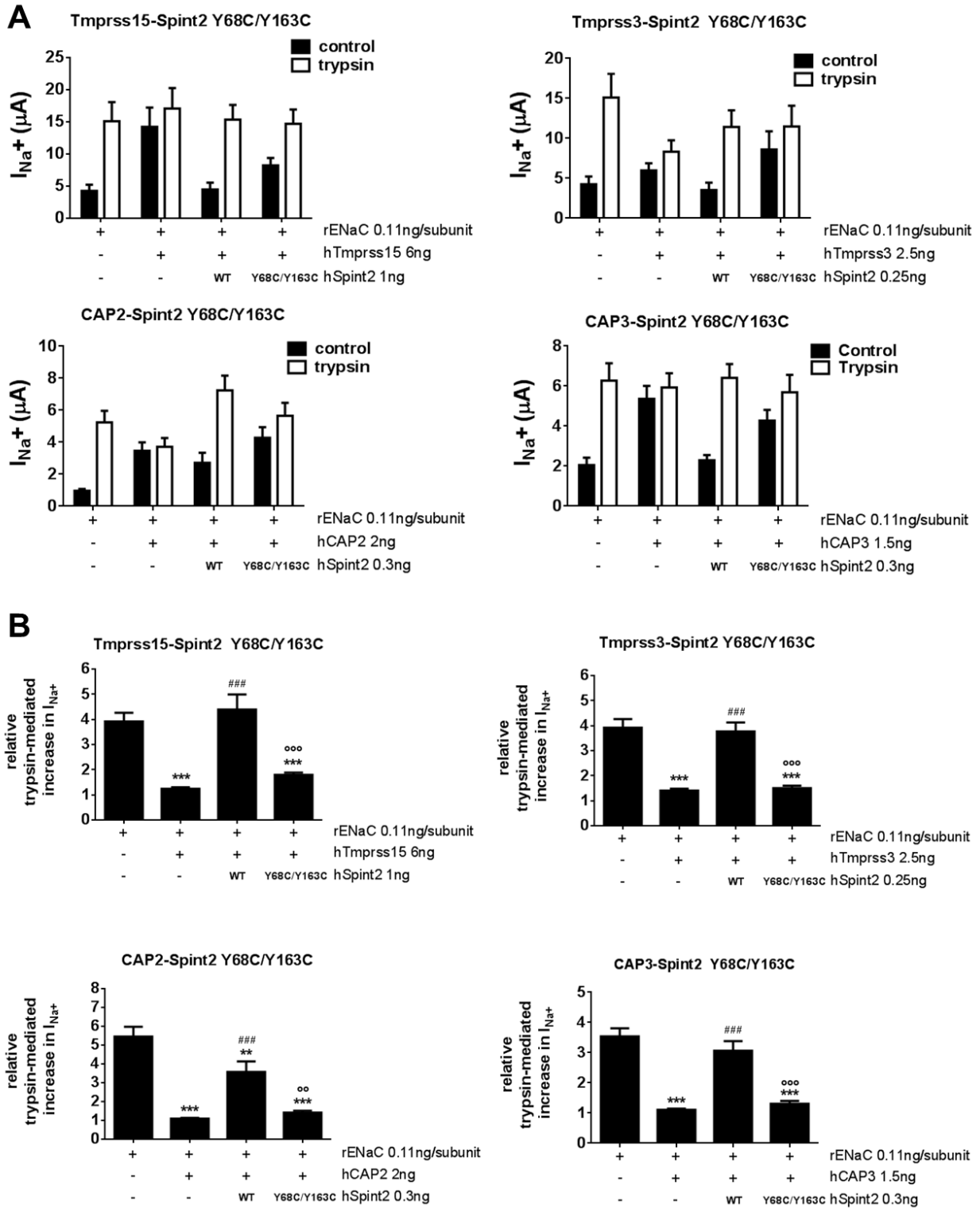


Figure 5

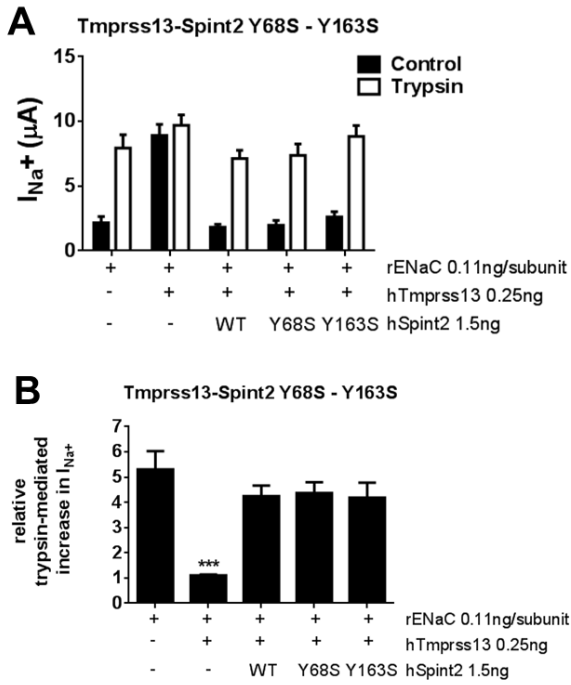
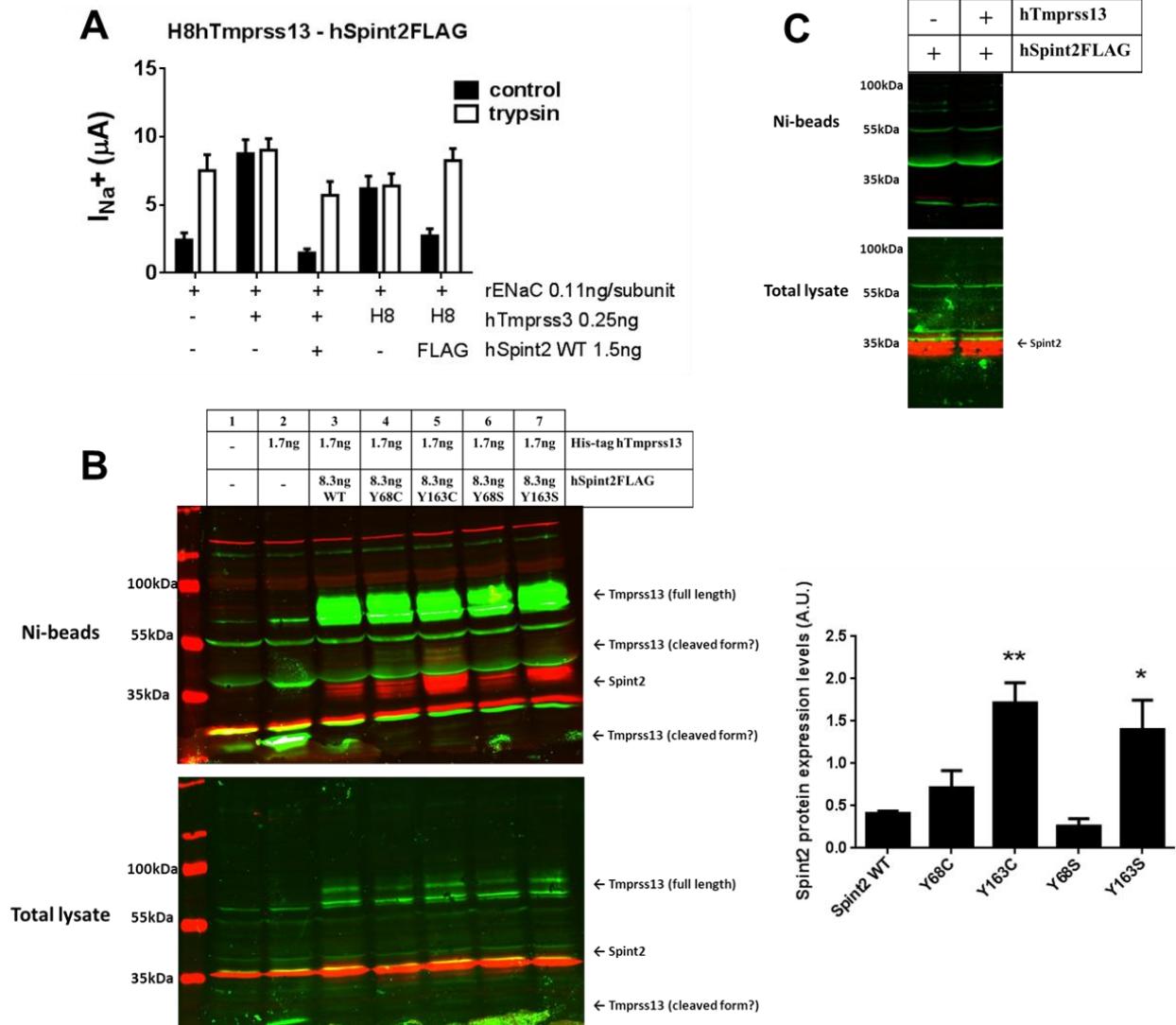


Figure 6



## Supplemental Data

### Functional analysis of a missense mutation in the serine protease inhibitor Spint2/HAI-2 associated with the congenital sodium diarrhea

Faller N, Gautschi I and Schild L

**Supplemental Table S1**

<b>Gene</b>	<b>Forward Primer</b>	<b>Reverse Primer</b>
<i>Actb</i>	ggctcctagcaccatgaaga	agctcagtaacagtccgcc
<i>Gapdh</i>	catggccttccgtgttcta	cctgcttcaccaccttctga
<i>Spint2</i> (long isoform)	tttatggaggctgtgaaggca	aagagtcggctccattcctg
<i>Spint2</i> (short isoform)	tagacgtccacgagaacacca	actcaggacagaagagtccg
<i>Prss8</i> (=CAP1)	agaaccgcacactatccagc	ccaagtaccagatgcctcc
<i>Tmprss4</i> (=CAP2)	cattcagaggggccagttgt	cagggtggatctgtccttgg
<i>St14</i> (=CAP3)	tccgaagctttgatgtcgct	agcgtgacaaggaagacgtt
<i>Hpn</i> (=Tmprss1)	ctgacatggcgaaggagg	cttggtacagtggctcctgg
<i>Tmprss2</i>	aaagcctggatcccgtgtg	ctggcttggatcccttggc
<i>Tmprss3</i>	tcagatgacaaggtgacggc	cgaggacatgtttccacca
<i>Tmprss11a</i>	ggcgaagaaccgtagggaaa	gctcgttgcacaatcttt
<i>Tmprss13</i>	gatggagtggaggactgcaa	tcgccagaagaccagagta
<i>Entk</i> (=Tmprss15)	gtggctgcaacaacttcagg	ggcacatagcccagtgttt

SUPPLEMENTAL TABLE S1. Sequences of the primers used for the quantitative PCR experiments on mouse tissues.